2003

Novel control design and strategy for load frequency control in restructured power systems

Dulpichet Rerkpreedapong
West Virginia University

Novel Control Design and Strategy for Load Frequency Control in Restructured Power Systems

by

Dulpichet Rerkpreedapong

Dissertation submitted to the
College of Engineering and Mineral Resources
at West Virginia University
in partial fulfillment of the requirements
for the degree of

Doctor of Philosophy
in
Electrical Engineering

Professor Asad Davari, Ph.D.
Professor Stratford Douglas, Ph.D.
Professor Ronald Klein, Ph.D.
Professor Powsiri Klinkhachorn, Ph.D.
Professor Ali Feliachi, Ph.D., Chair

Lane Department of Computer Science and Electrical Engineering

Morgantown, West Virginia
2003

Keywords: automatic generation control, decentralized control, ancillary services, regulation, NERC, control performance standards, deregulation

Abstract

Novel Control Design and Strategy for Load Frequency Control in Restructured Power Systems

by

Dulpichet Rerkpreedapong
Doctor of Philosophy in Electrical Engineering

West Virginia University

Professor Ali Feliachi, Ph.D., Chair

In restructured electric power systems, a number of generation companies and independent power producers compete in the energy market to make a profit. Furthermore, a new marketplace for *ancillary services* is established, providing an additional profit opportunity for those power suppliers. These services are essential since they help support the transmission of power from energy sources to loads, and maintain reliable operation of the overall system. This dissertation addresses *regulation*, a major ancillary service also known as the load frequency control (LFC) problem, and presents novel control designs and strategies for the LFC in restructured power systems.

A power system is an interconnection of control areas, which are operated according to control performance standards established by the North American Electric Reliability Council (NERC). LFC is a necessary mechanism in each control area because it maintains a balance between power demand and power generation while assuring compliance with NERC standards.

This dissertation first develops three new control designs that yield effective and robust load frequency control actions. All controllers developed here require only local measurements. The first control design is based on decoupling each area thru modeling of the interconnection effects of other control areas. The second control design relies on the robust H_∞ theory in terms of linear matrix inequalities (LMIs). The third control design is achieved by the collaboration between genetic algorithms (GAs) and LMIs. The first two control designs result in high-order dynamic controllers. The third design requires only a simple proportional-integral (PI) controller while yielding control performance as good as those resulting from the previous two designs. Consequently, the third control design is the most preferable due to its simplicity and suitability for industry practice. Furthermore, a stability analysis method based on perturbation theory of eigenvalues is developed to assess the stability of the entire power system being equipped by the proposed controllers.

Second, to comply with NERC standards, two LFC strategies are developed to direct LFC's actions. One strategy employs fuzzy logic to mimic a skillful operator's actions so that all decisions are made efficiently. The other strategy treats the compliance with NERC standards as constraints while minimizing the operational and maintenance costs associated with LFC actions. Three new indices are introduced to assess economic benefits from the strategy compared to the conventional methods. Simulation is performed to demonstrate performances of all proposed methods and strategies.

Acknowledgments

I would like to take this opportunity to express my cordial gratefulness to my advisor, Dr. Ali Feliachi, who gave me invaluable knowledge, and taught me how to be a good researcher. His continual support and guidance made me be the best I can be. Without him, this dissertation would not have been a complete success. I also want to extend my appreciation to my committee members: Dr. Asad Davari, Dr. Stratford Douglas, Dr. Ronald Klein, and Dr. Powsiri Klinkhachorn. Their creative ideas and suggestions definitely helped me maximize the worthiness of this dissertation.

I would like to acknowledge the US DOE/EPSCoR WV State Implementation Award, whose financial support made this dissertation possible. I am also very thankful to the Royal Thai Government, which financially supported me throughout my graduate program.

I would also like to thank Ali Karimi, Amer Al-Hinai, Amer Hasanović, Joshua Robinson, Karl Schoder, Kourosh Sedghisigarchi, and Nedžad Atić, my friends and colleagues at the Advanced Power Engineering Research Center (APERC) for being supportive and making my time at work enjoyable. I am very grateful to my best friends, Pisut Raphisak and Juchirl Park, who never let me have a lonely time, and always encourage me through my struggles. I truly thank them for their incredible friendship and being like my family here.

Finally, my hearty thanks go to my family in Thailand: my father, mother, sister, and brothers, who always love me, support me, and believe in me. For almost six years during my Master and Doctoral studies, they had been faithfully waiting for my success. This dissertation is dedicated to them with love and gratitude.

Contents

List of Figures

List of Tables

Chapter 1

Introduction

In recent years, structures of electric power systems have dramatically changed due to deregulation. It is the purpose of the Federal Energy Regulatory Commission[1] (FERC) to improve economic efficiency and lower electricity prices. As a result, vertically integrated utilities (VIUs) have become a number of independent specialized companies pursuing the goal of maximizing their own benefits. Those parties, Generation (Genco), Transmission (Transco), and Distribution (Disco) companies, make sales and purchases on amounts of energy and ancillary services [1] in competitive markets, whose structures may vary from one region to another [2]. Nevertheless, these players operate under the supervision of an independent system operator (ISO), whose responsibilities are to rule and approve their actions in order to maintain a good level of system reliability.

Regulation service [3] or load frequency control (LFC) is one of the ancillary services and is very essential for all interconnected power system control areas. This is because the LFC mechanism keeps the system interconnection frequency at 60 Hz, and also maintains the net interchange of each control area at the scheduled value. A system operator needs to prepare an adequate amount of regulation power, which can be purchased from generation companies or independent power producers (IPPs), to meet the regulation requirement.

Load frequency control is performed by an automatic generation control (AGC) system operated by the system operator. The balance between power generation and demand is traditionally achieved through automatic controls on the steam valves or water gates of speed governors, in

[1]Federal Energy Regulatory Commission (FERC), "FERC is an independent regulatory agency within the Department of Energy that regulates and oversees energy industries in the economic and environmental interest of the American public.", Washington, D.C., http://www.ferc.gov

order to adjust the amount of steam or water flowing into the turbines. Hence, they control the mechanical power on the shafts of the turbo generators.

In practice, a proportional-integral (PI) controller is widely employed for the load frequency control purpose. Normally, its control parameters are tuned about once a month based on trial and error techniques, which may not be efficient for all operating conditions. Additionally, specified control performance in areas such as transient response, oscillations, and settling time is unlikely to be easily obtained. This situation has led to a number of contributions from research focused on systematic controller design for load frequency control applications. Several decentralized controllers have been developed, while others have been designed to be adaptive or robust against uncertainties. However, most of them are either state feedback or full-order dynamic controllers, which are too complex for industry practices. Consequently, an effective control design, which provides robustness, decentralized structure, and if possible a proportional-integral (PI) based control scheme, is still needed in order to develop an ideal load frequency controller.

In February 1997, the North American Electric Reliability Council[2] (NERC) released new control performance standards [4] CPS1 and CPS2 to assess the effectiveness of the automatic generation control (AGC) of each control area. According to the EPRI report [5], the definition of a control area is given as:

> "*A control area is an electrical system which is bound by interconnect (tie-line) metering and telemetry. A control area continuously adjusts its generation and interchange schedules (via AGC) to match its system load and assists with the frequency regulation of the interconnected power system.*"

In more detail, the new standards were adopted to replace the old control performance criteria (CPC), which had been used in the past. According to observations [33], the CPC were found to be ineffective standards because when they were satisfied by the control areas, the interconnected system operation was often still poor. Also the old standards lacked a technical basis, while the new standards have mathematical support and are based on statistical theory. As a result, when they are complied with, the new standards yield a healthy interconnected system operation. However, regarding CPS data from NERC, some control areas have very good compliance with CPS1, while violating CPS2. Some of them even violate the standard for two or three months

[2]North American Electric Reliability Council (NERC) has operated as a voluntary organization to promote bulk electric system reliability and security - one dependent on reciprocity, peer pressure, and the mutual self-interest of all those involved, "NERC's mission is to develop, promote, and enforce reliability standards", Princeton, New Jersey, http://www.nerc.com

in a row, and are eventually penalized. In order to solve this problem, new control strategies, an objective of this research, have to be developed.

After deregulation, instead of a single utility having responsibility for load frequency control or regulation service within its territory, many competing companies cooperate and jointly share that responsibility according to contract agreements established within the marketplace. In the uniform price based market, the market price is set by the highest accepted bid where all bids are normally from the marginal cost of providing the service. Therefore, reducing the marginal cost should be a solution to lower the market price passed along to customers on the demand side.

While performing load frequency control, the mechanical equipment of generating units within the speed governor system is constantly moved up and down following the AGC signal obtained from the system operator. Such unit maneuvering causes wear and tear, and hastens the time frame of the maintenance schedule. Consequently, reducing incurred wear and tear is a strategy for cutting costs, a significant objective of those providing the regulation service. In this dissertation, several LFC strategies are developed to cooperate with the load frequency controller in order to minimize the LFC costs. The success of this research will benefit all market participants, and also bring the regulation price down in harmony with FERC's purpose.

This dissertation is organized as follows. A literature survey and work related to the investigated problems are discussed in Chapter 2. Next, background for this dissertation is given in Chapter 3. Afterwards, new robust decentralized load frequency control designs are described in Chapter 4 and are tested with a detailed model of power systems using the Power Analysis Toolbox (PAT) in Chapter 5. Subsequently, a new LFC strategy to comply with NERC's control performance standards is presented in Chapter 6. Taking into account economic incentives, the economy inspired load frequency control system is implemented in Chapter 7. Finally, conclusions and future work are given in Chapter 8.

Chapter 2

Literature survey

This chapter summarizes the ideas from existing work and publications related to load frequency control designs and strategies for restructured power systems. They are thoroughly reviewed and discussed in the following sections. Finally, the contributions of this dissertation, which have been designed mainly to improve upon previous work and overcome weakness in it, are described in section 2.3.

2.1 Power system load frequency control design

A large power system interconnection consists of a number of control areas interconnected through tie lines. Their fundamental role is to balance power generation and constantly changing demand, in order to maintain the interconnection frequency and net interchange at their scheduled values. The control area operator performs load frequency control (LFC), which is a balancing mechanism, through the automatic generation control (AGC) system. It automatically compensates for the difference between generation and load by using a proportional-integral (PI) controller, which uses area control error (ACE) as the input. The ACE signal can be obtained from measurements of interconnection frequency (f_a) and net interchange (NI_a), which sometimes is called tie-line power (P_{tie}), according to the following equation.

$$ACE = B * (f_a - f_s) + (NI_a - NI_s)$$

where

NI_s: scheduled net interchange (MW)
f_s: scheduled interconnection frequency (Hz)
B: frequency bias coefficient (MW/Hz)

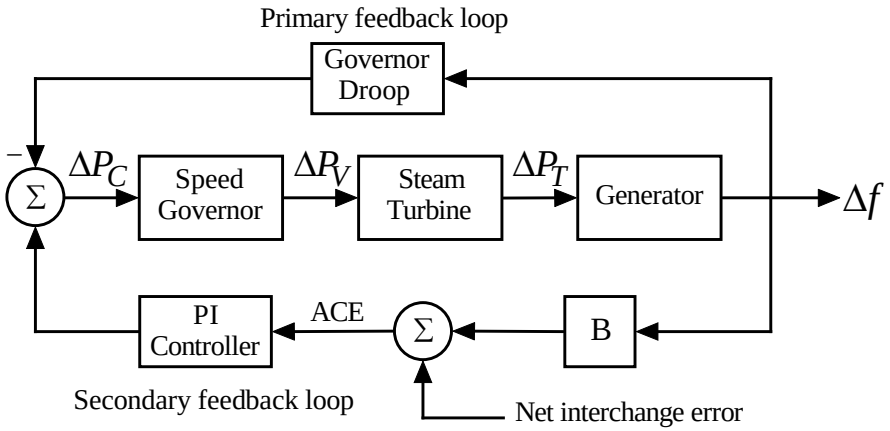

Figure 2.1: A simplified structure of load frequency control.

In Figure 2.1, the simplified structure of a conventional PI load frequency controller is illustrated. The raise/lower signal (ΔP_C) automatically adjusts the steam valve (ΔP_V) of the speed governor to increase or decrease the amount of steam flowing into the turbine. Hence, the mechanical power (ΔP_T) on the shaft of the turbo generator is controlled in order to drive the ACE to zero.

In real-world practice, the control parameters of conventional PI load frequency controllers are tuned online by trial and error, and only once in a long while. Thus, the obtained control parameters may not be efficient in a wide range of operations. In addition, the dynamic performance of such controllers is unlikely to be acceptable. There is a body of research contributing to the improvement of the transient performance of load frequency control, such as PI tuning algorithms and controller synthesis including decentralized, adaptive, robust control. Some of that work, which is significant and related to the proposed research are discussed next.

Proportional-integral (PI) control tuning and optimization

Several research studies have focused on tuning parameters of PI LFC controllers. The common objective is to improve the transient performance of load frequency control. This work is described as follows.

Robust control analysis and design for load frequency control is addressed in Stankovic et al.'s paper [6]. The LFC controller is of the integral type, and its control gain is selected to maintain stability robustness over parameter uncertainties using Quantitative feedback theory (QFT). QFT

is used to both analyze and shape the closed-loop responses in the frequency domain (bode plot) under parameter variations. In this paper, a lead controller is additionally cascaded to the integral LFC controller in order to reduce the response oscillations due to load disturbances during the transient period.

In another research area, load frequency control design is treated as an optimization problem. First, different performance indices, including power-imbalance terms (Δf, ΔP_{tie} or ACE) are developed. Subsequently, optimization techniques are used to determine the optimal LFC parameters that minimize those performance indices.

In Abdel-Magid and Dawoud's work [7], the parameters of the integral controller are searched for, in order to minimize given performance indices using Genetic Algorithms (GAs). This study investigates two performance indices. The first one is the integral of square of error (ISE), which is a typical performance criterion used in a number of control applications. This criterion tends to penalize all errors with respect to given weighting factors. The other performance index is the integral of time-multiplied absolute value of the error (ITAE) [8]. This criterion is also widely used. It includes the time (t), in order to penalize the settling time of the controlled system. For a two-area power system, the above performance indices are described by the following equations.

$$ISE = \int_0^\infty \left(\Delta P_{tie}^2 + \alpha \Delta f_1^2 + \gamma \Delta f_2^2\right) dt$$

$$ITAE = \int_0^\infty t \left(|\Delta P_{tie}| + \alpha |\Delta f_1| + \gamma |\Delta f_2|\right) dt$$

where α and γ are weighting factors that characterize the performance indices.

GAs are used in this work, since they are more likely to reach the global minimum rather than conventional optimizations. However, such an optimization needs to be performed through a number of simulations of the entire system, which require physical parameters for all control areas, and consequently might not be practical. In addition, the above performance indices include the frequency deviations of both areas, which is not preferable from a decentralized control point of view.

Under deregulation, load frequency control, as one of the ancillary services, is sold and purchased at marketplaces as commodities. Donde et al. [9] formulates an AGC simulation framework accounting for LFC contracts for a two-area power system following the ideas of Kumar et al. [10] and [11]. This paper also proposes an optimization based on a trajectory sensitivity

approach to obtaining the optimal parameter for the integral load frequency controller. In this work, the two areas are assumed identical, and the performance index used for optimization by a gradient Newton algorithm is illustrated as

$$Performance\ Index = \int_0^\infty \left[\alpha \Delta P_{tie}^2 + \beta \Delta f_1^2\right] dt$$

where α and β are weighting factors that characterize the performance index.

Similar to [7], the optimization process is done by a number of simulations, and all parameters of the global system are needed. This paper assumes that both areas are identical to simplify the problem, but it is not the case with real-world power systems.

In Kothari et al.'s paper [12], the proposed ideas are close to those in [9]. The LFC contracts are considered, but the parameters of integral controllers are optimized subject to the new performance index as shown below.

$$Performance\ Index = \sum_{k=1}^{n} \left[ACE_1^2(k) + ACE_2^2(k) + 200\varepsilon_1^2(k) + 0.2I_1^2(k)\right]$$

where

$$\begin{aligned} \varepsilon_1 &= \tfrac{1}{60}\int \Delta f_1 dt \\ I_1 &= \int \Delta P_{tie} dt \end{aligned}$$

An additional advantage of this performance index is that the obtained optimal control parameter tends to offset the inadvertent power and time error accumulation, which are caused by accumulations of ΔP_{tie} and Δf during the operation.

In the above work, all optimization methods require lengthy simulations, which need physical parameters for entire system to find the optimal control parameters of LFC controllers. In practical implementations, such parameters of a control area are unlikely to be available to the other areas. Therefore, a completely decentralized control design, which can be systematically obtained without relying on simulation and, moreover, needs only local measurements and parameters, is desirable for load frequency control applications.

2.1.1 Decentralized robust load frequency control

Electric power systems are known as one of the most complex networks, comprising a number of subsystems or control areas interconnected to one another by tie lines. Unlike the situation

of other small dynamic systems, employing a centralized controller that relies on global information from either measurements or state observers would not be practical and secure. Thus the decentralized control scheme that results in a controller, which needs only local information in controlling its own subsystem, is very desirable for the control design of power systems.

For a large power system including n interconnected subsystems, a state space form of generic subsystem i with its decentralized controller can be described as

$$\begin{aligned} \dot{x}_i &= A_{ii}x_i + B_i u_i + \sum_{\substack{j=1 \\ j\neq i}}^{n} A_{ij}x_j \\ y_i &= C_i x_i \\ u_i &= K_i(s) y_i \end{aligned}$$

where

$$\dot{x} = \begin{bmatrix} \dot{x}_1 \\ \vdots \\ \dot{x}_i \\ \vdots \\ \dot{x}_n \end{bmatrix} = \begin{bmatrix} A_{11} & \cdots & A_{1i} & \cdots & A_{1n} \\ \vdots & \ddots & & & \vdots \\ A_{i1} & & A_{ii} & & A_{in} \\ \vdots & & & \ddots & \vdots \\ A_{n1} & \cdots & A_{ni} & \cdots & A_{nn} \end{bmatrix} \begin{bmatrix} x_1 \\ \vdots \\ x_i \\ \vdots \\ x_n \end{bmatrix} + \begin{bmatrix} B_1 & & & & \\ & \ddots & & 0 & \\ & & B_i & & \\ & 0 & & \ddots & \\ & & & & B_n \end{bmatrix} \begin{bmatrix} u_1 \\ \vdots \\ u_i \\ \vdots \\ u_n \end{bmatrix}$$

x: state variables of entire system
x_i: state variables of subsystem i
y_i: output of subsystem i
u_i: input of subsystem i
$K_i(s)$: decentralized controller of subsystem i

For load frequency control problems, a control area is considered to be a subsystem of the power system interconnection. Several research studies being discussed here present a variety of decentralized control designs for load frequency control. Feliachi et al. apply the robust H_∞ control theory to obtain robustness for the closed-loop system against uncertainties such as demand changes and area interconnections [13], [14] and [15]. Some others use different control theories to solve the problems. They are described as follows.

Yang et al. [16] proposes a decentralized load frequency controller design based on structured singular values. In this paper, the open-loop subsystem of each control area has already included an integral controller. An additional decentralized controller is designed to improve the transient stability of the entire system. Such a controller is of a dynamic type, designed based on structured

singular values (μ); this is a frequency-response robust control design method. It increases the gain and phase margins of each subsystem, which results in the stability of the closed-loop system. However, employing both LFC controllers, including the integral and proposed ones, is relatively redundant and cost inefficient for control areas, since either one with good control design could achieve the same goal effectively.

A systematic based decentralized load frequency control design is presented in Aldeen et al.'s paper [17]. For each subsystem in their design, a local observer is developed to reconstruct global states. Those estimated states are used as the inputs of the proportional-integral (PI) controller, which formulates the decentralized control scheme. However, the PI controller used in Aldeen et al is much more complex than the traditional one, which requires only the ACE as the input. Also it results in the need for a state observer, which actually increases the order of the control system.

In Trinh et al. [18], a decentralized controller is proposed for the load frequency control problem. Based on singular perturbation methods, the decoupling is obtained by assuming that power systems are relatively weakly coupled systems [19]. With the approximately decoupled subsystem, the optimal decentralized controller is designed, using the linear quadratic regulator (LQR) technique. The assumption as given above is probably too optimistic. In fact, interconnections among power systems can be from weak to very strong depending on the distance between them. Consequently, the proposed decentralized controller may not perform well in strongly coupled power systems.

An inclusion principle with the emphasis on state observer and optimal controller design is applied to load frequency control applications by Stankovic et al. [20]. In their study, the state space model (S) of a two-area power system is formed, and is considered to be two overlapping subsystems. It is subsequently cast into an expanded system ($\tilde{\text{S}}$) that has a larger size, and contains all necessary information about S. Afterwards, the corresponding subsystems of S are extracted from $\tilde{\text{S}}$. Using a linear quadratic gaussian (LQG) technique, decentralized controllers are finally designed for the individual resulting subsystems. According to the proposed control scheme, the order of the observer based controller increases with the size of the subsystem depending on modeling details and the number of generating units. Moreover, the complexity of using an overlapping decentralization technique would increase exponentially with the number of subsystems, which is determined for only two in this paper, but could be more in real-world applications.

A robust decentralized controller for the LFC can be also obtained by using the Riccati-equation approach presented in Lim et al. [21] and [22]. The parameter variations and interference from all other areas are considered as uncertainties for individual subsystems. The control gains for each decentralized state-feedback controller are obtained by solving a Riccati equation, taking into account such uncertainties. The resulting decentralized controllers of all subsystems are guaranteed for stabilizing the overall system by a stability analysis based on the Lyapunov function given in Khargonekar et al.'s work [23]. Nevertheless, the proposed controller requires the measurements of all local states, and some of them are not measurable. Therefore, a state observer is needed, which increases the complexity of the control system when the number of states becomes large.

2.1.2 Intelligent adaptive load frequency control

The load frequency control problem has also attracted significant attention from researchers in the area of intelligent control, including neural networks and fuzzy logic. In Hsu et al.'s work [24], a fuzzy logic LFC controller is designed to replace the conventional one. The fuzzy rules are designed with expertise to regulate the ACE to zero. The frequency deviation and its rate are used as the inputs of the fuzzy logic system, whose output is the control signal of a control area. In an approach similar to this, Indulkar et al. [25] use the ACE and its rate as the fuzzy inputs.

In Djukanovic's study [26], the uncertainties of system parameters are taken into consideration, including power system time constant, frequency bias constant, and synchronizing power coefficient. Artificial Neural Networks (ANN) are used to adapt control gains to variations of those parameters in order to maintain good dynamic performance. The training sets are generated by solving the state-space LQR problems for different values of such parameters. To make this control scheme effective, however, the number of training sets needs to be large, and consequently network training unavoidably becomes very slow.

Subsequently, Talaq et al. used a Sugeno type fuzzy inference system as a gain scheduler [27] to replace the neural networks in [26]. This is because the fuzzy system design needs fewer training sets and is well suited for smoothly interpolating linear gains over the input space. In these papers, all optimal feedback gains are designed for the whole system rather than for individual control areas, which do not address the decentralized control scheme.

A number of load frequency control designs discussed in this section are employed mainly

to achieve good dynamic performance of the LFC operation. Yet, the structure and operational objective of load frequency control have been changing during the last few years due to power system deregulation and the adoption of NERC's new control performance standards. These issues are addressed in the next section.

2.2 Load frequency control in restructured power systems

Load frequency control is an essential mechanism for the reliable operation of an interconnected power system. It is also known as regulation service [3],[28] which is one of a number of ancillary services [1],[29]. In the past, LFC was provided by vertically integrated utilities (VIUs) for their own territories. After deregulation, it has become possible for different generation companies (Genco) and independent power producers (IPP) to participate in providing this service instead of the VIUs, which have become transmission companies (Transco). The transition from VIU to deregulated utility structure is illustrated in Figure 2.2.

Christie et al. [30] and Meliopoulos et al. [31] draw several possible scenarios of load frequency control service under deregulation. The main idea is that LFC becomes a commodity which can be sold and purchased in the market. Gencos and IPPs may choose either to sell it by submitting their bids to the independent system operator (ISO) or not to participate if the profit opportunity is rare. In such an environment, all market participants tend to maximize their benefits rather than enhancing power system reliability. The ISO, which is the middle man, needs to supervise and approve the actions of those market players to assure the reliability of the power system operation [32].

Especially for regulation service, the North American Electric Reliability Council (NERC) employed the control performance criteria (CPC), which include A1 and A2, for three decades to specify whether an area's generation is sufficiently controlled to make the interconnection frequency and net interchange meet their schedules. Criterion A1 requires that the ACE should cross zero at least once every ten minutes. Criterion A2 requires that ten minute averages of ACE should be less than an area specific parameter (L_d). However, using these criteria, it was found that when they were satisfied, interconnected system operation was often poor.

In February 1997, the new control performance standards including CPS1 and CPS2, developed from mathematical relations between the ACE and the frequency error, were adopted to replace the old criteria in order to eliminate the CPC's drawback [33]. CPS1 is a limit on the 12-month average of the product of the ACE and frequency error from its schedule. CPS2

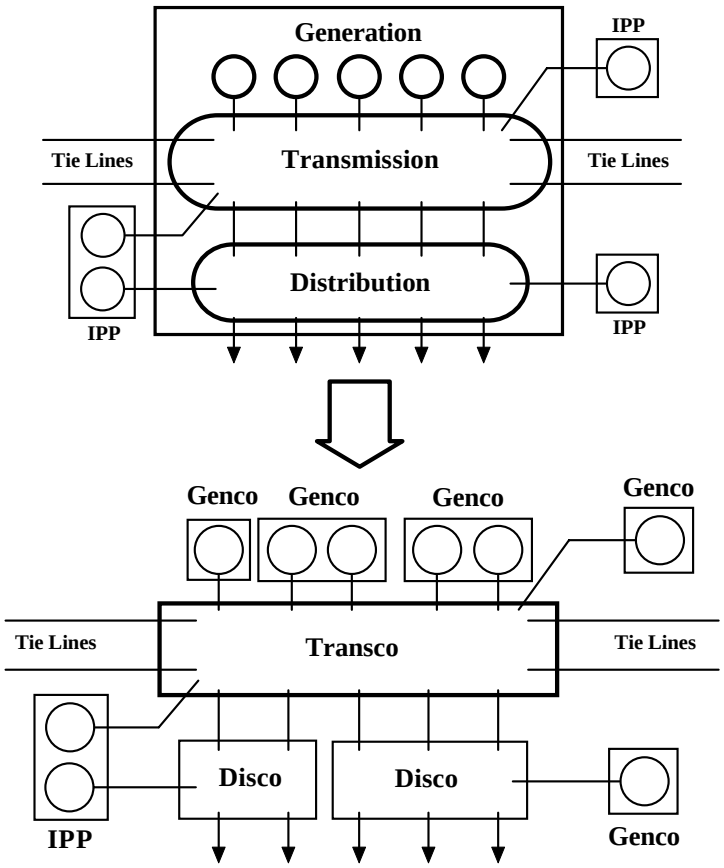

Figure 2.2: Transition from VIU to deregulated utility structure.

is similar to A2, but its specific limit is determined based on a statistical method and is much larger than A2's. From observations, CPS1 and CPS2, which have technical background support and are more flexible than the old criteria, allow less unit maneuvering, resulting in a saving of fuel costs and unit wear and tear.

Gross et al. [34] presents an analytic framework of CPS1 and CPS2 for LFC performance assessment. Probability and random processes concepts are used as a key tool for this analysis. The analytical results show that the two standards are redundant. More specifically, CPS2 is automatically satisfied when CPS1 is complied with under the following assumptions, where window length $W \geq 10$ minutes.

1) The random variable's $\overline{ACE}_i^n$ and $\overline{ACE}_j^n$ of two different control areas $i \neq j$ are independent, and

2) The mean value of $\overline{ACE}_i^n$ is equal to zero; $n = 1, 2, ..., N$.

where

$$\overline{ACE}_i^n \;=\; \frac{1}{K}\sum_{k=1}^{K} ACE_i\,(t_k), \qquad n = 1, 2, ..., N$$

To obtain a statistically meaningful assessment, the number N of W windows should be large. Corresponding to window n, the subinterval (I^n) is defined as

$$I^n \;=\; [t_0 + (n-1)\cdot W, t_0 + n\cdot W]$$

while the measurement time subset is:

$$\tau^n \;\triangleq\; \{t_k :\; t_k\, is\, a\, measurement\, point\, in\, I^n,\; k = 1, 2, ..., K\}$$

associated with the subinterval I^n.

From the preliminary work of this dissertation, however, it is found that the first assumption does not usually hold since the ACE of all control areas are partially obtained from the same interconnection frequency error. Moreover, the CPS data from NERC [35] show that some control areas still violate CPS2 even though they comply with CPS1.

A few studies present AGC logic for load frequency control, in compliance with NERC's standards and the goal of enhancing economic operations. Jaleeli et al. [36] present a tie-line bias prioritized energy control scheme that 1) regulates interconnection frequency, 2) reduces inadvertent energy and time error accumulations, and 3) lowers unnecessary generation maneuvering, resulting in a reduction of unit wear and tear. The simplified idea of this control scheme is that the ACE should be kept within a near-zero target boundary, but unconditionally forcing a small ACE to return to zero does not optimize operating objectives, and may not be economically optimal. The proposed control scheme is also called wedged control because the near-zero target boundary is wedge-shaped as shown in Figure 2.3.

The control strategy is that as long as the average of the ACE is within the boundary, there will not be generation maneuvering, corresponding to the ACE. A smaller boundary limit for a larger T yields a much closer match between the generation of each control area and its power demand, and hence improves its control performance. On the other hand, the wedge-shaped boundary has wider limits for shorter values of T. This characteristic results in reducing unnecessary unit maneuvering in order to match fast load fluctuations. However, Jaleeli et al do not provide an algorithm to tune wedge control. Also they do not address the issue of compatibility with NERC's new control performance standards.

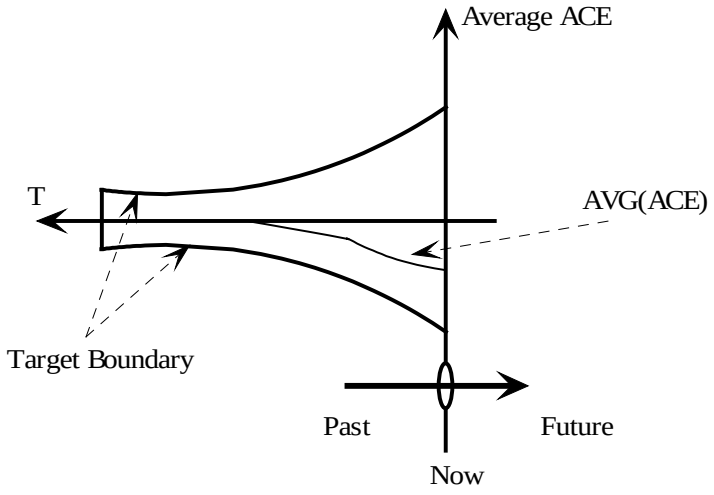

Figure 2.3: A target wedge boundary of tie-line bias prioritized energy control.

In Yao et al.'s study [37], an AGC logic based on NERC's new standards is developed. The logic system is composed of CPS1 and CPS2 control modules, which need to be coordinated orderly. The compliance factor of each CPS1 and CPS2 is defined and calculated every 4 seconds. The concept of the proposed logic is that as long as those compliance factors are less than their corresponding thresholds, the AGC signal to regulating units is set to zero, which means no control actions are induced. Otherwise, the AGC signal is set to the average of the raw ACE. Determination of the threshold values is very important, since they directly indicate the control tightness. In this paper, those thresholds are selected by searching for the values that result in the best compliance with CPS1 and CPS2. However, those values are constant and specifically chosen for the test system and would not be applicable to other power systems.

2.3 Contribution of the dissertation

From literature review, it can be observed that load frequency control is one of the most attractive research topics in this field. A number of studies involving the LFC have been carried out in the past three decades. Nevertheless, existing robust load frequency controllers are relatively complicated and impractical for implementation. Some studies employ centralized control, which rely on global measurements or high-order observers. Thus, an effective robust decentralized LFC controller which is attractive from implementation point of view needs to be developed. In

addition, the replacement of the old control performance criteria (CPC) with the new control performance standards (CPS) by NERC significantly influences control areas, requiring the development of new LFC strategies. In a market based environment, such strategies should result in not only compliance with the CPS, but also in saving operational and maintenance costs for power producers. Fulfilling the above requirements becomes the main objectives of this dissertation, addressed as follows.

- Develop robust decentralized load frequency control designs which result in effective robust performance and simple controller structure. Since industry's LFC controllers are conventionally of the PI control type, robust PI control design in particular is focused on in this research.

- Develop LFC strategies in compliance with NERC's new control performance standards. According to the historical data, some control areas often violated the standards, and they were penalized by NERC.

- Develop operational and control strategies that help generating units or generation companies in cutting down their operational and maintenance costs. Those costs partially result from inefficient control actions, which cause excess unit maneuvering and unnecessary reversals of unit equipment.

Chapter 3

Background

This chapter provides the basic background needed for this research. First, load frequency control problems will be described in section 3.1. Technical details of the LFC mechanism are also given in this section. Subsequently, a dynamic model of a control area, including multi-generating units is presented for solving LFC problems. This model is prepared to accommodate the proposed LFC control designs, and reflects new changes due to restructuring, such that of ramp rate as obtained from a bidding result. In section 3.3, more details in implementing load frequency control as an ancillary service will be explained. Finally, LFC or regulation service is assessed on a monthly basis by the control performance standards, CPS1 and CPS2, established by the North American Electric Reliability Council (NERC). A control area that fails to comply with these standards is likely to be penalized. The definitions and details of CPS1 and CPS2 will be given in section 3.4. An in-depth study of the standards would help the system operator better understand and meet the compliance requirements.

3.1 Load frequency control problems

For a few decades, load frequency control problems have been extensively studied by many researchers. The objective is to design an effective feedback controller, which helps a control area maintain the interconnection frequency and power interchanges at their schedules. The load frequency control mechanism can be depicted as in Figure 3.1. The turbine and speed governor, which are the prime-mover of the synchronous generator, are controlled by load frequency control to balance generated power and demand; thus the frequency deviation and the net interchange error from the scheduled values remain close to zero. Nowadays, the term “area control error

(ACE)", which is the combination of area frequency bias (B) times frequency deviation and net power interchange error, is used to measure the power imbalance.

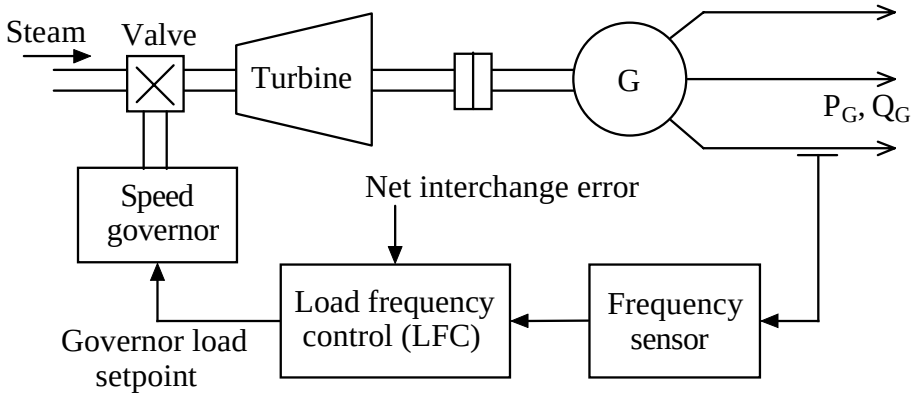

Figure 3.1: Load frequency control mechanism.

As shown in Figure 3.2, the schematic diagram of the speed governor system consists of four important parts: 1) the speed governor, 2) the linkage mechanism, 3) the hydraulic amplifier and 4) the speed changer. The centrifugal flyballs of the speed governor are driven by the turbine shaft. They yield upward and downward movements of the linkage mechanism proportional to changes in shaft speed. The hydraulic amplifier is needed to transform the governor movements into large mechanical forces in controlling the steam valve. Moreover, driven by a servomotor, the speed changer can raise and lower the governor links for scheduling load at nominal frequency. This can be done manually, or automatically by load frequency control. Generally, once the LFC senses the area control error signal, it will adjust the speed changer or governor load setpoint to compensate for the power imbalance.

Nevertheless, different types of LFC yield distinct control performances. They depend on the objective and property of control designs. In this dissertation, the goal of load frequency control is to provide robust operation of power system interconnection against possible contingencies. The LFC performance will be assessed by the control performance standards. Furthermore, a desirable LFC strategy should help reduce the unit maneuvering, as well as wear and tear during operation. An ideal load frequency control system which offers all the above advantages is developed in this dissertation. A dynamic model of the control area used for the proposed LFC designs will be first introduced in the next section.

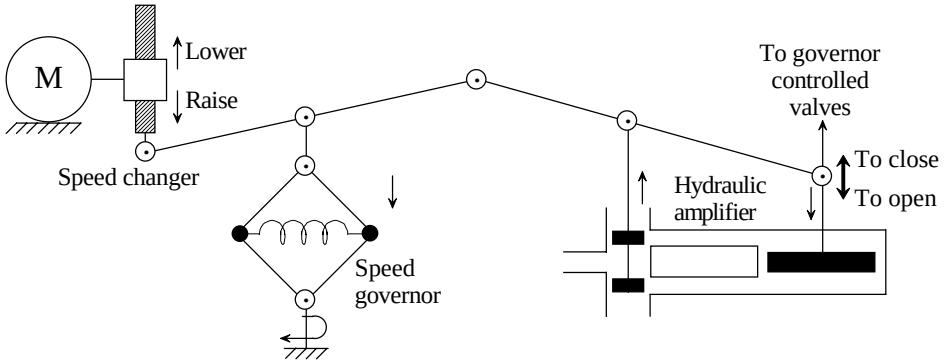

Figure 3.2: Speed governor system [38].

3.2 Dynamic model

The U.S. bulk power system is composed of three major networks or power grids including the Eastern, Western, and Texas interconnections [39]. Each one comprises high-voltage connections between individual utilities (control areas) which coordinate operations and buy and sell power among themselves.

A control area calls for the load frequency control or regulation service from generation companies and independent power producers. The primary function of LFC is to keep the interconnection frequency at 60 Hz, and to maintain the net interchange at the scheduled value. A system operator needs to prepare an adequate amount (MW) of regulation services to meet the regulation requirement in order to make sure that power imbalances are compensated for at all times.

Power generating units are composed of several crucial components such as generators, turbines, and speed governors. They are of time-delay systems, and their dynamic behaviors can be described by appropriate transfer functions.

In [40], a set of cascaded transfer functions is used to represent the dynamic of a generating unit. However, this model needs to be modified when a control area has more than one generating unit. In this case, all units are assumed to be coherent. All generators are lumped and represented by a transfer function whose output is the area frequency deviation. The dynamic model of a generic control area i for load frequency control problems used in this dissertation is shown in Figure 3.3.

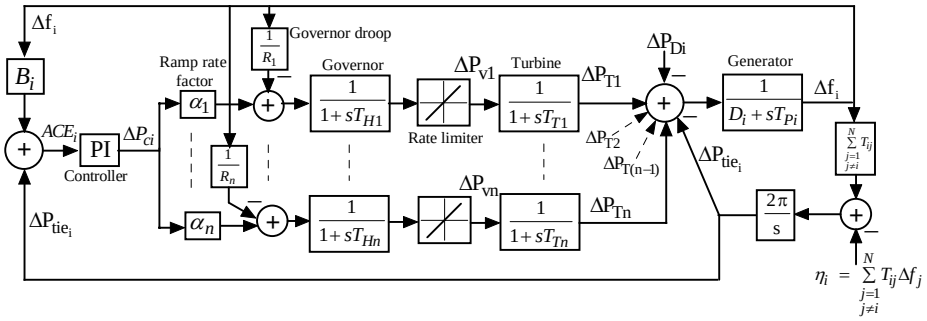

Figure 3.3: A dynamic model of control area i for the LFC problem.

P_T: turbine power — P_V: governor valve
P_C: governor setpoint — P_D: power demand
f: area frequency — P_{tie}: net interchange
ACE: area control error — η: interface
Δ: deviation from nominal values
T_{ij}: tie-line synchronizing coefficient between areas i and j
D: damping coefficient — T_P: constant of inertia
T_T: turbine time constant — T_H: governor time constant
R: droop characteristic — B: frequency bias factor
α: ramp rate factor — N: number of control areas

In Figure 3.3, control area i is interconnected with other areas through tie lines. A conventional LFC controller which is of proportional-integral (PI) type is used to drive the ACE, a combination of frequency deviation and tie-line power error, to zero. Power generation of each generating unit is ramped with respect to the corresponding ramp rate factors obtained from regulation contracts.

However, in terms of transfer functions the above dynamic model can be transformed into a state-space form as illustrated by eq. (3.1). This model is utilized throughout the dissertation.

$$\dot{x}_i = A_i x_i + B_{iu} u_i + B_{iw} w_i \tag{3.1}$$

where

$$x_i^T = \begin{bmatrix} x_{ia}^T & x_{i1}^T & x_{i2}^T & \dots & x_{in}^T \end{bmatrix}, \; u_i = \Delta P_{Ci}, \; w_i^T = \begin{bmatrix} \eta_i & \Delta P_{Di} \end{bmatrix}$$
$$x_{ia}^T = \begin{bmatrix} \Delta f_i & \Delta P_{tie_i} & \int ACE_i \end{bmatrix}, \; \eta_i = \sum_{\substack{j=1 \\ j \neq i}}^{N} T_{ij} \Delta f_j$$
$$x_{i1}^T = \begin{bmatrix} \Delta P_{T1} & \Delta P_{V1} \end{bmatrix}, \; \dots \; , \; x_{in}^T = \begin{bmatrix} \Delta P_{Tn} & \Delta P_{Vn} \end{bmatrix}$$

$$A_i = \begin{bmatrix} AREA_i & MP_i \\ DROOP_i & TG_i \end{bmatrix},\ B_{iu} = \begin{bmatrix} 0 \\ \bar{B}_{iu} \end{bmatrix},\ B_{iw} = \begin{bmatrix} \bar{B}_{iw} \\ 0 \end{bmatrix}$$

$$AREA_i = \begin{bmatrix} -\frac{D_i}{T_{Pi}} & \frac{-1}{T_{Pi}} & 0 \\ 2\pi \sum_{\substack{j=1 \\ j\neq i}}^{N} T_{ij} & 0 & 0 \\ B_i & 1 & 0 \end{bmatrix},\quad MP_i = \begin{bmatrix} \underbrace{\begin{pmatrix} \frac{1}{T_{Pi}} & 0 \\ 0 & 0 \\ 0 & 0 \end{pmatrix} \cdots \begin{pmatrix} \frac{1}{T_{Pi}} & 0 \\ 0 & 0 \\ 0 & 0 \end{pmatrix}}_{n \text{ blocks}} \end{bmatrix}$$

$$DROOP_i = \begin{bmatrix} \begin{pmatrix} 0 & 0 & 0 \\ \frac{-1}{R_1 T_{H1}} & 0 & 0 \end{pmatrix} \\ \vdots \\ \begin{pmatrix} 0 & 0 & 0 \\ \frac{-1}{R_n T_{Hn}} & 0 & 0 \end{pmatrix} \end{bmatrix},\quad TG_i = \begin{bmatrix} \begin{pmatrix} \frac{-1}{T_{T1}} & \frac{1}{T_{T1}} \\ 0 & \frac{-1}{T_{H1}} \end{pmatrix} & & 0 \\ & \ddots & \\ 0 & & \begin{pmatrix} \frac{-1}{T_{Tn}} & \frac{1}{T_{Tn}} \\ 0 & \frac{-1}{T_{Hn}} \end{pmatrix} \end{bmatrix}$$

$$\bar{B}_{iu} = \begin{bmatrix} \alpha_1 \begin{pmatrix} 0 \\ \frac{1}{T_{H1}} \end{pmatrix} \\ \vdots \\ \alpha_n \begin{pmatrix} 0 \\ \frac{1}{T_{Hn}} \end{pmatrix} \end{bmatrix},\quad \bar{B}_{iw} = \begin{bmatrix} 0 & \frac{-1}{T_{Pi}} \\ -2\pi & 0 \\ 0 & 0 \end{bmatrix}$$

According to the above equations, the state-space model x_i represents the state vector, while u_i is the area input, and w_i is the area disturbances including the area interface (η_i) and changes in local demand (ΔP_{Di}). In addition, this dynamic model is applicable for multiple generating units, and flexible in that it can be altered for various types of generating units.

3.3 Regulation service

According to Order 888, the Federal Energy Regulatory Commission (FERC) defines the set of *ancillary services* as they are [41]:

> "necessary to support the transmission of electric power from seller to purchaser given the obligations of control areas and transmitting utilities within those control areas to maintain reliable operations of the interconnected transmission system."

Load frequency control is also known as *regulation service*. It is one of the key ancillary services that transmission providers are required to offer, but customers can also self-supply or purchase from the third parties. A generator providing regulation service needs to be equipped with a governor system and to be under automatic generation control (AGC). The power generation is controlled by AGC signals in order to track real-time load fluctuations. Therefore, the time frame of this service is very short, usually less than 1 minute.

Only online generating units connected to the power grid and electrically close to the local control area can provide regulation. Ones that can quickly change their output (MW) to track moment-to-moment load fluctuations are preferable. This capability to change MW output within one minute is called *ramp rate* (MW/minute). In regulation auction markets, ramp rate is normally included in regulation bids along with the marginal cost ($/MW) of the service. Those who are selected to provide regulation must reserve their contracted megawatts, and will be responding to the AGC signals according to the offered ramp rates during the contract period.

3.4 NERC's control performance standards

In February 1997, the North American Electric Reliability Council (NERC) adopted two new control performance standards, CPS1 and CPS2. Each control area is required to monitor its AGC performance and to report its compliance with CPS1 and CPS2 to NERC at the end of each month. CPS1 and CPS2 are given as follows [4].

3.4.1 CPS1

CPS1 is defined as follows: over a sliding 12-month period, the average of the "clock-minute averages" of a control area's ACE divided by "ten times its area frequency bias" times the corresponding "clock-minute averages of the interconnection frequency error" shall be less than the square of a given constant, ε_1, representing a targeted frequency bound. This is expressed by

$$AVG_{12-month}\left[\left(\frac{ACE_i}{-10B_i}\right)_1 * \Delta F_1\right] \leq \varepsilon_1^2 \tag{3.2}$$

where

ΔF	interconnection frequency error
B_i	frequency bias of the i^{th} control area in MW/0.1Hz
ε_1	targeted frequency bound for CPS1
$(\cdot)_1$	clock-1-minute average

To calculate the frequency-related parameter, CPS1, a compliance factor (CF) and a 1-minute average compliance factor ($CF1$) are introduced

$$CF = AVG_{12-month}\left[CF_1\right] \tag{3.3}$$

$$CF_1 = \left[\left(\frac{ACE}{-10B}\right)_1 * \left(\frac{\Delta F}{\varepsilon_1^2}\right)_1\right] \tag{3.4}$$

Then CPS1 is obtained from the following equation

$$CPS1 = (2 - CF) * 100\% \tag{3.5}$$

To comply with NERC, CPS1, as obtained from eq. (3.5), should not be less than 100%.

3.4.2 CPS2

The second performance standard, CPS2, requires that the 10-minute averages of a control area's ACE be less than a constant (L_{10}) given in the equation below.

$$AVG_{10-\text{minute}}\left(ACE_i\right) \leq L_{10} \tag{3.6}$$

$$L_{10} = 1.65\varepsilon_{10}\sqrt{(-10B_i)\,(-10B_s)} \tag{3.7}$$

Note that B_s is the summation of the frequency bias settings of all control areas in the considered interconnection, and ε_{10} is the targeted frequency bound for CPS2.

To comply with this standard, each control area must have its level of compliance at no less than 90%. A compliance percentage is calculated from the following equation

$$CPS2 = \left[1 - \frac{Violations_{month}}{Total\,periods - Unavailable\,periods}\right] * 100\% \tag{3.8}$$

where $Violations_{month}$ are a count of the number of periods that the clock-10-minute averages of ACE are greater than L_{10} in one month.

Chapter 4

Robust decentralized load frequency control design

Normally, a power system interconnection, which includes a number of control areas, is geographically distributed, and the tie-lines that link interconnected areas are often long. These characteristics cause huge difficulties for centralized load frequency control in terms of reliability of remote data transmissions, and high costs of communication links. Consequently, achieving an effective decentralized control design is very desirable to the system operators. This is because the use of communication links and their back-up systems can be significantly reduced, and also the controller requires only local measurement. In this chapter, three robust decentralized control designs which are developed in this dissertation will be described in the following sections.

4.1 Decentralized load frequency control via interface modeling

In this section, a decentralized control design via interface modeling is proposed for load frequency control application [42], [43]. The main concept of decentralization is that interface is treated as a disturbance which can be modelled. Once the dynamic model of the disturbance is obtained, it is included in the system model, which results in an augmented model.

However, the disturbance model is fictitious because it is acquired by observing the dynamical characteristic of the interface instead of by classical identification. As a result, a Kalman filter is employed as an state observer to increase the accuracy of the estimation. Its advantage is that only local measurements yielding a completely observable system are needed as inputs.

In order to control the system, a state feedback controller based on the linear quadratic

regulator (LQR) technique is designed for the augmented system, which has taken into account disturbance effects. As a result, decentralized control can be achieved.

According to the state-space model given by eq. (3.1), a power system interconnection, including multiple control areas, is decentralized into a number of decoupled control areas. All area interfaces (η_i) are treated as disturbances together with the changes in area demand (ΔP_{Di}). Unfortunately, those disturbances are immeasurable, and make control designs more difficult for classical linear regulator problems. However, complication of control designs may be alleviated if such disturbances can be estimated.

For instant, a nearly constant disturbance (w_i) can be modelled as a linear system [44] driven by white noise (ν_i) as

$$\dot{w}_i = A_{iw} w_i + \nu_i \tag{4.1}$$

The dynamic of the disturbance is then integrated with that of the system in eq. (3.1) which results in an augmented system as

$$\begin{bmatrix} \dot{x}_i \\ \dot{w}_i \end{bmatrix} = \begin{bmatrix} A_i & B_{iw} \\ 0 & A_{iw} \end{bmatrix} \begin{bmatrix} x_i \\ w_i \end{bmatrix} + \begin{bmatrix} B_{iu} \\ 0 \end{bmatrix} u_i + \begin{bmatrix} 0 \\ \nu_i \end{bmatrix} \tag{4.2}$$

where the output is given by

$$y_i = \begin{bmatrix} C_i & 0 \end{bmatrix} \begin{bmatrix} x_i \\ w_i \end{bmatrix} \tag{4.3}$$

With use of a Kalman filter, above states and disturbances can be estimated if the measured outputs results in an observable system, and the variance of the white noise is known.

According to the above system, an optimization criterion in terms of the quadratic integral form expressed in (4.4) becomes the objective of the optimal control design.

$$\int_{t_o}^{t_1} \left[y_i^T(t) Q_i y_i(t) + u_i^T(t) \Re_i u_i(t) \right] dt + x_i^T(t_1) P_1 x_i(t) \tag{4.4}$$

where Q_i and $\Re_i$ are positive definite matrices, and P_1 is nonnegative definite symmetric.

For a given input $u_i(t)$ and realization of the disturbances $\nu_i(t)$ from t_0 to t_1, the criterion is a measure for the deviations of $y_i(t)$ and $u_i(t)$ from zero. However, this criterion cannot be directly measured due to the stochastic behavior of the disturbances. Consequently, the average over any possible realizations of the disturbances is considered instead [45], which is referred to

as the stochastic linear optimal regulator problem.

$$E\left\{\int_{t_o}^{t_1}\left[y_i^T(t)\,Q_i y_i(t)+u_i^T(t)\,\Re_i u_i(t)\right]dt+x_i^T(t_1)\,P_1 x_i(t)\right\} \tag{4.5}$$

The solution of the classical linear quadratic regulator problem is deterministic and well known. However, [45] gives the proof that the presence of white noise (ν_i) in the system equation (4.6) does not change the solution other than increasing the minimal value of the criterion.

$$\dot{x}_i = A_i x_i + B_{iu} u_i + \nu_i \tag{4.6}$$

where ν_i is white noise with intensity $V(t)$. The initial state x_{i0} is a stochastic variable and independent of white noise ν_i, with

$$E\left\{x_{i0}x_{i0}^T\right\} = Q_0 \tag{4.7}$$

and its optimal solution is given as

$$u_i(t) = -K_i(t)\,x_i(t) \tag{4.8}$$

where

$$K_i(t) = \Re_i^{-1} B_{iu}^T P(t). \tag{4.9}$$

At $P(t)$ is the solution of the Riccati equation

$$-\dot{P}(t) = C_i^T Q_i C_i - P(t)\,B_{iu}\Re_i^{-1}B_{iu}^T P(t) + A_i^T P(t) + P(t)\,A_i \tag{4.10}$$

with the final condition

$$P(t_1) = P_1. \tag{4.11}$$

Finally, the minimal value of the criterion is obtained by

$$tr\left[P(t_0)\,Q_0 + \int_{t_0}^{t_1} P(t)\,V(t)\,dt\right] \tag{4.12}$$

The above control design is then applied to solve the stochastic LQR problem for the augmented system (4.2). To accommodate the augmented states

$$\tilde{x}_i = \begin{bmatrix} x_i \\ w_i \end{bmatrix}, \tag{4.13}$$

the solution $P(t)$ of the Riccati equation is partitioned as

$$P(t) = \begin{bmatrix} P_{11}(t) & P_{12}(t) \\ P_{12}^T(t) & P_{22}(t) \end{bmatrix}. \tag{4.14}$$

Hence, this procedure results in partitioning the feedback gain as

$$K_i(t) = \begin{bmatrix} K_{ix}(t) & K_{iw}(t) \end{bmatrix} \tag{4.15}$$

where

$$K_{ix}(t) = \Re_i^{-1} B_{iu}^T P_{11}(t) \tag{4.16}$$

and

$$K_{iw}(t) = \Re_i^{-1} B_{iu}^T P_{12}(t). \tag{4.17}$$

The above feedback gains are obtained by partitioning the matrix Riccati equation, so that P_{11}, P_{12}, and P_{22} are the solutions of the following differential equations.

$$\begin{cases} -\dot{P}_{11}(t) = C_i^T Q_i C_i - P_{11}(t) B_{iu} \Re_i^{-1} B_{iu}^T P_{11}(t) + A_i^T P_{11}(t) + P_{11}(t) A_i \\ P_{11}(t_1) = P_1 \end{cases} \tag{4.18}$$

$$\begin{cases} -\dot{P}_{12}(t) = P_{11}(t) B_{iw} + [A - B_{iu} K_{ix}]^T P_{12}(t) + P_{12}(t) A_{iw} \\ P_{12}(t_1) = 0 \end{cases} \tag{4.19}$$

$$\begin{cases} -\dot{P}_{22}(t) = -P_{12}^T(t) B_{iu} \Re_i^{-1} B_{iu}^T P_{12}(t) + B_{iw}^T P_{12}(t) + P_{12}^T(t) B_{iw} + A_{iw}^T P_{22}(t) + P_{22}(t) A_{iw} \\ P_{22}(t_1) = 0 \end{cases} \tag{4.20}$$

Finally, the proposed LFC controller, using the Kalman filter to estimate states and disturbances is illustrated in Figure 4.1. This control design is based on stochastic linear quadratic regulator technique and is completely decentralized. With the known system and approximate disturbance models expressed by eq. (4.2), the Kalman filter can estimate all states as well as disturbances accurately if the chosen variances of the fictitious white noises (ν_i) driving the disturbance model in eq. (4.1) are appropriate. The feedback gains are then designed based on LQR technique. The controller characteristic is tailored by choosing the appropriate weighing matrices Q_i and $\Re_i$ in the criterion (4.5).

To illustrate the effectiveness of this proposed control design, a decentralized controller is designed for each control area of a three-area power system as shown in Figure 4.2. Each control

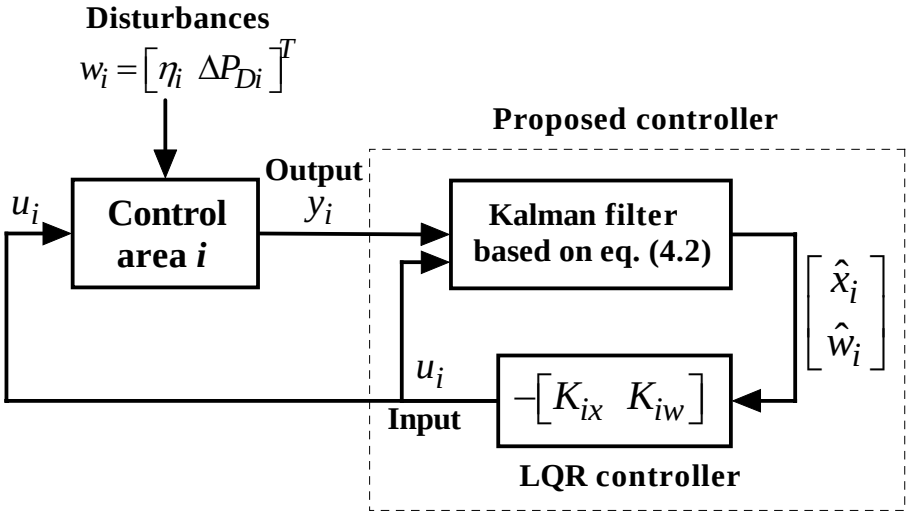

Figure 4.1: An LQR controller based on disturbance modeling using a Kalman filter.

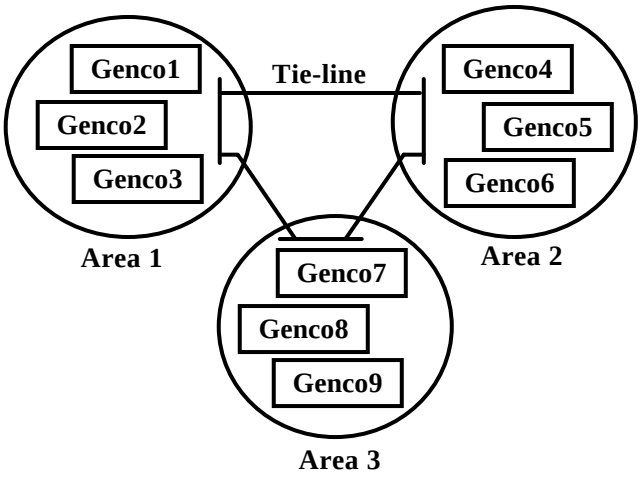

Figure 4.2: A three-area power system.

Table 4.1: Numerical parameters of generating units

Parameters	**Genco**								
MVA_{base} (1000 MW)	1	2	3	4	5	6	7	8	9
Rate (MW)	1000	800	1000	1100	900	1200	850	1000	1020
D (pu/Hz)	0.0150	0.0140	0.0150	0.0160	0.0140	0.0140	0.0150	0.0160	0.0150
T_P (pu.sec)	0.1667	0.1200	0.2000	0.2017	0.1500	0.1960	0.1247	0.1667	0.1870
T_T (sec)	0.4	0.36	0.42	0.44	0.32	0.40	0.30	0.40	0.41
T_H (sec)	0.08	0.06	0.07	0.06	0.06	0.08	0.07	0.07	0.08
R (Hz/pu)	3.00	3.00	3.30	2.7273	2.6667	2.50	2.8235	3.00	2.9412
B (pu/Hz)	0.3483	0.3473	0.3180	0.3827	0.3890	0.4140	0.3692	0.3493	0.3550
α	0.4	0.4	0.2	0.6	0	0.4	0	0.5	0.5
Ramp rate (MW/min)	8	8	4	12	0	8	0	10	10

area has three generation companies (Genco) providing generated power to balance the demand. All parameters of generating units are tabulated as shown in Table 4.1.

Subsequently, the obtained controllers are tested with a step load change in each area as follows: $\Delta P_{D1} = 100$ MW, $\Delta P_{D2} = 80$ MW and $\Delta P_{D3} = 50$ MW. A desired control performance can be achieved by choosing appropriate weighting matrices Q_i and $\Re_i$, which need to be positive definite. For this system, the measured outputs (y_i) are the frequency deviation, net interchange error, and integral of ACE as expressed by eq. (4.21). The Kalman filter utilizes those measurements in estimating the states that are used as the inputs of the LFC controller.

$$y_i = \begin{bmatrix} \Delta f_i \\ \Delta P_{tie_i} \\ \int ACE_i \end{bmatrix} \tag{4.21}$$

Further, the dynamic responses of the load frequency controllers are illustrated through nonlinear simulation. Figures 4.3, 4.4 and 4.5 present the area control error (ACE), frequency deviation (Δf), and governor load setpoint (ΔP_C) of Areas 1, 2 and 3 respectively.

From simulation results, the area control error and frequency deviation of all areas are quickly driven back to zero, which indicates a good balance between generated power and load. The governor load setpoints of generating units are adjusted by the controllers to reach such a balancing. Therefore, it can be concluded that a decentralized control scheme based on interface modeling is effective and well suited for load frequency control applications.

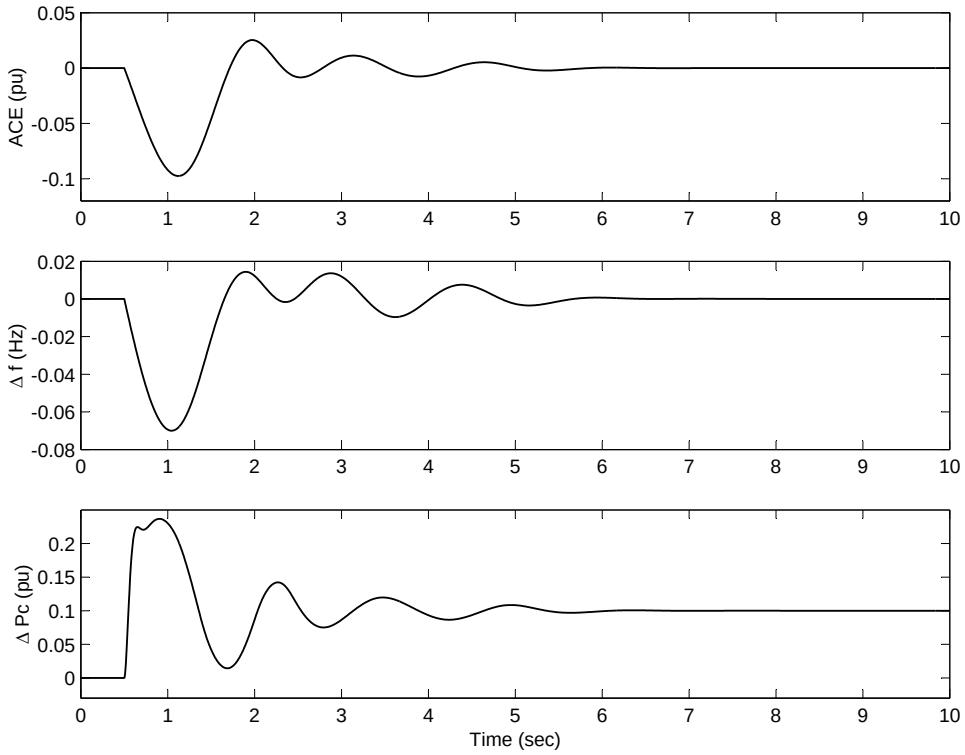

Figure 4.3: Area 1: ACE, frequency deviation and governor load setpoint.

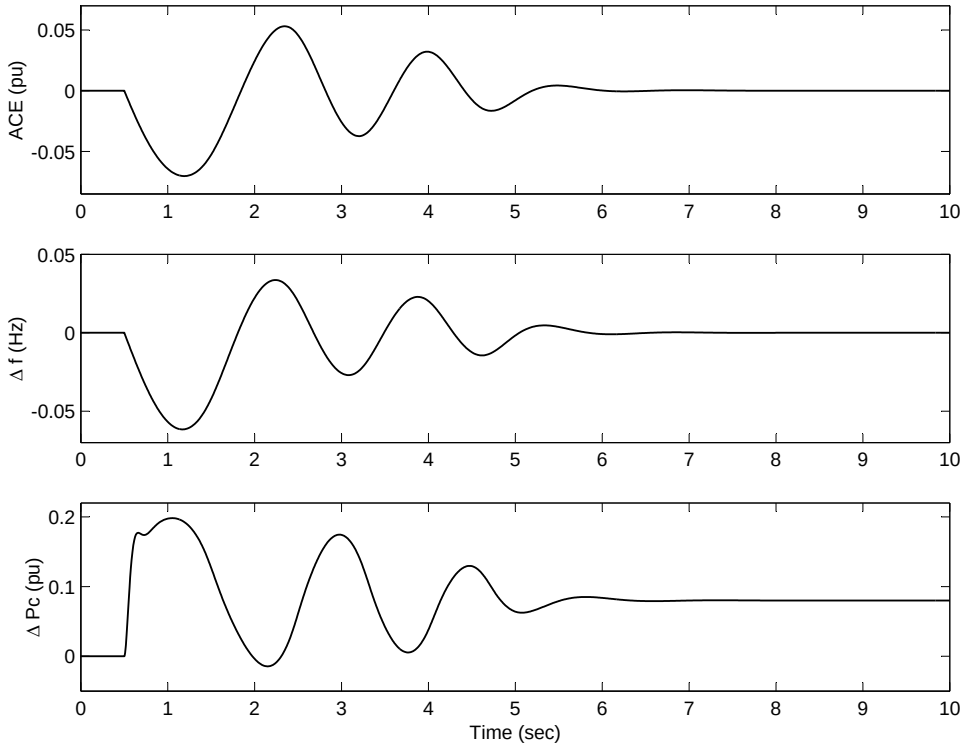

Figure 4.4: Area 2: ACE, frequency deviation and governor load setpoint.

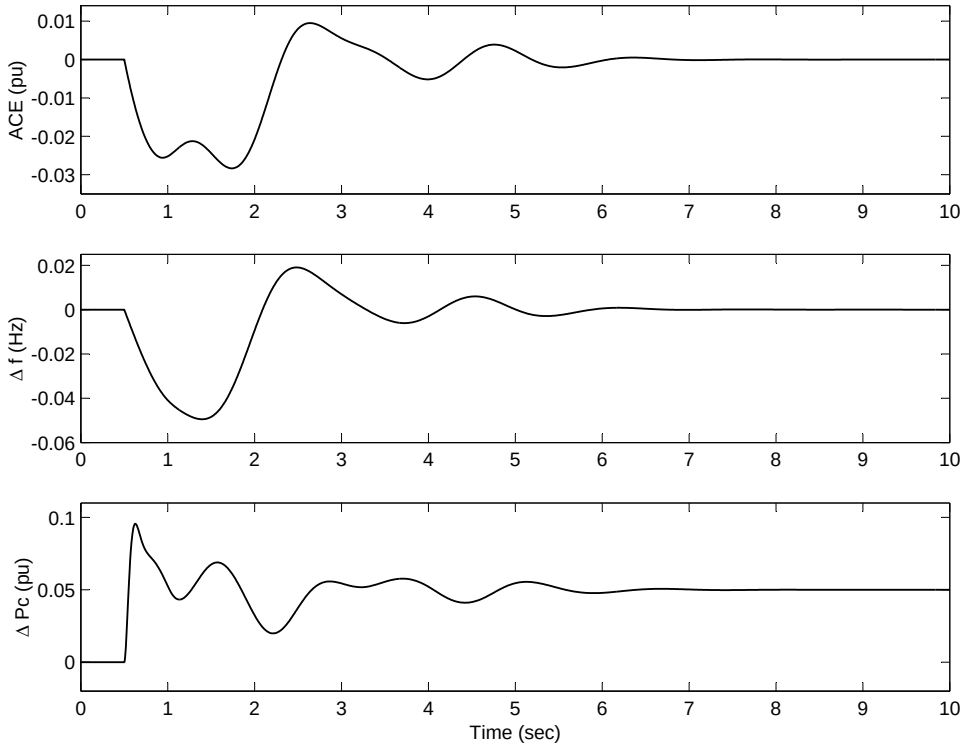

Figure 4.5: Area 3: ACE, frequency deviation and governor load setpoint.

4.2 Decentralized robust H_∞ load frequency control

In the previous section, the interface variable was treated as a disturbance, which is subsequently observed by the Kalman filter. The decentralized LQR based controller then feeds back the estimates of states and disturbances to regulate the controlled variables.

In this section, the robust H_∞ control design is proposed to solve the decentralized load frequency control problem. Similar to the previous control design, this robust control technique treats the interface as a disturbance, but it tends to minimize the worst-case disturbance effects on the controlled variables rather than using it as the feedback variables.

Over the past two decades, robust control theory has been useful as applied to control system designs that require robustness against possible disturbances such as parameter uncertainties, system modeling errors, plant and measurement noises, and external disturbances.

One major objective of robust control is to synthesize a controller that will guarantee the internal stability of the system when bounded perturbations are present. This proposed control design is different from other previous work. Specifically, the control design is casted into a linear matrix inequality (LMI) formulation, so that the powerful LMI control toolbox can be used to solve the constrained optimization problem to achieve the desired robustness [47].

Here, the robust H_∞ control theory is adopted to design a decentralized controller for load frequency control. This well-known approach provides the closed-loop system with robustness against bounded uncertainties. According to the decentralized LFC problem, the area interface (η) is considered as a bounded disturbance. Hence it can be handled by the proposed technique.

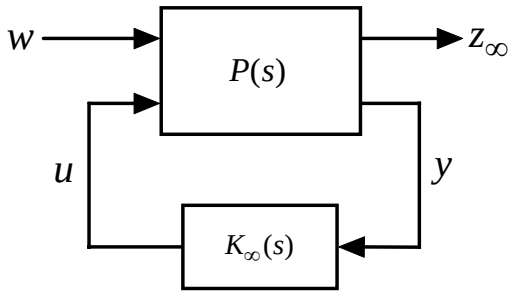

Figure 4.6: Close-loop system via robust H_∞ control.

Fig. 4.6 shows a classical block diagram of the robust H_∞ control problem. The objective is to

design a control law u based on the measured variables y such that the effects of the disturbance w on the controlled variables z_∞, as expressed by the infinity norm of its transfer function $\|T_{z_\infty w}\|_\infty$, do not exceed a given value, γ, defined as guaranteed robust performance. In order to synthesize an H_∞ controller via LMI approach, state space realizations of the system *P(s)* and controller $K_\infty(s)$ are needed. They are given by eq. (4.22) and eq. (4.23) respectively.

State Space System Model

$$\begin{aligned} \dot{x} &= Ax + B_1 w + B_2 u \\ z_\infty &= C_\infty x + D_{\infty 1} w + D_{\infty 2} u \\ y &= C_y x + D_{y1} w \end{aligned} \tag{4.22}$$

(A, B_2) is stabilizable, and (A, C_y) is detectable.

State Space Controller Model

$$\begin{aligned} \dot{\zeta}_\infty &= A_{k\infty}\zeta_\infty + B_{k\infty} y \\ u &= C_{k\infty}\zeta_\infty + D_{k\infty} y \end{aligned} \tag{4.23}$$

Combining the above equations results in the following closed-loop system:

$$\begin{aligned} \dot{x}_{cl} &= A_{cl} x_{cl} + B_{cl} w \\ z_\infty &= C_{cl1} x_{cl} + D_{cl1} w \end{aligned} \tag{4.24}$$

where

$$x_{cl} = \begin{bmatrix} x \\ \zeta_\infty \end{bmatrix}, \; A_{cl} = \begin{bmatrix} A + B_2 C_{k\infty} C_y & B_2 C_{k\infty} \\ B_{k\infty} C_y & A_{k\infty} \end{bmatrix}$$

$$B_{cl} = \begin{bmatrix} B_1 + B_2 C_{k\infty} D_{y1} \\ B_{k\infty} D_{y1} \end{bmatrix}$$

$$C_{cl1} = \begin{bmatrix} C_\infty + D_{\infty 2} D_{k\infty} C_y & D_{\infty 2} C_{k\infty} \end{bmatrix}$$

$$D_{cl1} = D_{\infty 1} + D_{\infty 2} D_{k\infty} D_{y1}$$

The following lemma [46] relates H_∞ control design to LMI.

Lemma1: *the closed-loop RMS gain or H_∞ norm of the transfer function from w to z_∞, $\|T_{z_\infty w}\|_\infty$, does not exceed γ, if and only if there exists a symmetric matrix X_∞ such that*

$$\begin{bmatrix} A_{cl}X_\infty + X_\infty A_{cl}^T & B_{cl} & X_\infty C_{cl1}^T \\ B_{cl}^T & -I & D_{cl1}^T \\ C_{cl1}X_\infty & D_{cl1} & -\gamma^2 I \end{bmatrix} < 0 \tag{4.25}$$

$$X_\infty > 0 \tag{4.26}$$

An optimal H_∞ control design can be achieved by minimizing the guaranteed robust performance index, γ, subject to the constraints given by the matrix inequalities (4.25) and (4.26). The MATLAB's LMI control toolbox provides the function "hinflmi" to solve an H_∞ control problem directly. This function returns the controller parameters, $K_\infty(s)$, as shown in (4.23) with the optimal robust performance index γ^*. The obtained controller is a dynamic type, whose order is the size of the system matrix.

In section 4.3, the performance of the proposed H_∞ controllers will be illustrated through the simulation results of the three-area power system given in section 4.1 with a variety of disturbances. In fact, the main purpose is to compare the results with those of the GALMI based PI controllers presented in the following section.

4.3 Decentralized robust load frequency control using GALMI

This section proposes a novel decentralized robust control design, which is developed in favor of practicality in terms of controller implementation. This control design allows designers to customize a feasible feature of the controller such as state or output feedback, and number of order if a dynamic type is needed. It is fully suitable for load frequency control applications which commonly employ the proportional-integral (PI) control, while the other control designs yield observer-based controllers whose size can be large for real-world power systems.

The concept of this control design lies in the cooperation of genetic algorithms (GAs) and linear matrix inequalities (LMIs). More specifically, this so called GALMI control design uses genetic algorithms (GAs) to search for the best control parameters for the PI controller subject to the robust H_∞ control constraints in terms of LMIs as (4.25) and (4.26), which are solved by the LMI control toolbox. The objective is to acquire a good property of the H_∞ control that promises system robustness against bounded uncertainties under the PI control structure.

Here, the proposed control design will be used for the PI controller in Figure 3.3. The area control error (ACE_i) signal is used as the input of the controller. However, the state space model

given in eq. (3.1) includes the frequency deviation (Δf_i), tie-line power error (ΔP_{tie_i}), and the integral of the ACE ($\int ACE_i$) as a portion of the states (x_i). They can form the system output (y_i) as follows.

$$y_i = \begin{bmatrix} ACE_i \\ \int ACE_i \end{bmatrix} = C_i x_i \tag{4.27}$$

where

$$ACE_i = B_i \Delta f_i + \Delta P_{tie_i} \tag{4.28}$$

Unlike the dynamic controller presented in section 4.2, a static output feedback controller is designed to be used as the PI controller, while conserving the good robust performance of the H_∞ controller whose controlled variable is given as

$$z_{i\infty} = C_{i\infty} x_i + D_{i\infty} u_i \tag{4.29}$$

where $C_{i\infty}$ and $D_{i\infty}$ are robust weighing factors which penalize the states and inputs based on the objective of control design.

The PI control law (u_i) with proportional (K_{Pi}) and integral (K_{Ii}) gains can be expressed as

$$u_i = \Delta P_{Ci} = K_{Pi} ACE_i + K_{Ii} \int ACE_i \tag{4.30}$$

$$u_i = [K_{Pi} \;\; K_{Ii}] \begin{bmatrix} ACE_i \\ \int ACE_i \end{bmatrix} \tag{4.31}$$

$$u_i = K_i y_i \tag{4.32}$$

From the above equations, the desired controller is only a simple static output feedback controller and is much less complex than the one obtained from the conventional H_∞ control design shown in eq. (4.23). To determine the control parameter vector (K_i), eq. (4.27) is first substituted into eq. (4.32), which results in eq. (4.33). Next, (4.33) is substituted into eq. (3.1) and (4.29), and the closed-loop system is finally obtained as eq. (4.34).

$$u_i = K_i C_i x_i \tag{4.33}$$

$$\begin{aligned} \dot{x}_i &= A_{cl} x_i + B_{cl} w_i \\ z_{i\infty} &= C_{cl1} x_i + D_{cl1} w_i \end{aligned} \tag{4.34}$$

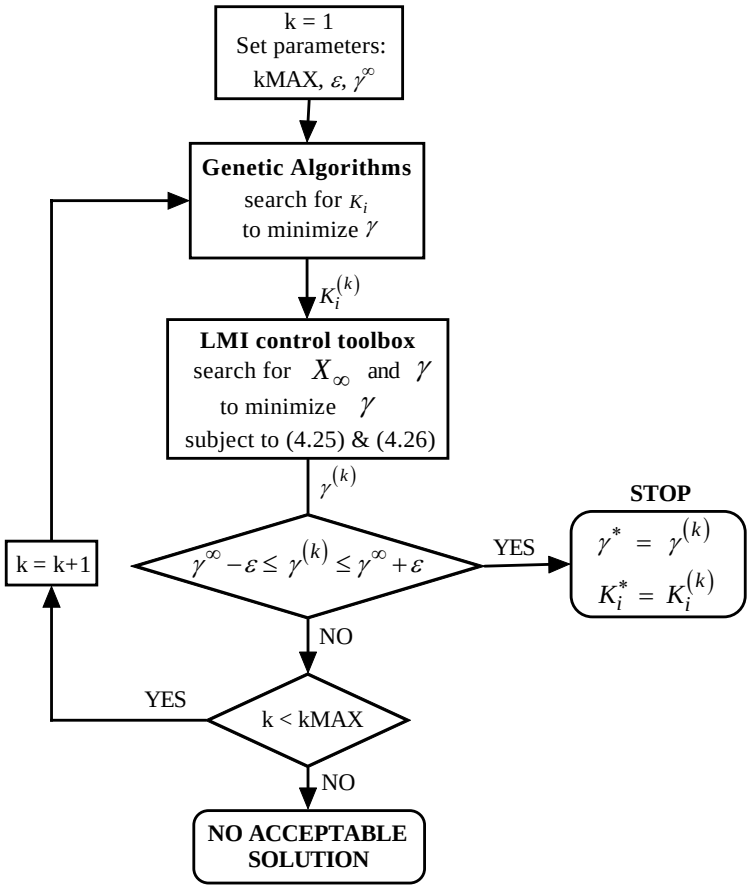

Figure 4.7: Robust control design via GALMI optimization.

where

$$A_{cl} = A_i + B_{iu}K_iC_i, \quad B_{cl} = B_{iw}$$
$$C_{cl1} = C_{i\infty} + D_{i\infty}K_iC_i, \; D_{cl1} = [\underline{0}]$$

Subsequently, K_i is searched for in order to minimize the performance index, γ, subject to robust control constraints given by matrix inequalities (4.25) and (4.26). However, a solution of the consequent nonconvex constrained optimization problem cannot be achieved by using LMI techniques alone. Therefore, the proposed genetic algorithm (GA) optimization technique is utilized to search for the control parameters (K_i) of the PI load frequency controller at the upper level, whereas the LMI control toolbox is used at the lower level to solve the linear matrix inequalities given as constraints for robust H_∞ control design. The algorithm that describes the

Table 4.2: Robust performance index

Control Design	γ_{area1}	γ_{area2}	γ_{area3}	Control Structure
GALMI	500.0090	500.0085	500.0086	PI
H_∞	500.0152	500.1470	500.0183	9^{th} order

GALMI optimization is shown in Figure 4.7. The parameter kMAX is the maximum number of iterations. While the number of iterations (k) is less than kMAX, the optimization routine continues to search for the robust PI parameters unless the current robust performance index ($\gamma^{(k)}$) is found close enough to the robust performance index (γ^{∞}) resulting from the H_∞ control design. In this case, the optimization routine is terminated earlier, and the current PI parameters ($K_i^{(k)}$) become the solution of this optimization. These PI parameters (K_i^*) yield the robust performance as good as that obtained from the H_∞ control design.

The same test system as given in Figure 4.2, consists of three control areas. Each area has three generating units that are owned by different generation companies (Gencos). Two types of robust decentralized load frequency controllers, 1) robust H_∞ control, designed according to the procedure described in section 4.2, and 2) robust GALMI tuned PI control, designed based on the proposed GALMI algorithm presented in this section, are implemented in each area. The obtained robust performance indices (γ) of both designs are almost identical as shown in Table 4.2. These results show no degradation on the GALMI tuned PI control design. However, its structure is much simpler than the robust H_∞ design, whose order is the number of system states (or the size of A_i) that increases with the modeling details and the number of units, and it can be very large. In this section, the performance of the robust PI controllers is compared with that of the dynamic H_∞ controllers for three scenarios of load disturbances.

For Scenario 1, random load changes, shown in Figure 4.8(a), representing expected load fluctuations, are applied to the three control areas. The area control error (ACE), frequency deviation (Δf), and governor load setpoint (ΔP_C) closed-loop responses are shown in Figure 4.8(b)-4.8(d). From the results, both controllers effectively ramp generated power to match the load fluctuations. The performance of the GALMI tuned PI controllers is almost identical to that of full order H_∞ controllers. In addition, Figure 4.9 shows the raise/lower signals allocated to all generating units in Area 1 conforming to their offered ramp rates.

For Scenario 2, a large disturbance, a step increase in demand, is applied to each area: ΔP_{D1} = 100 MW, ΔP_{D2} = 80 MW, and ΔP_{D3} = 50 MW. The purpose of this scenario is to test the

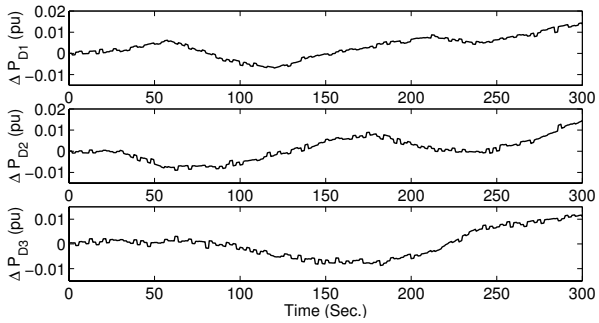

(a) Load changes for Scenario1

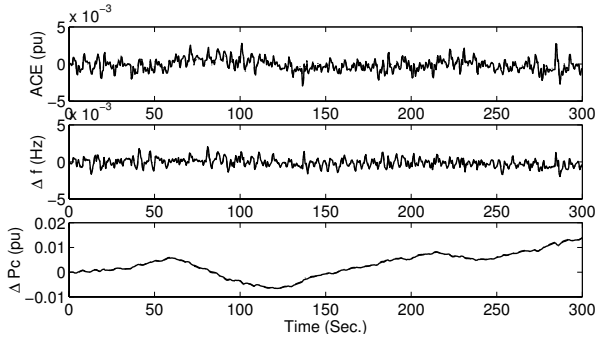

(b) Area 1

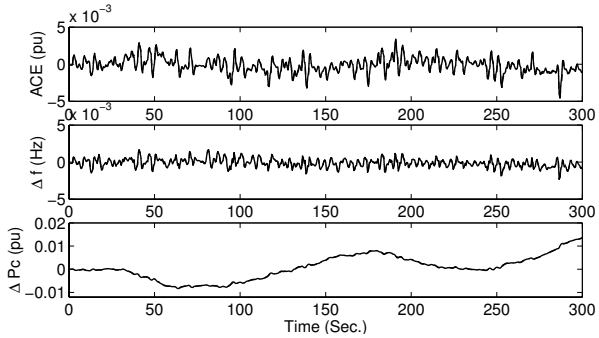

(c) Area 2

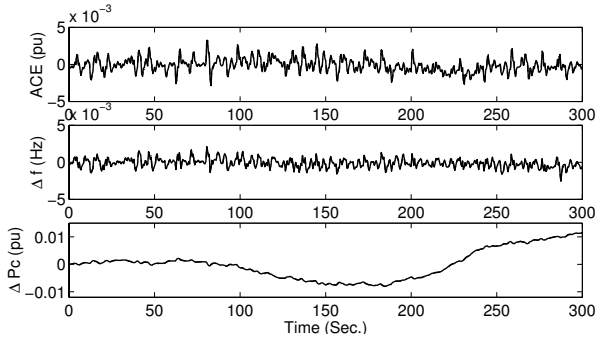

(d) Area 3

Figure 4.8: System response for Scenario 1. Solid (GALMI), Dash-dotted (H_∞)

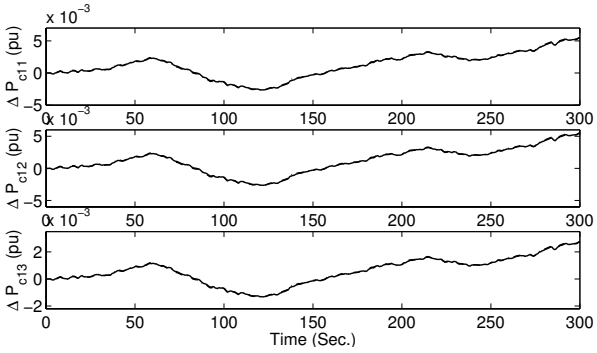

Figure 4.9: Raise/lower signals of units in area1. Solid (GALMI), Dash-dotted (H_∞)

robustness of the proposed controllers against large disturbances. In fact, these large step changes in demand rarely occur since a party which causes a serious mismatch between actual and forecast load is likely to be penalized. Figure 4.10(a), 4.10(b) and 4.10(c) show the responses of Areas 1, 2 and 3 respectively. The ACE and frequency deviation (Δf) are effectively damped to zero with very small oscillations by the GALMI tuned PI controllers. The control input (ΔP_C) is also smoothly increased to the expected value without overshoot or oscillations. These controllers perform as well as the robust H_∞ controllers. The above step changes in power demand are considered significant because of the large overshoot (0.1 Hz) in the frequency deviations.

For Scenario 3, large step increases in demand are applied to Areas 2 and 3: $\Delta P_{D2} = 100$ MW, and $\Delta P_{D3} = 50$ MW. To make the scenario drastic, it is assumed that LFC reset controllers of Areas 2 and 3 are out of service. As a result, the frequency deviation of all areas cannot be driven to zero, which causes the area interface (η), treated as a system disturbance, to remain nonzero all the time. The purpose of the scenario is to investigate the response of the system to such a severe condition, when only Area 1 proposed LFC controller is kept active. The responses of Area 1, given in Figure 4.11(a), show that the ACE is driven to zero successfully, and the governor load setpoint has very small oscillations during the transient phase and goes back to zero in a very short time. The response of the governor load setpoint of GALMI tuned PI controller is slightly degraded compared with that of the H_∞ controller. This is because the H_∞ controller is a high order dynamic controller, with an order as large as the number of states of the system. In this case, the H_∞ controller is of 9^{th} order, but the GALMI controller is a simple PI controller. Incidentally, the responses of the ACE and frequency deviation of the H_∞ and GALMI tuned PI controllers are almost the same. In addition, the responses of Areas 2 and 3 are shown in

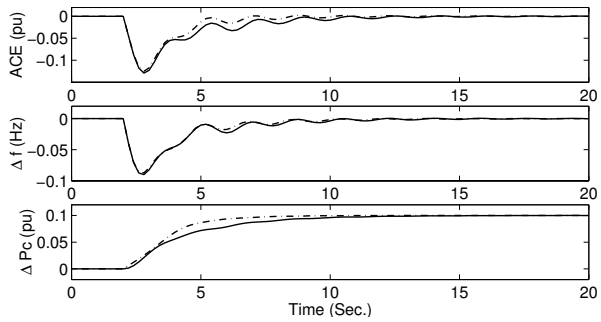

(a) Area 1

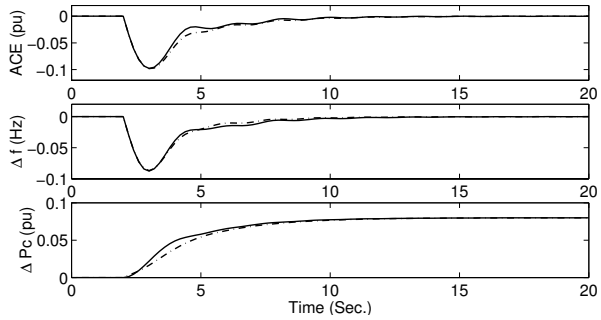

(b) Area 2

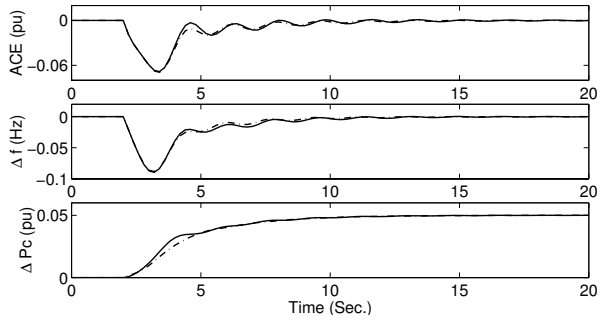

(c) Area 3

Figure 4.10: System response for Scenario 2. Solid (GALMI), Dash-dotted (H_∞)

Figure 4.11(b) and 4.11(c). Without the LFC controller, the ACE of both areas cannot be driven back to zero.

In this section, the proposed GALMI technique coordinates genetic algorithms with the LMI control toolbox optimization in order to obtain the control parameters, K_P and K_I, of a traditional PI controller that satisfies the robust H_∞ constraints. A three-area power system is used as the test system with three scenarios of load disturbances. Finally, the simulation results show that the responses of GALMI tuned PI load frequency controllers are almost the same as those of the robust H_∞ controllers, which have effective control performance and robustness against possible disturbances.

4.4 Global stability analysis

Previously, the decentralized control designs for load frequency control were illustrated. The resulting controllers require only local measurements which guarantee a decentralized control scheme. In addition, they have been tested with different power systems under a variety of contingencies, and yield impressive results. Nevertheless, the dynamic stability of the entire power system while all decentralized controllers are in use has not yet been fully analyzed. Therefore, this section will perform a global stability analysis for the proposed control designs.

4.4.1 Perturbation theory of eigenvalues

In more detail, a large interconnected power system is considered as a number of decoupled subsystems or control areas where area interfaces are treated as area disturbances. Although a decentralized controller of each area can handle such a disturbance from a local point of view, the effect of area interconnections still remain from the point of view of the global system. The question arises as to whether or not decentralized controllers can compensate for such an effect.

The above interconnection effect is considered as the perturbation (E), while the diagonal matrix (A_{cl}) is composed of decoupled closed-loop subsystems as expressed by eq. (4.35). This matrix is also called *ideal system matrix*, as in this dissertation. The addition of the ideal system

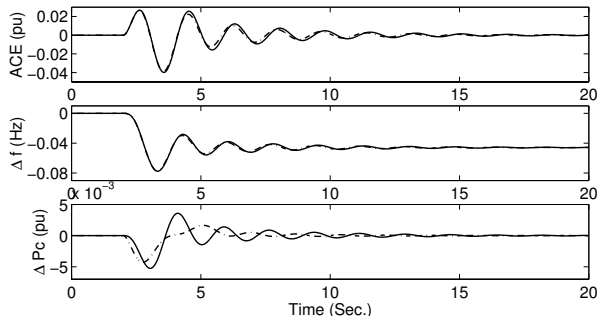

(a) Area 1

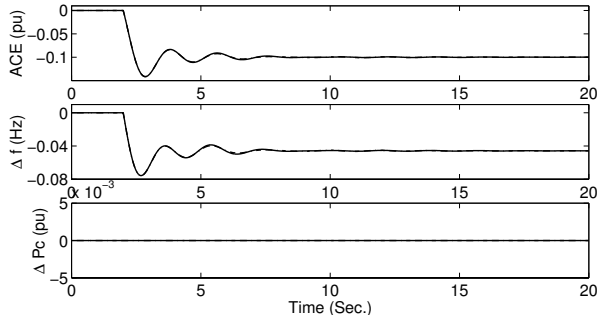

(b) Area 2

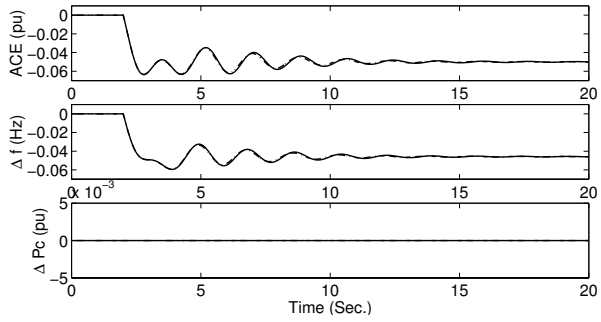

(c) Area 3

Figure 4.11: System response for Scenario 3. Solid (GALMI), Dash-dotted (H_∞)

matrix and its perturbation yields the *actual closed-loop system matrix* ($\tilde{A}_{cl}$) as given by eq. (4.36).

$$A_{cl} = \begin{bmatrix} A_{cl,1} & & & 0 \\ & A_{cl,2} & & \\ & & \ddots & \\ 0 & & & A_{cl,N} \end{bmatrix} \tag{4.35}$$

$$\tilde{A}_{cl} = A_{cl} + E \tag{4.36}$$

Perturbation theory with regard to eigenvalues is a key issue in evaluating the stability of the actual closed-loop system [55],[56],[57]. An objective is to determine the perturbation bound of the system eigenvalues, which is used to bound the displacement ($\left|\tilde{\lambda} - \lambda\right|$) of the ideal system eigenvalues (λ) caused by the perturbation (E), where $\tilde{\lambda}$ represents the eigenvalues of the actual closed-loop system.

According to investigation, conventional perturbation theories such as Bauer-Fike theorem and Gerschgorin's theorem, provide very conservative bounds. The resulting bounds are unreasonably large, so the stability of most closed-loop systems cannot be concluded. Nevertheless, for a special structure where a system matrix (A_{cl}) is almost diagonal, Theorem 4.1 can result in sharper perturbation bounds.

Theorem 4.1. *Let λ be a simple eigenvalue of the matrix A, with right and left eigenvectors x and y, and let $\tilde{A} = A+E$ be a perturbation of A. Then there is a unique eigenvalue $\tilde{\lambda}$ of $\tilde{A}$ such that* [55]

$$\tilde{\lambda} = \lambda + \frac{y^H E x}{y^H x} + O\left(\varepsilon^2\right) \tag{4.37}$$

Proof. Define $\tilde{x}$ = x+δx and $\tilde{\lambda} = \lambda + \delta\lambda$ to be an eigenvector and eigenvalue of $\tilde{A}$ corresponding to $\tilde{\lambda}$.

Therefore,

$$\tilde{A}\tilde{x} = \tilde{\lambda}\tilde{x} \tag{4.38}$$

$$(A+E)(x+\delta x) = (\lambda + \delta\lambda)(x+\delta x) \tag{4.39}$$

Expand both sides of eq. (4.39):

$$Ax + A\delta x + Ex + E\delta x = \lambda x + \lambda\delta x + \delta\lambda x + \delta\lambda\delta x \tag{4.40}$$

Disregard the second order terms $E\delta x$ and $\delta\lambda\delta x$, and note that $Ax = \lambda x$:

$$A\delta x + Ex = \lambda\delta x + \delta\lambda x + O\left(\varepsilon^2\right) \tag{4.41}$$

Next, multiply eq. (4.41) by y^H:

$$y^H A\delta x + y^H Ex = y^H \lambda \delta x + y^H \delta\lambda x + O\left(\varepsilon^2\right) \tag{4.42}$$

$$y^H Ex = \delta\lambda y^H x + O\left(\varepsilon^2\right) \tag{4.43}$$

Finally,

$$\delta\lambda = \frac{y^H Ex}{y^H x} + O\left(\varepsilon^2\right) \tag{4.44}$$

$$\tilde{\lambda} = \lambda + \frac{y^H Ex}{y^H x} + O\left(\varepsilon^2\right) \tag{4.45}$$

Q.E.D.

The $\delta\lambda$ in eq. (4.44) is the estimated displacement of λ after the system matrix (A) is perturbed. In addition, the condition number, $cond(\lambda)$, as given in eq. (4.46) is used to indicate the sensitivity of the eigenvalue (λ) to the perturbation. A large condition number indicates that the corresponding eigenvalue would be displaced far away from its initial position by a perturbation. Subsequently, a perturbation bound (B_P) can be determined by multiplying eq. (4.46) by the norm of the perturbation as expressed in eq. (4.47).

$$cond\left(\lambda\right) = \frac{\|y\| \cdot \|x\|}{|y^H x|} \tag{4.46}$$

$$B_P = \frac{\|y\| \cdot \|x\|}{|y^H x|} \|E\| \tag{4.47}$$

The resulting perturbation bounds are shaper than ones obtained from other methods. Nevertheless, it would make less sense to use only these bounds as a criterion to judge the system stability. A new indicator named "departure angle" is introduced in this dissertation to enhance the analysis of eigenvalue sensitivity. The departure angle (ϕ_d) is the angle of eigenvalue that departs from its original location to a new one. It is specially helpful when a perturbation bound turns out to be large, and overlaps the right-half plane (RHP). In this case, the departure angle can reshape the bound, frequently removing the overlap. An example will be illustrated as a case study given in section 4.4.2.

4.4.2 Case study

To perform the stability analysis, the three-area power system equipped with the robust PI controllers described in section 4.3 is used as a case study. Nevertheless, it is not straightforward

to formulate the system (A) and perturbation (E) matrices mentioned in the previous section. To convey this work to readers, the formulation algorithm is given as follows.
According to eq. (3.1), the dynamic model of area i is expressed as:

$$\dot{x}_i = A_i x_i + B_{iu} u_i + B_{iw} w_i \tag{4.48}$$

The disturbance portion $B_{iw} w_i$ is decomposed into two terms.

$$\dot{x}_i = A_i x_i + B_{iu} u_i + G_i \eta_i + H_i \Delta P_{Di} \tag{4.49}$$

Since $\eta_i = \sum_{\substack{j=1 \\ j \neq i}}^{N} T_{ij} \Delta f_j$, it can be rewritten as:

$$\eta_i = \sum_{\substack{j=1 \\ j \neq i}}^{N} T_{ij} S_j x_j \tag{4.50}$$

where $S_j = \begin{bmatrix} 1 & 0 & 0 & \cdots & 0 \end{bmatrix}$ with its number of columns equal to the size of area j.
Here, the composite system of all areas can be expressed as:

$$\dot{x} = Ax + Bu + H\Delta P_D \tag{4.51}$$

$$y = Cx \tag{4.52}$$

$$u = Ky \tag{4.53}$$

where

$$x = \begin{bmatrix} x_1^T & x_2^T & \cdots & x_N^T \end{bmatrix}^T, \quad u = \begin{bmatrix} u_1 & u_2 & \cdots & u_N \end{bmatrix}^T, \quad y = \begin{bmatrix} y_1^T & y_2^T & \cdots & y_N^T \end{bmatrix}^T$$

$$\Delta P_D = \begin{bmatrix} \Delta P_{D1} & \Delta P_{D2} & \cdots & \Delta P_{DN} \end{bmatrix}^T, \qquad G_{ij} = G_i T_{ij} S_j$$

$$A = \begin{bmatrix} A_1 & G_{12} & \cdots & G_{1N} \\ G_{21} & A_2 & & G_{2N} \\ \vdots & & \ddots & \vdots \\ G_{N1} & G_{N2} & \cdots & A_N \end{bmatrix}, \quad B = \begin{bmatrix} B_{1u} & 0 & \cdots & 0 \\ 0 & B_{2u} & & \vdots \\ \vdots & & \ddots & 0 \\ 0 & \cdots & 0 & B_{Nu} \end{bmatrix}$$

$$C = \begin{bmatrix} C_1 & 0 & \cdots & 0 \\ 0 & C_2 & & \vdots \\ \vdots & & \ddots & 0 \\ 0 & \cdots & 0 & C_N \end{bmatrix}, \quad K = \begin{bmatrix} K_1 & 0 & \cdots & 0 \\ 0 & K_2 & & \vdots \\ \vdots & & \ddots & 0 \\ 0 & \cdots & 0 & K_N \end{bmatrix}$$

Meanwhile, the ideal system disregarding interconnection effects (G_{ij}) are given as:

$$A_{ideal} = \begin{bmatrix} A_1 & 0 & \cdots & 0 \\ 0 & A_2 & & \vdots \\ \vdots & & \ddots & 0 \\ 0 & \cdots & 0 & A_N \end{bmatrix} \tag{4.54}$$

and the perturbation matrix (E) that represents interconnection effects is defined as:

$$E = \begin{bmatrix} 0 & G_{12} & \cdots & G_{1N} \\ G_{21} & 0 & & G_{2N} \\ \vdots & & \ddots & \vdots \\ G_{N1} & G_{N2} & \cdots & 0 \end{bmatrix} \tag{4.55}$$

As a result, they can be related as:

$$A = A_{ideal} + E \tag{4.56}$$

Finally, the closed-loop system of eq. (4.56) is obtained by feeding back $u = KCx$.

$$A + BKC = (A_{ideal} + BKC) + E \tag{4.57}$$

$$\tilde{A}_{cl} = A_{cl} + E \tag{4.58}$$

where $\tilde{A}_{cl}$ is the actual closed-loop system matrix, and A_{cl} is the ideal actual closed-loop system matrix.

Next, Theorem 4.1 will be applied to perform the stability analysis in terms of the perturbation of eigenvalues. The objective is to investigate the eigenvalue sensitivity of the ideal closed-loop system to the interconnection effects. Analyzed results will imply the stability margin of the entire power system, which is equipped with decentralized load frequency controllers, configured distributively.

As shown in Table 4.3, the ideal closed-loop power system (A_{cl}) results in 26 eigenvalues, which are all in the left-half plane (LHP). It has been shown that all decentralized controllers are perfectly designed. However, those eigenvalues are displaced when the interconnections between areas are considered. They are estimated by Theorem 4.1, and also tabulated in Table 4.3 in comparison with the actual values directly determined from the real closed-loop system ($\tilde{A}_{cl}$).

In addition, the condition numbers of all eigenvalues are given in Column 4 of the Table. This parameter indicates the eigenvalue sensitivity to the interconnection effects. However, the

Table 4.3: Analysis results: perturbation of eigenvalues

#	Ideal eigenvalues	Estimated eigenvalues	Actual eigenvalues	Condition numbers	Perturbation bounds	Departure angles
1	-0.1026	-0.1026	-0.1027	0.0001	0.0002	180.00
2	-0.4108	-0.4107	-0.4178	0.5090	1.6683	180.00
3	-0.4400	-0.4399	-0.4334	0.0212	0.0696	0.00
4	-0.9855	-0.9857	-1.1921	0.5496	1.8011	180.00
5	-1.4587	-1.4589	-1.5718	0.4249	1.3925	180.00
6	-0.9907 - 1.9785i	-0.9907 + 1.9785i	-0.9995 - 1.9554i	0.7395	2.4238	110.82
7	-0.9907 + 1.9785i	-0.9907 - 1.9785i	-0.9995 + 1.9554i	0.7395	2.4238	-110.82
8	-2.3727	-2.3727	-2.3726	0.0064	0.0209	0.00
9	-2.4338	-2.4338	-2.4336	0.0012	0.0039	0.00
10	-2.4697	-2.4697	-2.4701	0.0003	0.0009	180.00
11	-2.6793	-2.6793	-2.6781	0.0036	0.0118	0.00
12	-0.4308 - 2.6623i	-0.4307 + 2.6623i	-0.3411 - 3.0319i	0.4873	1.5972	-76.36
13	-0.4308 + 2.6623i	-0.4307 - 2.6623i	-0.3411 + 3.0319i	0.4873	1.5972	76.36
14	-2.9116	-2.9116	-2.9094	0.0173	0.0568	0.00
15	-3.0118	-3.0117	-3.0647	0.0412	0.1351	180.00
16	-0.3321 - 3.1145i	-0.3320 + 3.1145i	-0.2327 - 3.5860i	0.4964	1.6268	-78.09
17	-0.3321 + 3.1145i	-0.3320 - 3.1145i	-0.2327 + 3.5860i	0.4964	1.6268	78.09
18	-12.6255	-12.6255	-12.6234	0.0088	0.0287	0.00
19	-12.6446	-12.6446	-12.6443	0.0020	0.0065	0.00
20	-12.6520	-12.6520	-12.6526	0.0012	0.0039	180.00
21	-14.2857	-14.2857	-14.2857	0	0	0.00
22	-14.4057	-14.4057	-14.4057	0.0013	0.0044	180.00
23	-14.6552	-14.6552	-14.6480	0.0257	0.0842	0.00
24	-16.6667	-16.6667	-16.6667	0	0	0.00
25	-16.8126	-16.8126	-16.8126	0.0015	0.0050	180.00
26	-16.9213	-16.9213	-16.9214	0.0014	0.0046	180.00

sensitivity would be more perceivable, if the perturbation bounds given in the next column are considered instead. This parameter is, in fact, the product of the condition number and norm of interconnection effects ($\|E\|$). This bound may be depicted as a circle with its center at the location of an ideal eigenvalue as shown in Figure 4.12.

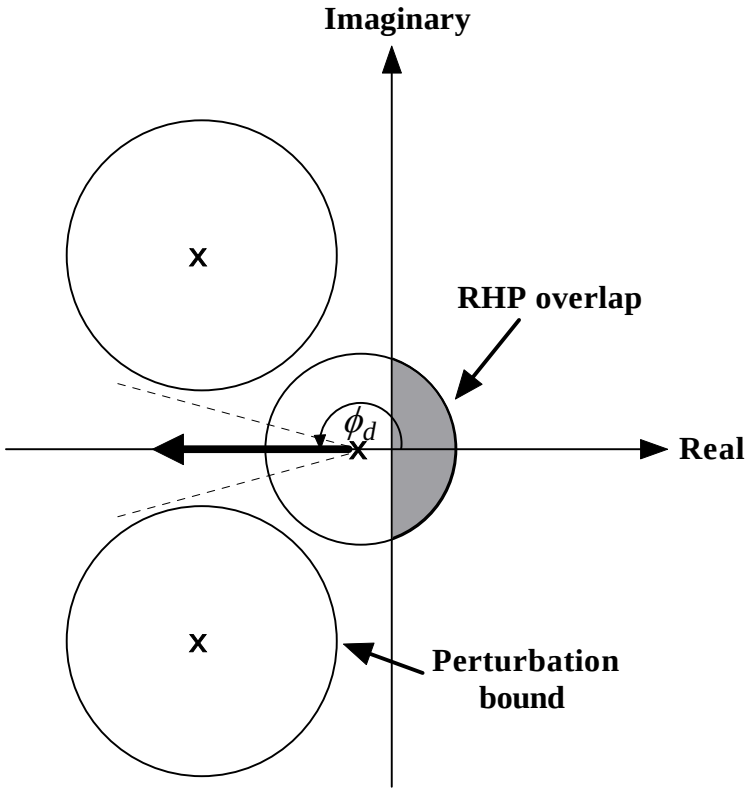

Figure 4.12: Perturbation bounds of eigenvalues.

A large condition number yields a wide perturbation bound, which may overlap the right-half plane when the corresponding ideal eigenvalue is close to the imaginary axis. In this case, care must be taken because the eigenvalue may move to the right-half plane, i.e. a system that is unstable, when the norm of perturbation increases. Nevertheless, this instability may not be the case, if the eigenvalue moves in directions other than the horizontally right direction (zero degree). As a result, the departure angles (ϕ_d) given in Column 6 of Table 4.3 will be used to enhance this analysis.

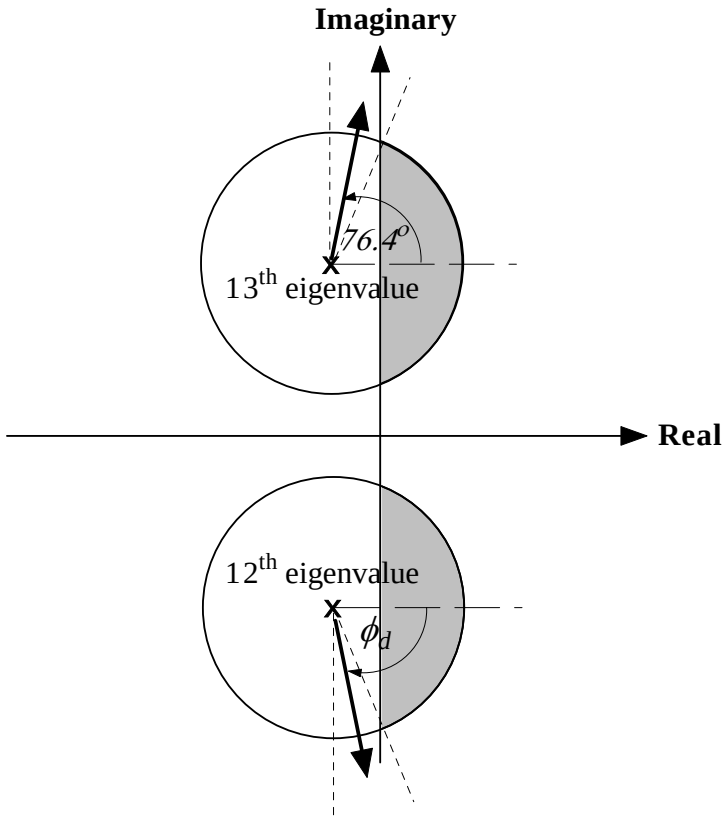

Figure 4.13: Perturbation bounds of the 12^{th} and 13^{th} eigenvalues.

For instance, the 2^{nd} and 4^{th} ideal eigenvalues have the perturbation bounds overlapping the right-half plane. Nevertheless, they have their departure angles of 180 degrees, which shows that they are moving away from the right-half plane. For another example, the 12^{th} and 13^{th} eigenvalues, which are the worst case, also have their perturbation bounds overlapping the right-half plane as shown in Figure 4.13. The complex conjugate eigenvalues have departure angles of -76.36 and 76.36 degrees respectively. According to Figure 4.13, both eigenvalues are likely to move in the southeast and northeast directions rather than to the right-half plane directly. This indicates an amount of stability strength of the closed-loop system, which can endure an increase in perturbation. The above analytical method is also applied to the remaining eigenvalues. Finally, it can be concluded that the whole power system equipped with the proposed controllers still retains stability after taking into account the interconnection effects, and is also capable of enduring increased interconnection strength.

Chapter 5

Detailed simulation of load frequency control using PAT

This chapter is dedicated to the nonlinear simulation of load frequency control using the Power Analysis Toolbox (PAT) [49]. PAT is a powerful simulation software package developed for testing and analyzing behaviors of real-world electric power systems. In simulating a power system, the use of PAT results in a much shorter simulation time than those of conventional software packages such as Power System Toolbox (PST) [50]. Furthermore, it provides a user-friendly simulation environment using MATLAB's Simulink for power system dynamic studies. It also allows a user to integrate interested add-on devices such as fuel cells, micro-turbines, different types of turbine-governors, and so forth, without difficulty.

As is widely known in load frequency control area, the turbine-governor system is a major mechanism, which steers a synchronous generator to change electrical power up and down. In section 5.1, a detailed model of the turbine-governor is developed and integrated in PAT. This model is relatively universal since it can represent different types of turbine-governors such as steam and hydro types by altering the model parameters. This would increase PAT's simulation potential for coping with several types of turbine-governors other than the existing one.

In Chapter 4, the studied power systems with their proposed controllers are built in a Simulink environment. These models are exactly the same as ones used in control design. Although they are widely used and well suited for load frequency control problems, it will be interesting to investigate the performance of these controllers, when used to control a detailed power system model including the voltage loop. This task will be performed in section 5.2, which shows the

comparison between the dynamics of the classical model and detailed model controlled by the proposed load frequency control.

5.1 Turbine-governor models in PAT

To simulate a variety of load frequency control studies using the Power Analysis Toolbox (PAT), it becomes necessary to develop other types of turbine-governors different from that which is available. According to Debs [40], a detailed model of the turbine-governor system is presented as shown in Figure 5.1. This model can represent a wide range of turbine-governor types by changing its parameters as illustrated in Tables 5.1 and 5.2.

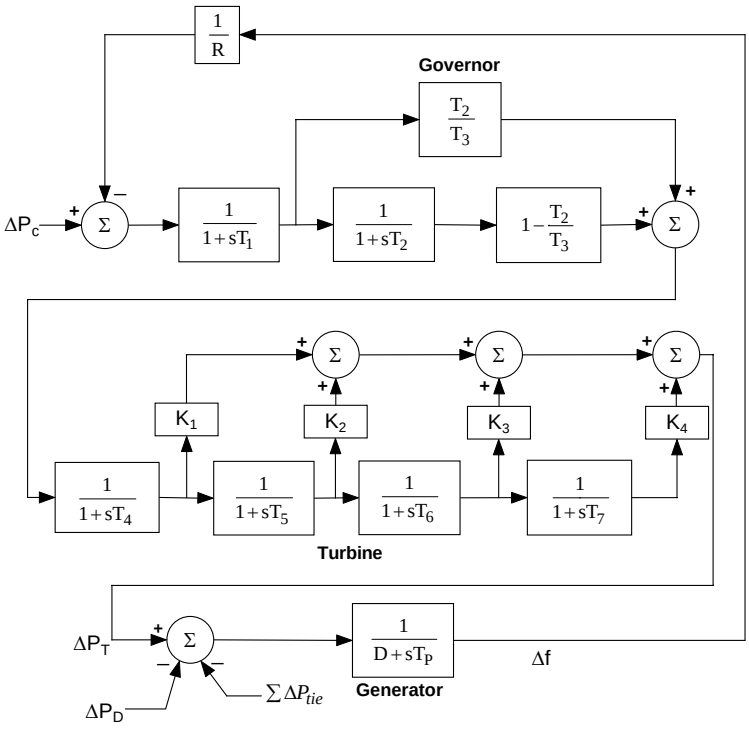

Figure 5.1: General turbine-governor model.

All generating units used in the test systems are based on the above turbine-governor model. As a result, the model is built as an add-on device for PAT as shown in Figure 5.2. This Figure also shows an example of the input code, including the turbine-governor parameters required in the PAT data file.

Table 5.1: Typical parameters for speed governors

	Mechanical hydraulic	Electro-hydraulic w/o steam feedback	Electro-hydraulic with steam feedback
T_1	0.2-0.3	0	2.8
T_2	0	0	1.0
T_3	0.1	0.025-0.1	0.15

Table 5.2: Typical parameters for turbines

	Non-reheat	Single-reheat	Double-reheat	Hydro
T_4	0.3	0.2	0.2	0
T_5	0	7.0	7.0	0.25-2.5
T_6	0	0	7.0	0
T_7	0	0.4	0.4	0
K_1	1	0.3	0.22	-2
K_2	0	0.4	0.22	3
K_3	0	0.3	0.3	0
K_4	0	0	0.26	0

```
% Turbine-governor data
% column         data                          unit
%  1   turbine model number (=3)
%  2   machine number
%  3   speed set point                  wf    pu
%  4   steady state gain               1/R    pu
%  5   maximum power order             Tmax   pu
%  6   servo time constant              T1    sec
%  7   governor time constant           T2    sec
%  8   transient gain time constant     T3    sec
%  9   HP section time constant         T4    sec
% 10   reheater time constant           T5    sec
% 11   Time constant for Universal TG   T6    sec
% 12   Time constant for Universal TG   T7    sec
% 13   Gain constant for turbine        K1
% 14   Gain constant for turbine        K2
% 15   Gain constant for turbine        K3
% 16   Gain constant for turbine        K4
% 17   power loop 0/1 = off/on
% 18   frequency loop 0/gain = off/on

% Universal TG (Type=3)
tg_con = [...
% 1  2  3   4   5    6    7     8    9    10   11   12   13   14   15   16  17  18
  3  1  1  25  1.0  0.08  1.0  0.15 0.20  6.0  7.0  0.5  0.2  0.2  0.4  0.2  0  1;
  3  2  1  25  1.0  0.00  0.0  0.06 0.36  0.0  0.0  0.0  1.0  0.0  0.0  0.0  0  1;
  3  3  1  25  1.0  0.00  0.0  0.08 0.41  0.0  0.0  0.0  1.0  0.0  0.0  0.0  0  1];
```

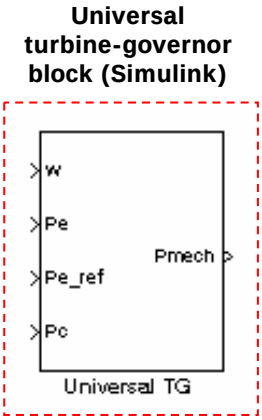

Figure 5.2: A Simulink block of the universal turbine-governor and its input code for PAT.

5.2 Effects of the excitation system on load frequency control

In section 5.1, a universal turbine-governor device is developed to be used in PAT. This device plays a very significant role in load frequency control studies. In this section, an excitation system, a feature which has been neglected in previous control designs and simulations, will be included in the analysis. Meanwhile, the classical model of generator, which mainly describes only mechanical dynamics, is replaced by a detailed model of a synchronous machine, representing full dynamics. These modifications make the power system being studied even more realistic.

Generally, the excitation system is used to provide DC current to the field winding of the synchronous machine. In terms of control functions, the system controls the field voltage, and thus the field current, to regulate the voltage and reactive power flow. Its input is the terminal voltage (V_t), while the output is the exciter voltage (E_{fd}). In typical load frequency control design, the excitation system is normally neglected since its dynamic response is much faster than that of the mechanical loop. Therefore, it barely affects the performance of load frequency control associated with the mechanical loop responses directly. Here, the purpose of this section is to confirm the above assumption by testing the proposed load frequency control in the environment of a full-blown power system.

The test considers two three-area power systems, where each area consists of three generating units. The first power system is based on the classical model, which describes only the mechanical dynamics of the generator without an excitation system. The other system uses the detailed model of synchronous generator connected with an excitation system. In addition, both are steered by the identical turbine-governor systems. Subsequently, the proposed PI load frequency controller presented in section 4.3 is designed for the first power system. However, it is also used to control the other power system in order to study the effects of voltage loops caused by the excitation system. In the simulation, stress is applied to both power systems by increasing the load by 10%, 20%, and 50%. Nevertheless, all cases yield the same conclusion. Therefore, only the case of a 20% increase in load is illustrated, and simulation results are given as follows.

Figures 5.3 and 5.4 illustrate dynamic responses of the power system, based on the classical model. They include the generator speed, area control error, relative angle, governor load setpoint, mechanical power, electrical power, and generator voltage. Meanwhile, the dynamic responses of the other power system, which use the detailed model, are shown in Figures 5.5 and 5.6. In this case, Figure 5.6 also includes the field voltage (E_{fd}), which is the output of the excitation system.

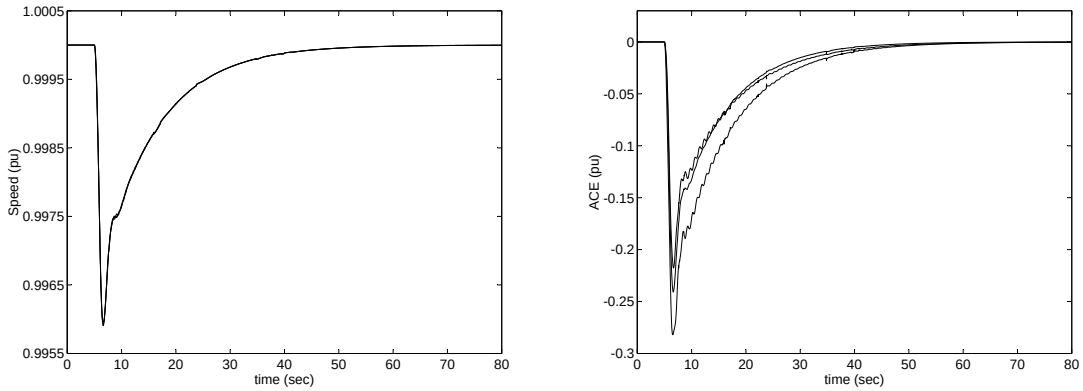

(a) Generator speed

(b) Area control error

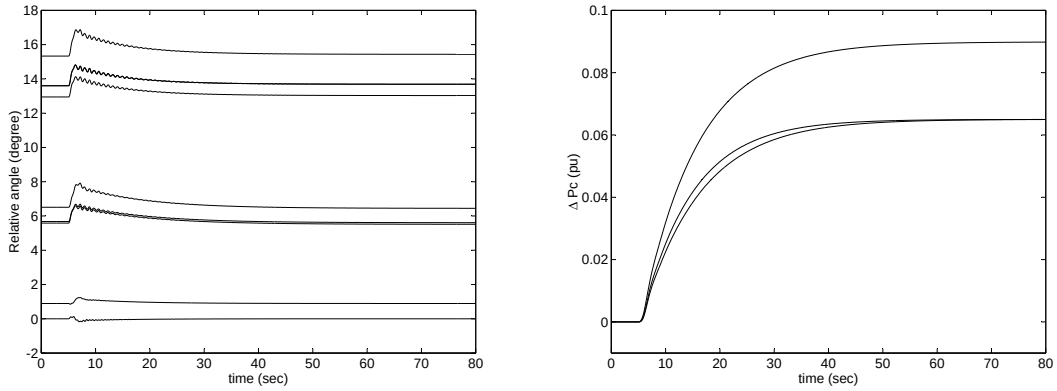

(c) Relative angle

(d) Governor load setpoint

Figure 5.3: Classical model: Dynamic responses at load increase by 20%.

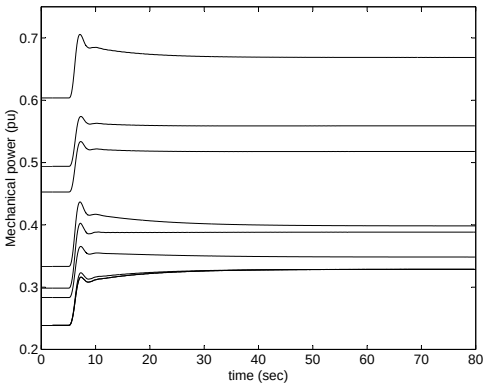

(a) Mechanical power

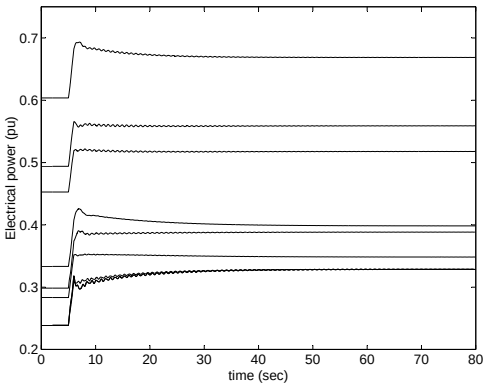

(b) Electrical power

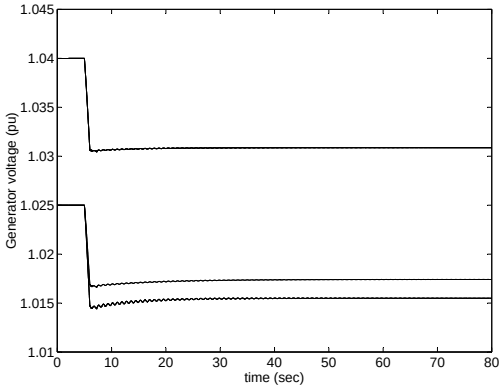

(c) Generator voltage

Figure 5.4: Classical model: Dynamic responses at load increase by 20%.

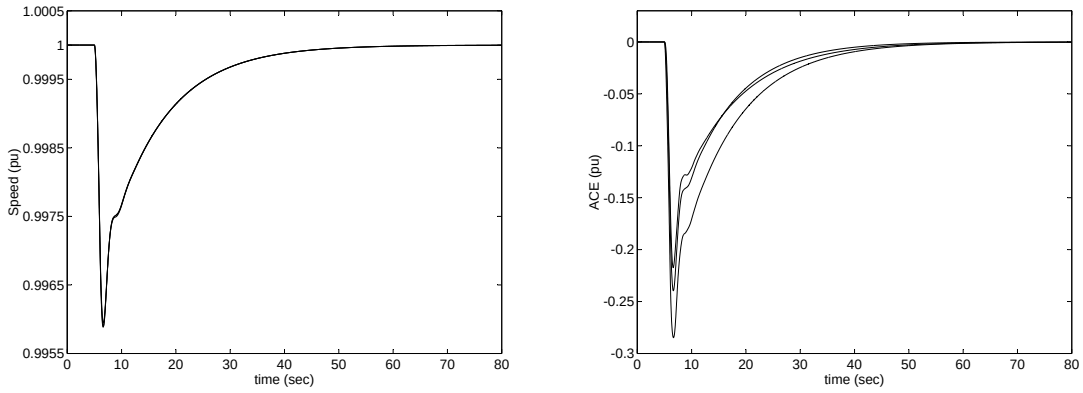

(a) Generator speed

(b) Area control error

(c) Relative angle

(d) Governor load setpoint

Figure 5.5: Detailed model: Dynamic responses at load increase by 20%.

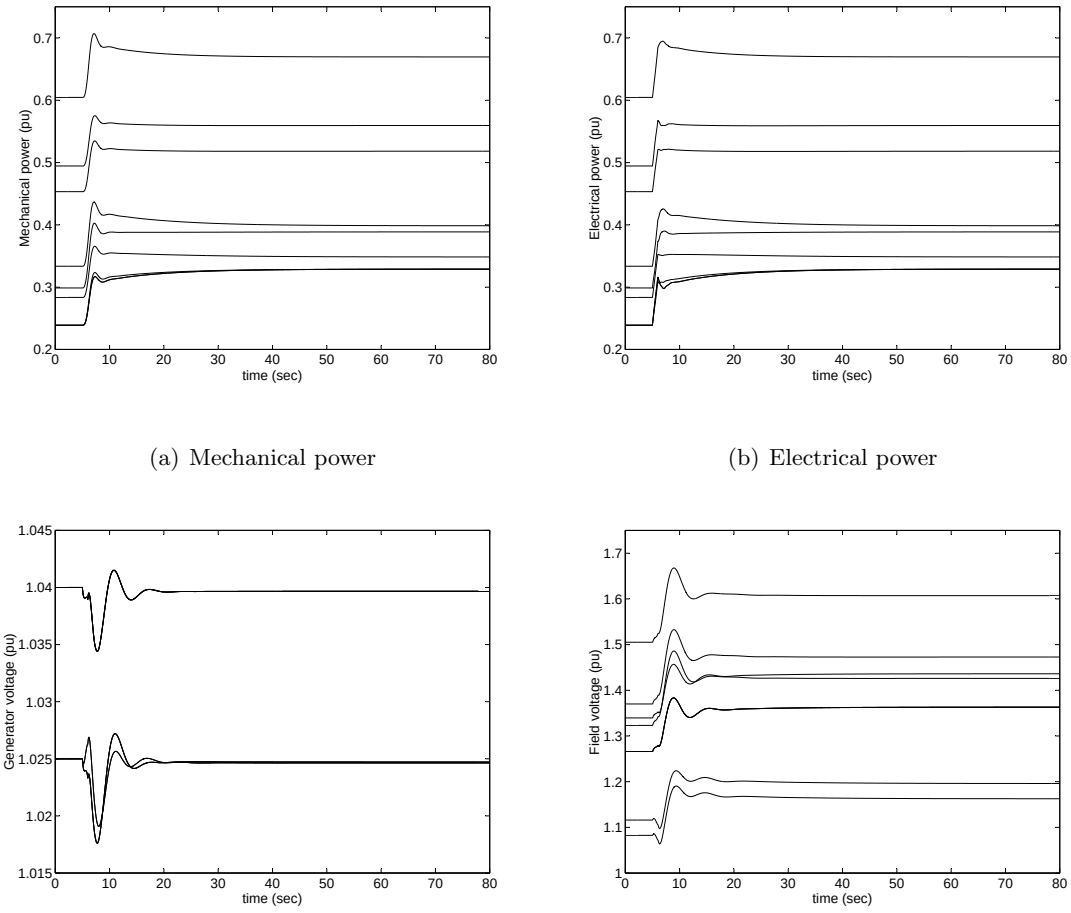

(a) Mechanical power

(b) Electrical power

(c) Generator voltage

(d) Field voltage

Figure 5.6: Detailed model: Dynamic responses at load increase by 20%.

According to the above results, the responses associated with the mechanical loop, including the generator speed, area control error, governor load setpoint, and mechanical power, are almost identical for both power systems. From a close observation, however, the responses of the classical model contain small oscillations during the transient phase. Meanwhile, most of responses associated with the voltage loop are different. Within the classical model after the 20% increase in load, the generator voltages drop and remain at the new levels. In contrast, the detailed model with the excitation system can bring the voltages back to the pre-disturbance values. These results show an improved voltage stability for the power system including its excitation system.

Nevertheless, from a load frequency control point of view, which tends to balance generation and demand, there is no noticeable deterioration caused by voltage-loop effects on the responses of the detailed model. The generator speed and area control error are perfectly controlled. Consequently, this study has shown the robustness of the proposed control design against effects of the excitation system.

Chapter 6

NERC's standards oriented load frequency control strategy

The objectives of this dissertation are not only to develop new decentralized load frequency control designs, but also to assure that the resulting controller promises compliance with NERC's control performance standards. This is crucial since violating the standards may cause serious interconnection problems, and NERC will subsequently penalize the one who is responsible. The following sections will describe proposed LFC strategies to comply with the NERC standards, and also to reduce operational and maintenance costs associated with LFC service. Finally, a performance assessment will be given at the end of this chapter.

6.1 Fuzzy logic load frequency control in compliance with NERC's control performance standards

All power system control areas are required to direct their interconnection operations in compliance with NERC's control performance standards. Operating automatic generation control (AGC) or LFC with tight control actions should result in good compliance with the standards, but it may cause 1) unnecessary fuel consumption due to excess maneuvering and 2) serious unit wear and tear because of incessantly rapid equipment excursions. Moreover, the NERC's historical data show that several control areas cannot comply with CPS2, even though they satisfy CPS1. To deal with the above problems, an intelligent system, which can manipulate the LFC controller to benefit whom with interest in LFC, is to be developed. Fuzzy logic is an ideal option

for this purpose.

6.1.1 Why fuzzy logic?

Fuzzy logic is a problem-solving control system method. It provides an easy way to reach an explicit conclusion based on information that is ambiguous, imprecise, or missing input and involves complex systems [51]. In addition, the fuzzy logic technique mimics how a human would make decisions within a much faster time frame.

An advantage of a fuzzy logic system is that a designer does not need to technically understand the system or to use mathematical system model to design a controller. On the other hand, a fuzzy logic system is empirically designed based on an expert's knowledge by developing if-then rules to solve the control problem.

Fuzzy logic plays a key role in control applications. It has been applied to solve many control problems, and proved to be an attractive choice because it imitates human control logic. To deal with input data, an imprecise but descriptive language more like human operator is used in fuzzy logic. In addition, its robustness helps to acceptably control the system, even when first implemented without tuning.

6.1.2 Fuzzy logic design for NERC's standards oriented load frequency control

In this section, fuzzy logic is employed as an automatic operator to control the actions of the LFC controller. This control strategy is based on the operational and economical logic of the experienced system operator [52]. To operate a control area effectively, the operator should 1) comply with NERC's control performance standards, 2) cut down operational and maintenance costs by diminishing excess unit maneuvering. Both can be achieved by an appropriate design for the fuzzy logic system. The structure of fuzzy logic based load frequency control is illustrated in Figure 6.1.

The above fuzzy logic system uses information that reflects compliance with CPS1 and CPS2 as inputs. Then it adjusts its output, the tuning parameter, to tune the control parameter of the LFC controller according to fuzzy rules. The proposed fuzzy logic system is designed to lower the control parameter when the value of either input rises. On the other hand, that control parameter will be increased when the value of either input falls. This algorithm will reduce wear and tear on the unit equipment since the governor setpoint or raise/lower signal (ΔP_c) generated from the controller is modified with much lower frequency while the control area has high compliance. For

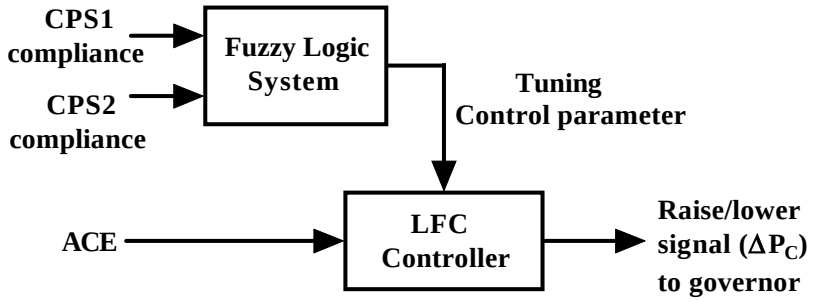

Figure 6.1: Fuzzy logic based load frequency control.

Table 6.1: Fuzzy logic rules for load frequency control

CPS1 compl. factor	Logical operation	CPS2 compl. factor	Tuning parameter
High			Very high
Medium	AND	High	High
Medium	AND	Medium	Medium
Medium	AND	Low	Low
Low	AND	High	Medium
Low	AND	Medium	Low
Low	AND	Low	Very low

instance, a set of fuzzy rules designed for this purpose is given in Table 6.1.

From Table 6.1, the CPS1 compliance factor as the first input is weighed more importantly than the other. This is because the CPS1 compliance factor is normally calculated in terms of an average of twelve month data, whereas the CPS2 compliance factor is determined based on an average of ten minute data. The high CPS1 compliance factor, for example, indicates poor compliance with CPS1 considered as ill interconnection operation, which needs to be recovered immediately. On the other hand, the high CPS2 compliance factor indicates less poor operation if the CPS1 compliance factor is not high. Membership functions will be used to define characteristic of the inputs and output (very low, low, ..., very high) as curves that map each point in the input space to a membership value between 0 and 1.

Generally, a system operator do not desire to have too high compliance since it frequently requires tight control actions which cause excess maneuvering and unit wear and tear. A solution to surviving this scenario is to operate the loosest load frequency control that still maintains

acceptable compliance with CPS1 and CPS2. This is the objective of the proposed fuzzy logic based load frequency control as illustrated below.

To develop such a fuzzy logic system, its inputs and outputs must first be defined. To assure compliance with CPS1 and CPS2, nothing is better than using measures that reflect the level of compliance with CPS1 and CPS2 as the inputs. The first input of the proposed fuzzy logic system is called *accumulatively average compliance factor* ($\mathrm{CF_{ac}}$). It is used to indicate the compliance level with CPS1, and is expressed by eq. (6.1).

$$CF_{ac} = AVG_{X\rightarrow Y}\left[CF_1\right] \tag{6.1}$$

$$CF = AVG_{X\rightarrow Z}\left[CF_1\right] \tag{6.2}$$

Figure 6.2: Twelve-sliding month time line for calculating compliance factors.

Figure 6.2 illustrates the important time intervals used in calculating $\mathrm{CF_{ac}}$. Specifically, point Y represents the current time where $\mathrm{CF_{ac}}$ is calculated in every minute. Point Z represents the end of a twelve-sliding-month period starting from point X. In addition, each control area is required to report its levels of compliance (CPS1 and CPS2) to NERC at the end of each month. Therefore, the compliance factor (CF) defined by eq. (3.3) can also be expressed by eq. (6.2), which is the 12-month average of the 1-minute average compliance factors ($\mathrm{CF_1}$).

According to eq. (3.4), $\mathrm{CF_1}$ is defined as the product of the area control error (ACE) and frequency deviation (ΔF). Thus poor compliance with CPS1 is indicated, when this value is high. On the other hand, a control area is in good compliance with CPS1, when this value is low. The other fuzzy input is the *10-minute window average of the ACE divided by* L_{10}, which is briefly expressed as ($\mathrm{AVG_{10}[ACE]/L_{10}}$). It is used to measure the level of compliance with CPS2 based on the ACE. This input is also calculated every minute in order to fire the fuzzy logic output.

To close the feedback loop, the output is the fuzzy gain (α) used to tune the control parameter (K_i) of the integral controller. Finally, the proposed secondary loop of the generating units or fuzzy logic load frequency control can be graphically illustrated in Figure 6.3.

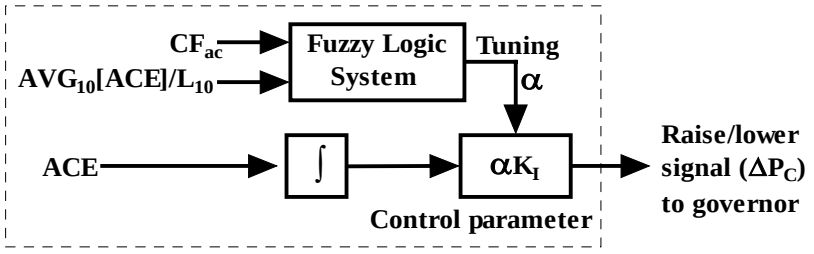

Figure 6.3: Fuzzy logic load frequency control.

Subsequently, the input and output membership functions based on Mamdani's method [53] are described in Figures 6.4 and 6.5 respectively. According to the fuzzy rules developed in

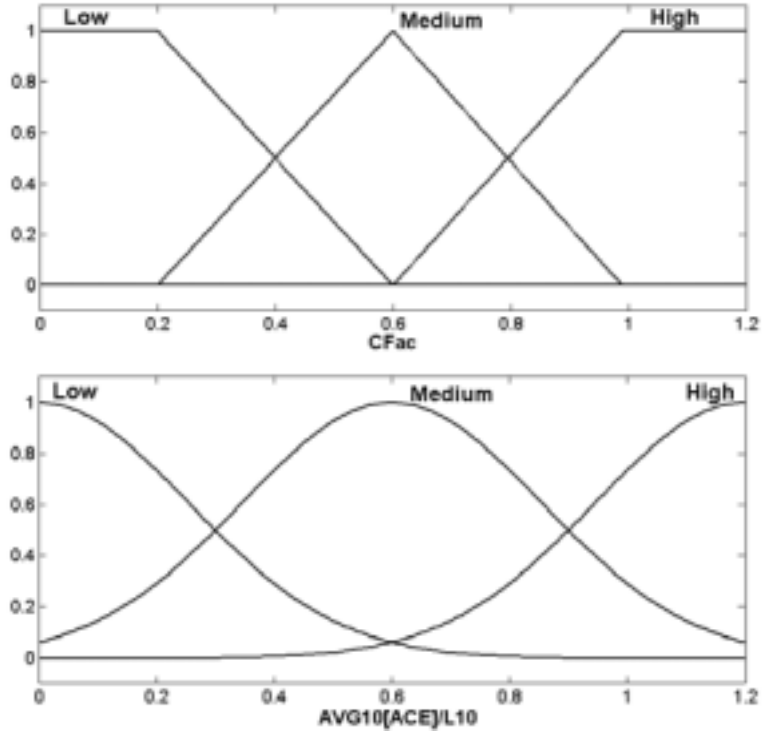

Figure 6.4: Input membership function.

Table 6.1, the fuzzy logic toolbox is used to draw the relationship between the inputs and output as a three-dimensional mesh surface as shown in Figure 6.6.

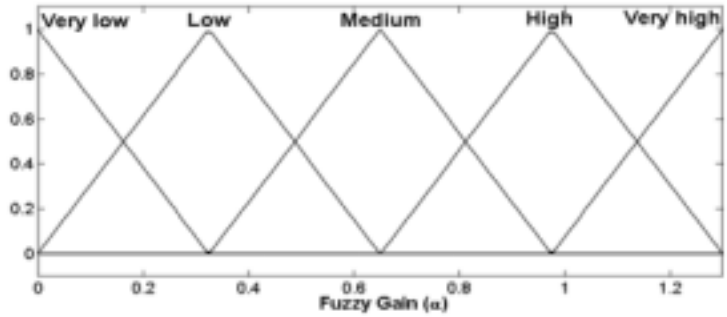

Figure 6.5: Output membership function.

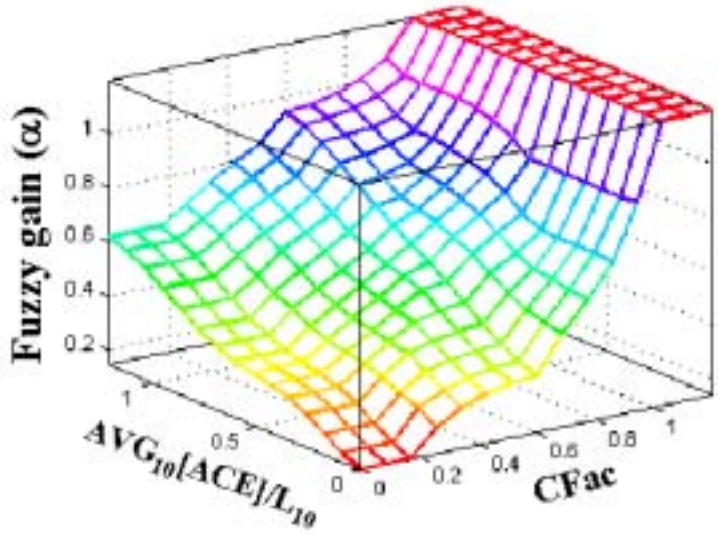

Figure 6.6: Relationship of fuzzy logic inputs and output.

6.2 Simulation results

To demonstrate the performance of the proposed strategy, a three-area power system as shown in Figure 6.7 is chosen as a test system. It includes five Gencos and three Discos. Area 1 and Area 2 each have two Gencos and one Disco, while Area 3 has only one Genco and one Disco. All parameters of generating units whose models are introduced in section 5.1 are given in Table 6.2. The tie-line synchronizing coefficients between areas are: $T_{12} = 60$ MW/rad, $T_{13} = 200$ MW/rad and $T_{23} = 100$ MW/rad.

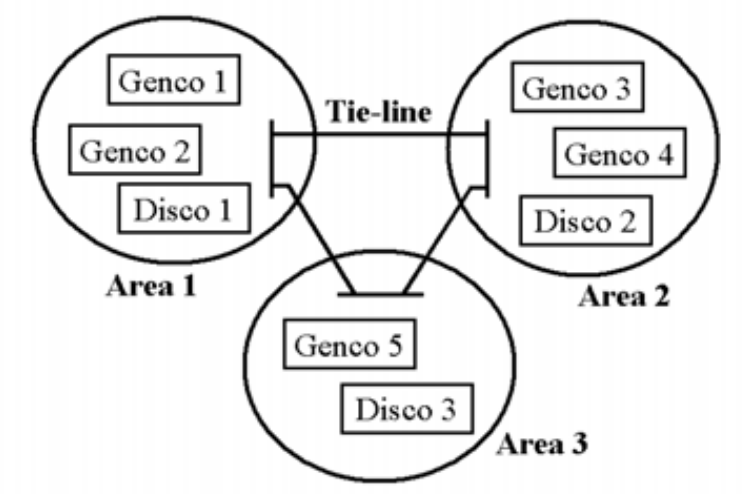

Figure 6.7: A three-area power system.

Table 6.2: Generating unit parameters

PARAMETERS	GENCO1	GENCO2,3	GENCO4	GENCO5
Rating (MW)	1000	750	700	2000
Droop characteristic: R	5%	4%	4%	5%
Damping: D (pu MW/Hz)	20	15	14	18
Constant of inertia: H (s)	5	5	5	5
T1	2.8	3	2.7	2.5
T2	1	0	0	0
T3	0.15	1	1	1
T4	0.2	0.4	0.35	0.5
T5	6	0	0	5
T6	7	0	0	0
T7	0.5	0	0	0
K1	0.2	1	1	0.4
K2	0.2	0	0	0.6
K3	0.4	0	0	0
K4	0.2	0	0	0

These Gencos generate electric power in terms of load following and regulation services to the Discos. The Gencos providing load following services will ramp their generation to follow slow load fluctuations. Such a load can be forecast according to time of day, day of week, weather, etc. On the other hand, those providing regulation services take care of discrepancies in fast load fluctuations and load following power. In the case study, load following and regulation contracts are given in Tables 6.3 and 6.4.

Table 6.3: Load following contract

	DISCO1	DISCO2	DISCO3
GENCO1	80%	20%	-
GENCO2	-	-	-
GENCO3	-	50%	-
GENCO4	-	-	-
GENCO5	20%	30%	100%

Table 6.4: Regulation contract

	ACE1	ACE2	ACE3
GENCO1	-	-	-
GENCO2	100%	-	-
GENCO3	-	50%	-
GENCO4	-	50%	-
GENCO5	-	-	100%

According to the above load following and regulation contracts, the proposed load frequency control of each area is used to satisfy power demand during a load pick-up hour as shown in Fugure 6.8. Again, the linear components of load fluctuations are satisfied by the load following service, and the random fluctuations will be met by the regulation service.

As follows, the performance of fuzzy rule based load frequency control is assessed through nonlinear simulation. Its performance is compared to two conventional control designs: a conventional design with existing control parameters, which are currently used by the control areas, identified as Case 1, and another conventional design using much lower control parameters, identified as Case 3. The proposed control design is identified as Case 2. The reasons for choosing these three cases for assessing the proposed load frequency controller are to show that 1) the proposed controller can reduce unnecessary wear and tear by lowering the values of the original control parameters and also 2) these new adjustable control parameters designed by the fuzzy

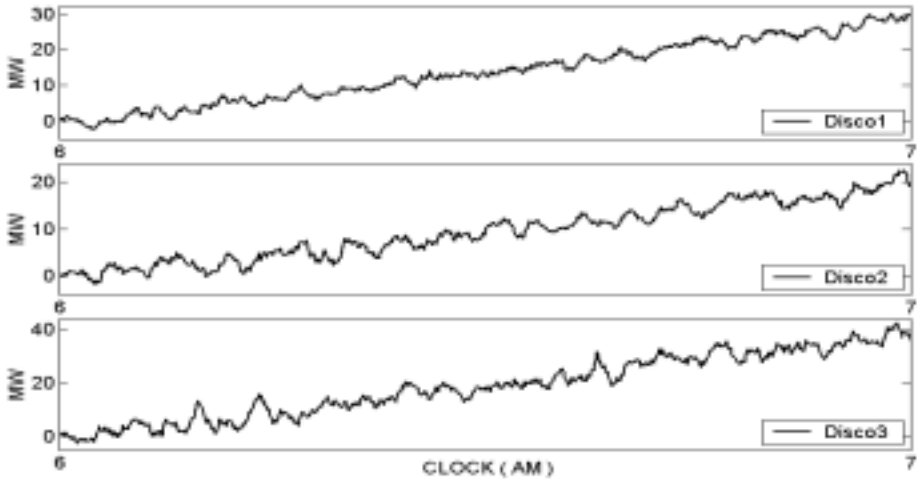

Figure 6.8: Demand changes of each Disco during a load pick-up hour.

logic system are capable of helping the control areas comply with CPS2. Case 3 shows how using control parameters that are too low causes the control areas to violate CPS2, although wear and tear is reduced.

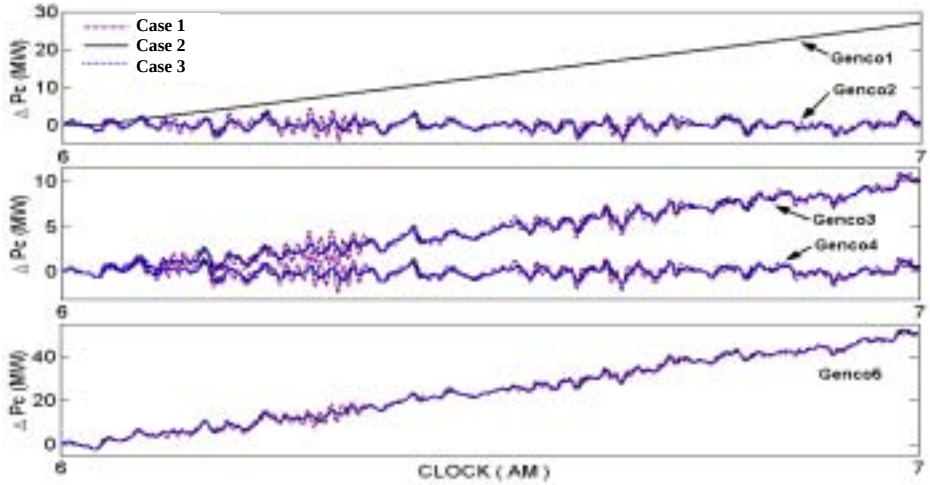

Figure 6.9: Governor load setpoint of each Genco.

Figure 6.9 shows the plots of changes in the governor load setpoint or raise/lower signals (ΔP_c) of each generating unit for the three cases. The signals for Cases 2 and 3 are similar, and

have many fewer high frequency components than those of Case 1. The excess maneuvering of the conventional LFC from Case 1 is better seen in Figure 6.10, where the difference between the raise/lower signals from Case 1 and Case 2 is plotted to show the superior performance of the fuzzy rule based load frequency control. The latter reduces unit maneuvering and high frequency components.

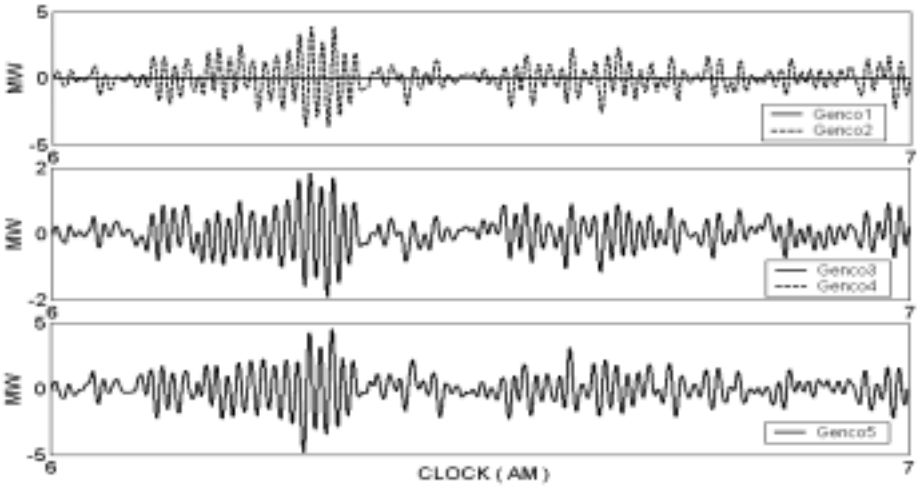

Figure 6.10: Excess governor load setpoint of conventional LFC over proposed fuzzy logic LFC.

The control parameters, omitting the negative signs from three cases, are plotted in Figure 6.11. The control parameters of the fuzzy rule based LFC from Case 2 are automatically tuned to reduce wear and tear, and to help the control areas compliant with the NERC standards, whereas those for the other cases are fixed, and not as versatile as the proposed one. In the case study, all areas are assumed to be highly compliant with CPS1 and, therefore, high above the standards. The proposed controller logically lowers the level of this compliance to gain benefits from the reduction of wear and tear. The percentages of compliance with CPS1 for each control area are plotted in Figure 6.12.

In Table 6.5, the 10-minute averages of the ACE of control areas are calculated and compared with the constants (L_{10}) at 10-minute periods. The results from the three cases are tabulated and compared. The control parameters from Cases 1 and 2 successfully help the control areas comply with CPS2, but those for Case 3 (low control parameters) could not keep the 10-minute averages of the ACE of Area 2 and Area 3 within the limits L_{10} during the period between 6:10-6:20 am.

Finally, simulation results show that excess maneuvering, which normally exists for the con-

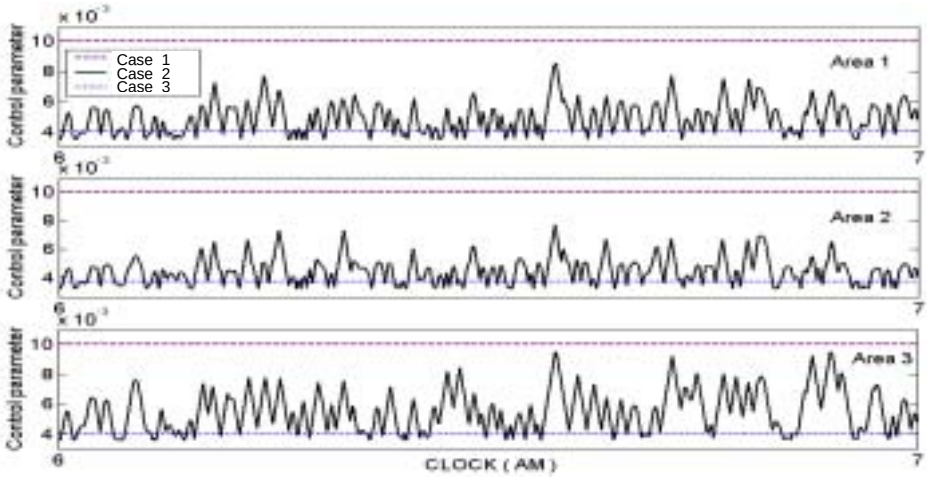

Figure 6.11: Control parameters of different load frequency control designs.

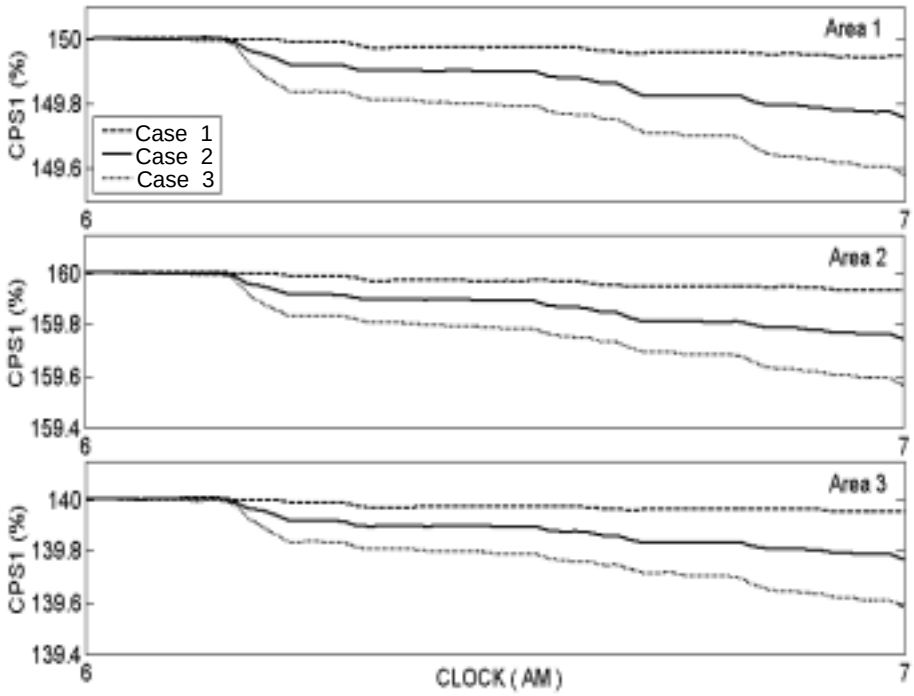

Figure 6.12: Percentage of compliance with CPS1 of each control area.

Table 6.5: 10-minute average of ACE compared with L_{10}

Time	AVG_{10}(ACE1)			AVG_{10}(ACE2)			AVG_{10}(ACE3)		
	Case 1	Case 2	Case 3	Case 1	Case 2	Case 3	Case 1	Case 2	Case 3
6:00-6:10	0.2113	0.6013	0.6797	0.3115	0.8287	0.9309	0.4110	0.9421	1.0464
6:10-6:20	0.3360	0.6232	0.9570	0.6057	1.0213	1.4271	0.4670	0.8821	1.3058
6:20-6:30	0.0671	0.1327	0.1756	0.1856	0.0828	0.2301	0.0577	0.1844	0.2378
6:30-6:40	0.0554	0.4802	0.4326	0.0093	0.4698	0.4942	0.0907	0.3639	0.2268
6:40-6:50	0.0068	0.4462	0.5737	0.3213	0.0072	0.1256	0.1670	0.2350	0.1917
6:50-7:00	0.0753	0.3092	0.4009	0.0183	0.2161	0.2433	0.1085	0.2794	0.1445
L_{10}	1.0732			1.0350			1.0763		

ventional LFC, is diminished by the proposed controllers. In addition, the control parameters of the proposed LFC, which are logically tuned, are effective in helping the control areas comply with CPS2. In contrast, the other conventional LFC, which uses lower control parameters, was not able to keep the 10-minute averages of the ACE under the limits L_{10} for a certain period.

Chapter 7

Economy inspired load frequency control system

In the previous chapter, the fuzzy logic based load frequency control was implemented to help the control areas comply with NERC's control performance standards. Moreover, the proposed control strategy reduces excess unit maneuvering, which causes expensive LFC costs.

To achieve the same target, this chapter presents a hybrid LFC system which incorporates the wedge-shaped control philosophy [36] and robust GALMI control design in terms of an adaptive control scheme. The wedge-shaped control method was first introduced by Jaleeli and VanSlyck. It claims that while n-minute averages of area control error (ACE) are within a specific wedge-shaped boundary, the generation needs not be changed to follow the demand in order to meet the NERC standards. This idea yields great advantages for LFC providers by significantly reducing unit maneuvering and reversals. More details will be given in section 7.1.

Furthermore, in this dissertation the robust GALMI control design described in section 4.3 is used to determine PI control parameters for the load frequency controller. It will be operated in an adaptive control fashion. More specifically, when the average of the ACE goes outside the wedge-shaped boundary, the load frequency controller will be activated. At the same time, its control parameters are automatically adjusted with respect to how far the ACE average is outside the boundary. The farther away it goes, the higher controller tightness would be needed to bring it back in bound.

With the integration of the above concepts, the new load frequency control strategy will yield more efficient LFC operations, which in turn will significantly reduce operational and mainte-

nance costs assessed on the basis of the level of unit maneuvering as well as on the number of reversals. Meanwhile, the compliance with NERC's control performance standards is guaranteed. Simulation results of a three-area power system will be given after the proposed strategy is illustrated.

7.1 Wedge-shaped control criteria

7.1.1 Background

The wedge-shaped control philosophy, also called tie-line bias priority-based control, was established by Jaleeli and VanSlyck [36]. This method, derived from an in-depth analysis of NERC's control performance standards, is designed to minimize the need for generation response to fast varying components of demand and also to comply with the standards. The analysis is initiated from the mathematical expression of area control error (ACE) as given in eq. (7.1).

$$ACE_i = \Delta NI_i - 10B_i\Delta F \tag{7.1}$$

where

NI_i net interchange error of the i^{th} control area
B_i frequency bias of the i^{th} control area in MW/0.1Hz
ΔF interconnection frequency error

Summation of the ACE for all areas in an interconnection yields:

$$\sum_i ACE_i = \left(-10\sum_i B_i\right)\Delta F \tag{7.2}$$

$$= -10B_s\Delta F \tag{7.3}$$

or

$$\Delta F = \sum_i \frac{ACE_i}{-10B_s} \tag{7.4}$$

The above relationship between ACE_i and ΔF will be used in the following explanations.

NERC's control performance standards consist of CPS1 and CPS2. Their conditions can be expressed by [33]:

CPS1: over any 12 consecutive months

$$RMS\left\{\overline{\Delta F}_1\right\} \leq \varepsilon_1 \tag{7.5}$$

CPS2: over any 10 consecutive minutes

$$RMS\left\{\overline{\Delta F}_{10}\right\} \;\leq\; \varepsilon_{10} \tag{7.6}$$

where $\overline{\Delta F}_m$ is the m-minute average of ΔF. The ε_1 and ε_{10} are the targeted RMS of 1-minute and 10-minute average frequency errors from their schedules respectively. Nevertheless, the square of $RMS\left\{\overline{\Delta F}\right\}$ for an n-equal area interconnection can be decomposed as follows.

$$\begin{aligned}
RMS^2\left\{\overline{\Delta F}\right\} &= AVG\left\{\left(\overline{\Delta F}\right)^2\right\} = AVG\left\{\overline{\Delta F}\times\overline{\Delta F}\right\} && (7.7)\\
&= AVG\left\{\left(\sum_i \overline{\left\{\frac{ACE_i}{-10B_s}\right\}}\right)\times\overline{\Delta F}\right\} && (7.8)\\
&= AVG\left\{\left(\overline{\left\{\frac{ACE_1}{-10B_s}\right\}}+\ldots+\overline{\left\{\frac{ACE_i}{-10B_s}\right\}}+\ldots+\overline{\left\{\frac{ACE_n}{-10B_s}\right\}}\right)\times\overline{\Delta F}\right\} && (7.9)\\
&= \underbrace{\ldots+AVG\left\{\overline{\left\{\frac{ACE_i}{-10B_s}\right\}}\times\overline{\Delta F}\right\}+\ldots}_{n\,terms} && (7.10)
\end{aligned}$$

To satisfy the CPS1 condition:

$$\begin{aligned}
\left(\ldots+AVG\left\{\overline{\left\{\frac{ACE_i}{-10nB_i}\right\}}\times\overline{\Delta F}\right\}+\ldots\right) &\leq \varepsilon_1^2 && (7.11)\\
AVG\left\{\overline{\left\{\frac{ACE_i}{-10nB_i}\right\}}\times\overline{\Delta F}\right\} &\leq \frac{\varepsilon_1^2}{n} && (7.12)\\
AVG\left\{\overline{\left\{\frac{ACE_i}{-10B_i}\right\}}\times\overline{\Delta F}\right\} &\leq \varepsilon_1^2 && (7.13)
\end{aligned}$$

Since all n areas are assumed equal, it would be reasonable for each to be required to satisfy the condition (7.12). The above derivation has illustrated how the CPS1 standard is established as shown in eq. (7.13). In an extended analysis, eq. (7.4) is rewritten as:

$$\overline{\Delta F} \;=\; \frac{\overline{ACE}_i+\overline{ACE}_j}{-10\left(B_i+B_j\right)} \tag{7.14}$$

where

ACE_i and B_i are the ACE and area bias of the i-th area.

ACE_j and B_j are the summation of ACE and area bias of the other areas.

Next, substitute eq. (7.14) into (7.13) and obtain:

$$AVG\left\{\frac{\overline{ACE}_i^2+\overline{ACE}_i\times\overline{ACE}_j}{100\left(B_i+B_j\right)B_i}\right\} \;\leq\; \varepsilon_1^2 \tag{7.15}$$

or

$$RMS^2\left\{\overline{ACE}_i\right\} + AVG\left\{\overline{ACE}_i \times \overline{ACE}_j\right\} \leq 100\,(B_i + B_j)\,B_i\varepsilon_1^2 \tag{7.16}$$

The term $AVG\left\{\overline{ACE}_i \times \overline{ACE}_j\right\}$ in eq. (7.16) is called "ACE coincidence". A decrease in the ACE coincidence yields more allowance for $RMS^2\left\{\overline{ACE}_i\right\}$. Consequently, less unit maneuvering is needed to comply with the NERC standards.

In the EPRI report TR-107813, it is stated that with the Priority-based Control Engineering (PCE) mechanism

> "*to minimize ACE coindence with other ACEs, k-minute sliding averages of ACE are required to be 68.3% of the narrowest funnel. The same averages are required to be within the second funnel 95.4%, and within the largest funnel 99.7%, of the time.*"

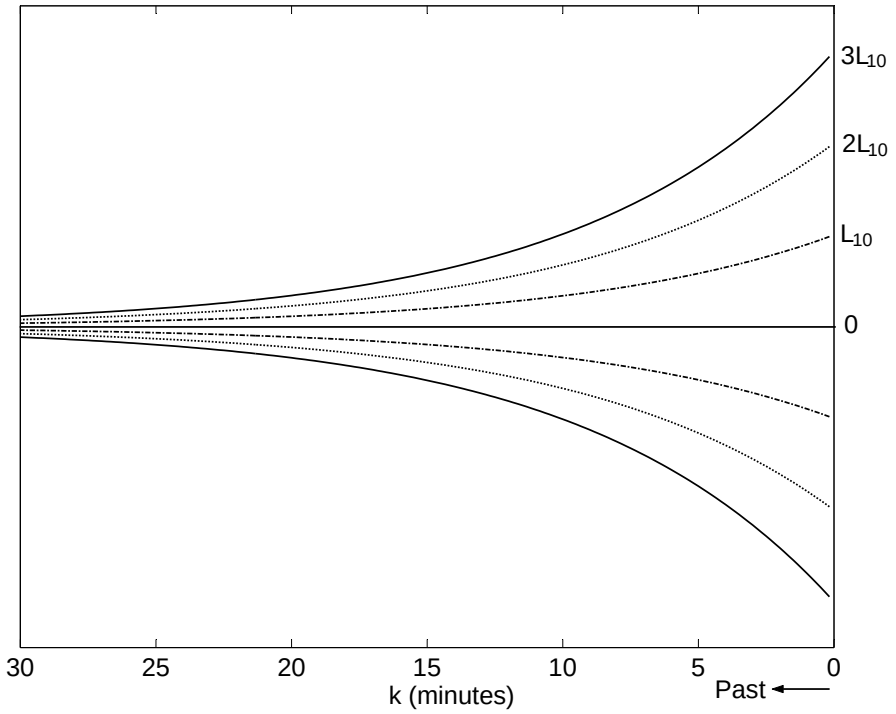

Figure 7.1: Wedge-shaped boundary.

The above funnels or wedge-shaped curves are depicted in Figure 7.1. All curves are equally spaced, and converge to zero as the width (k-minutes) of the sliding average window increases. The

narrowest, larger, and largest curves begin at the CPS2 limits (L_{10}), $2L_{10}$, and $3L_{10}$ respectively. The largest curve converges to L_{10} where k equals 10 minutes to bound the 10-minute sliding average of the ACE within the L_{10}. This is because the CPS2 standard requires the consecutive 10-minute averages of the ACE not to exceed the limit L_{10}, 90% of the time.

7.1.2 Control criteria

In this section, control criteria based on the wedge-shaped boundary will be developed. Here, for the sake of simplicity, only the main wedge-shaped boundary, i.e. the largest funnel, is used. The sliding k-minute averages of ACE are inputted and plotted in comparison with the wedge-shaped boundary as shown in Figure 7.2.

The shaded areas, called the "violation area", measure the amount of violation in the sliding k-minute averages of the ACE that are outside the boundary. Next, the value of the total violation area (TVA), a sum of all violation areas, is checked for any violation. In case there is no violation, the TVA equals zero, and no change in generation is needed. On the other hand, one or more violations will result in a positive TVA. A larger TVA will need a tighter control action, i.e. higher control tightness. Finally, the total violation area is scaled into an appropriate control tightness needed for adaptive robust load frequency control presented in section 7.2.

7.2 Adaptive robust load frequency control

In section 7.1, the wedge-shaped control criteria is described. While the sliding averages of the ACE remain within the wedge-shaped boundary, the LFC does not need to change the generated power to follow the demand. On the contrary, when the sliding averages of the ACE move outside the boundary, the LFC is needed to adjust generation to match the demand, in order to reduce the area control error. The LFC control parameters will be changed with respect to the amount of violation against the wedge-shaped boundary. For instance, loose control, i.e. low control parameters, will be used when a small violation is detected.

This section introduces an adaptive load frequency control scheme, whose PI control gains are adjusted according to the control tightness varied by the wedge-shaped control criteria [58]. More specifically, the control tightness is increased while the control area exhibits poor interconnection operation, i.e. a large average of the ACE. On the other hand, the control tightness is decreased to relieve mechanical stress on generating units under good operating conditions. This concept

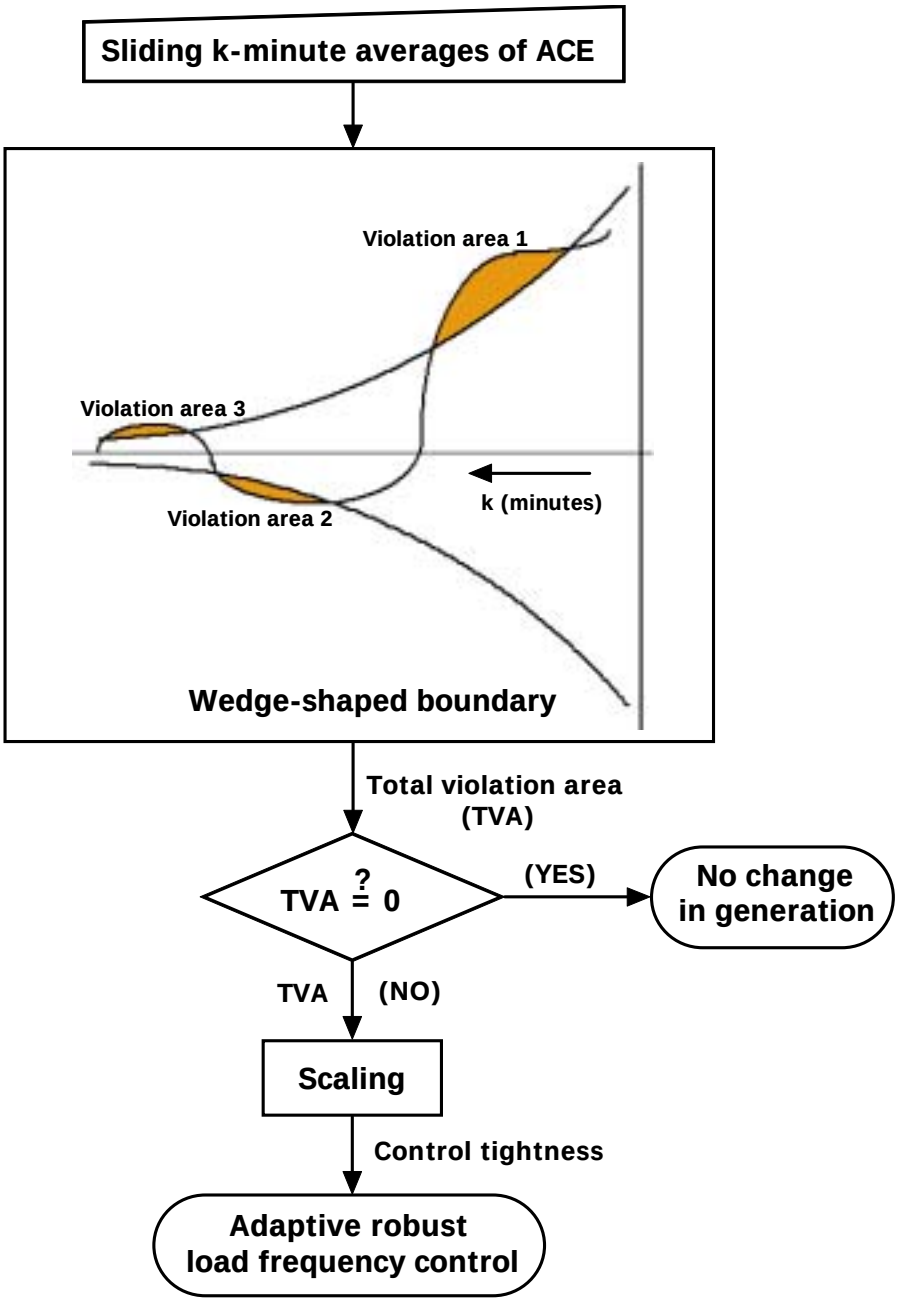

Figure 7.2: Wedge-shaped control criteria.

is more appealing than that of the conventional LFC using fixed PI gains, which often steers generating units to comply with NERC's standards, incurring the high costs associated with excess unit maneuvering and unnecessary wear and tear. The robust PI control design, incorporating genetic algorithms and linear matrix inequalities (GALMI), is used to determine the PI control parameters for the LFC. To be implemented as an adaptive control, this algorithm needs to be performed once, and again when the tightness of control is changed. However, this technique takes a few minutes to converge to a solution. In other words, it cannot instantly determine new gains, when it is asked for them. This becomes a major obstacle in implementing the adaptive LFC.

Here, spline techniques are used to solve the above problem. Specifically, the GALMI algorithm will be run off-line for different values of control tightness. Next, the resulting control parameters for a variety of control tightness values will be used as data for spline approximation. Then a PI control parameter path or "gain path" will be obtained which helps solving the problem involving the converging time of the GALMI algorithm.

The adaptive LFC is based on the concept that it is not necessary to closely follow the demand all the time. In other words, it will be better off for generation companies if the LFC marginally complies with the standards, but reduces by a great amount the LFC costs. Consequently, the control gains (K_P and K_I) of the adaptive LFC will be adjusted to lower the control effort so that fuel costs and unit wear and tear are reduced. On the contrary, the control gains will be adjusted to increase the control effort, once the LFC is close to violating NERC's standards. This adaptive control scheme, as shown in Figure 7.3, will reduce LFC operational costs, and also assure that the area complies with the standards. The proposed control scheme includes two important units, which are 1) the wedge-shaped control criteria and 2) the spline based gain paths. The first unit's function is to determine and adjust the control tightness for the PI controller. The criteria are based on the wedge-shaped control concept described in section 7.1, which decides when the controller takes a tight control action to comply with NERC's standards, or a loose control action to relieve the stress associated with the up and down movements of the generating units. The other unit is called spline based gain scheduler. It acquires the determined control tightness from the first unit, and in real-time schedules a pair of robust PI gains or control parameters for the PI controller. These gains are chosen from the PI gain paths constructed by a spline technique illustrated in the following section.

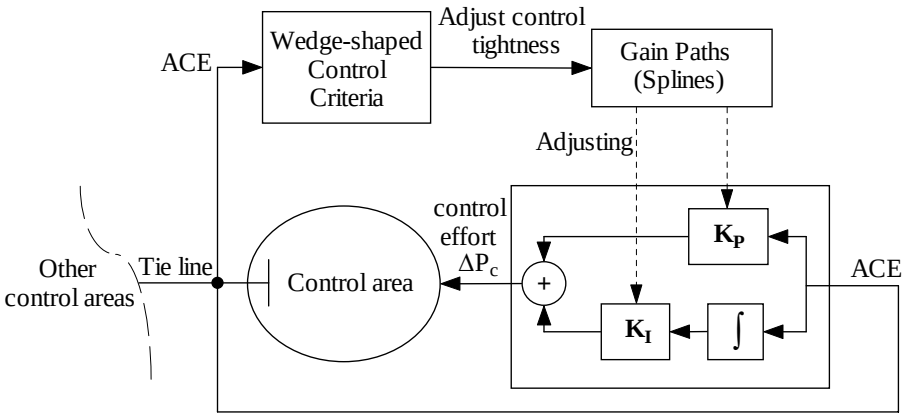

Figure 7.3: Adaptive load frequency control scheme.

7.2.1 Spline based PI gain paths

Before a spline technique is applied, the GALMI control design is run off-line to find PI control gains for different levels of control tightness, quantified by integers from 1 to 800. A number of resulting control parameters, K_P and K_I, each with corresponding control tightness are plotted in Figures 7.4 and 7.5.

According to Figure 7.4, the proportional gains change slightly with an increase in the control tightness. On the other hand, the trend of integral gains continues to rise while the control tightness increases as shown in Figure 7.5. Interestingly, the values of PI gains determined by the GALMI algorithm appear scattered all over the control tightness axis. This may be explained by the fact that there are multiple solutions for the robust control optimization problem solved by the GALMI technique. To obtain the PI gain paths, those data will be managed, utilizing a spline method.

Generally, spline theory is used to solve problems associated with a large amount of data or information, which needs to be described in a simple form. The theory can be used to interpolate between data using mathematical equations. Meanwhile, a large quantity of data can also be replaced by a single curve, which minimizes the distance between all data points and the curve using spline approximation methods. More details about the theory and definitions can be found in [59].

In this section, the spline technique is used to approximate the PI gain data as shown in Figures 7.4 and 7.5. This application will result in continuous gain paths along the control

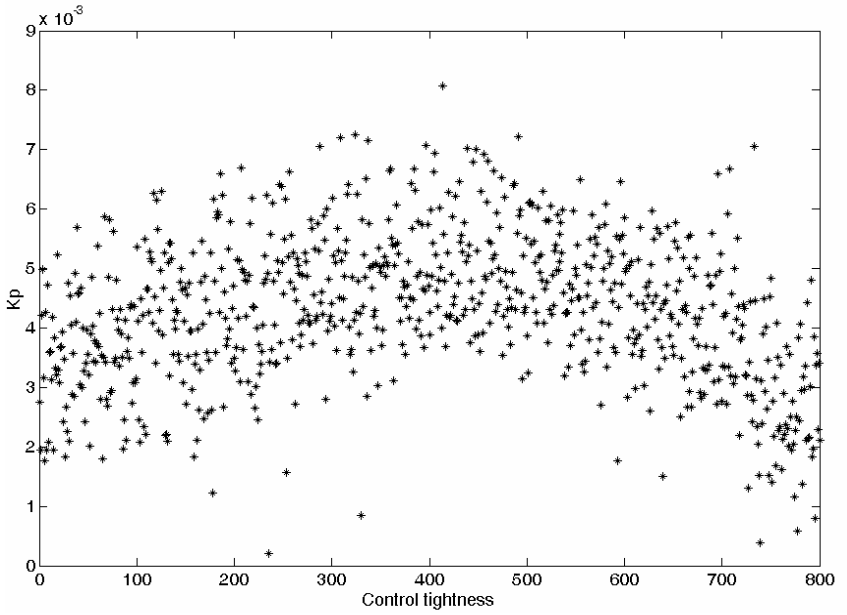

Figure 7.4: Proportional gain (K_P) vs. control tightness.

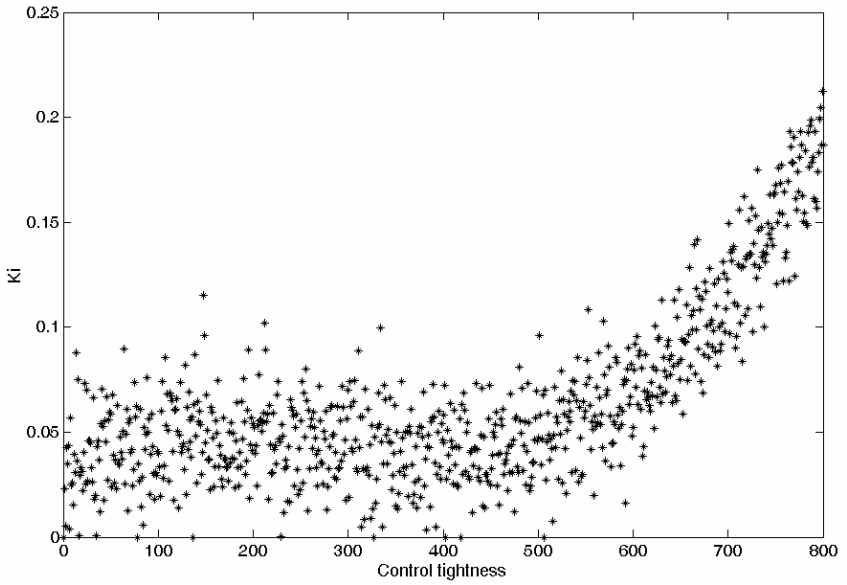

Figure 7.5: Integral gain (K_I) vs. control tightness.

tightness axis. More specifically, when any value of control tightness is chosen by the wedge-shaped control criteria, a pair of PI gains are promptly determined by a corresponding coordinate on the gain paths.

Here, the fourth-order least-squares spline approximation method will be used to smooth out the gain paths using the MATLAB command "SPAP2". The resulting gain paths are shown in Figures 7.6 and 7.7. In this approximation, six extra knots at 5, 10, 50, 175, 200 and 600 have been inserted between the control tightness at 1 and 800 to shape the gain paths, so as make them more reasonable.

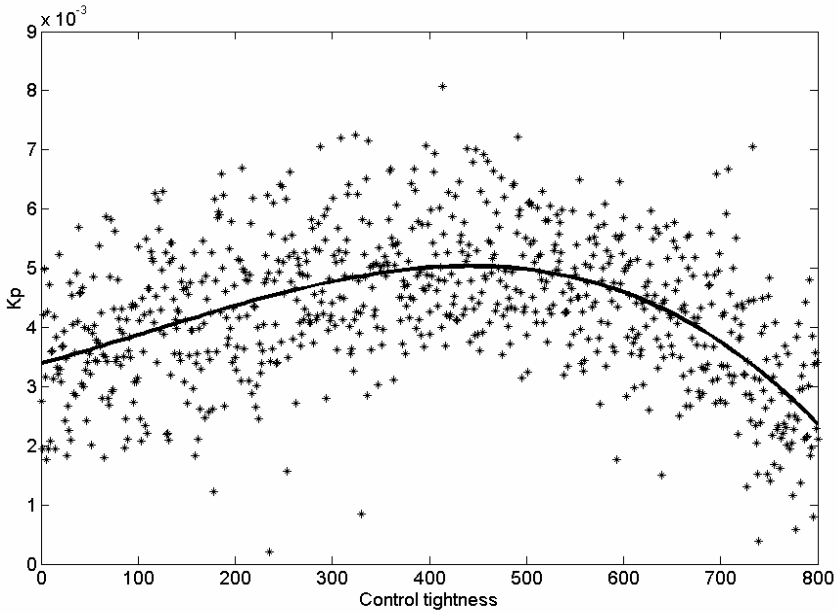

Figure 7.6: Proportional gain path by least-squares spline approximation.

The K_P and K_I gain paths obtained from the least-squares spline approximation are obviously smooth and practical in terms of simplicity of implementation. Subsequently, the gain paths will be incorporated with the wedge-shaped criteria to formulate the adaptive control scheme. Finally, the proposed hybrid load frequency control system introduced at the beginning of the chapter will be tested with a three-area power system. The simulation results will be presented in the following section.

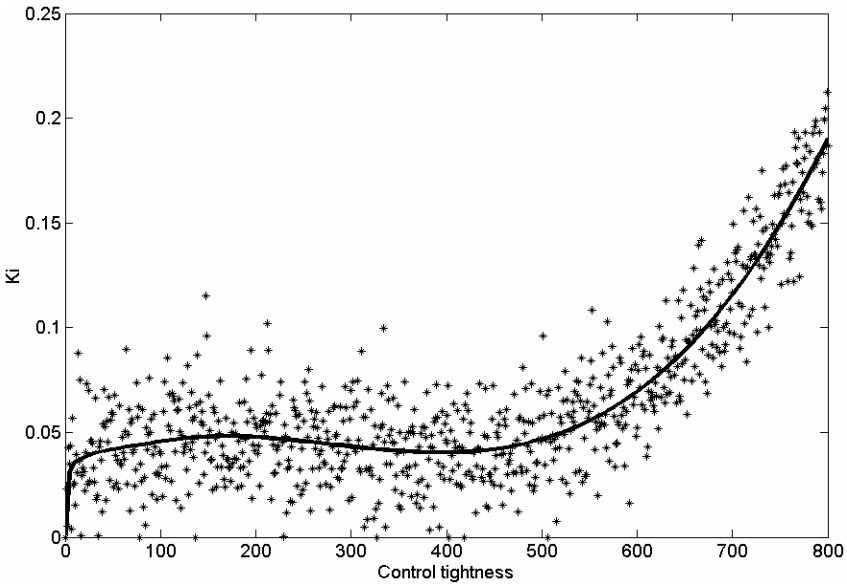

Figure 7.7: Integral gain path by least-squares spline approximation.

7.3 Simulation results

In this section, the dynamic simulation of a three-area power system will be performed to illustrate the performance of the proposed load frequency control system. Simulation results will include 1) the electric demand fluctuation, 2) the adjusted proportional gain, 3) the adjusted integral gain, 4) 10-minute averages of the area control error (ACE) associated with CPS2-NERC compliance, 5) the change in governor load setpoint (ΔP_C) and 6) the root means square (RMS) of ΔP_C. In addition, the results from using two types of conventional fixed gain LFC (loose and tight control) will be plotted in the same graph with those of the adaptive LFC system in order to compare their performances.

The demand fluctuations applied to each control area over one hour are shown in Figure 7.8. Nevertheless, simulation results of only Area 1 will be illustrated, since they are similar to those of the other areas. In Figure 7.9, the proportional gain (K_P) is varied along the proportional gain path as time increases. Meanwhile, the proportional gain for both the tight and loose LFC is fixed at $3.5\text{x}10^{-3}$ all the time. On the other hand, the integral gains (K_I) of the proposed LFC, tight LFC, and loose LFC are plotted all together in Figure 7.10. The gain of the proposed LFC is varied along the integral gain path, while the control tightness is adjusted by the wedge-shaped

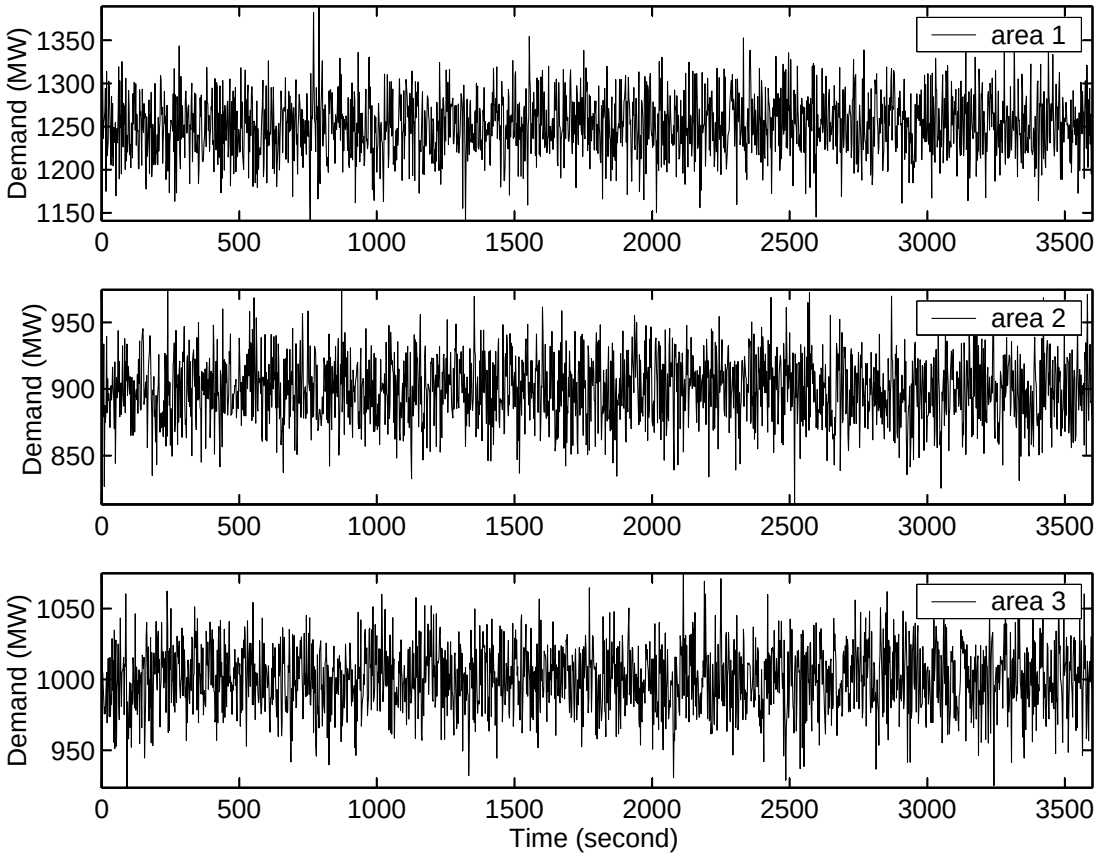

Figure 7.8: Demand applied to each area.

control criteria. The integral gain of the tight LFC equals 0.03, which is ten times higher than that of the loose LFC. As a result, the tight LFC will react to the area control error much faster and more actively than the loose LFC does.

To show the level of compliance with NERC's control performance standards, 10-minute averages of the ACE of three types of LFC are plotted against the specified limit L_{10} in Figure 7.11. The tight and proposed LFCs all have 10-minute averages of the ACE which are below the limit, complying with CPS2. In contrast, the loose LFC has one period of 10-minute averages above the limit, which indicates poor compliance. This is because the response of the loose LFC is too weak and slow to handle rapid changes in demand.

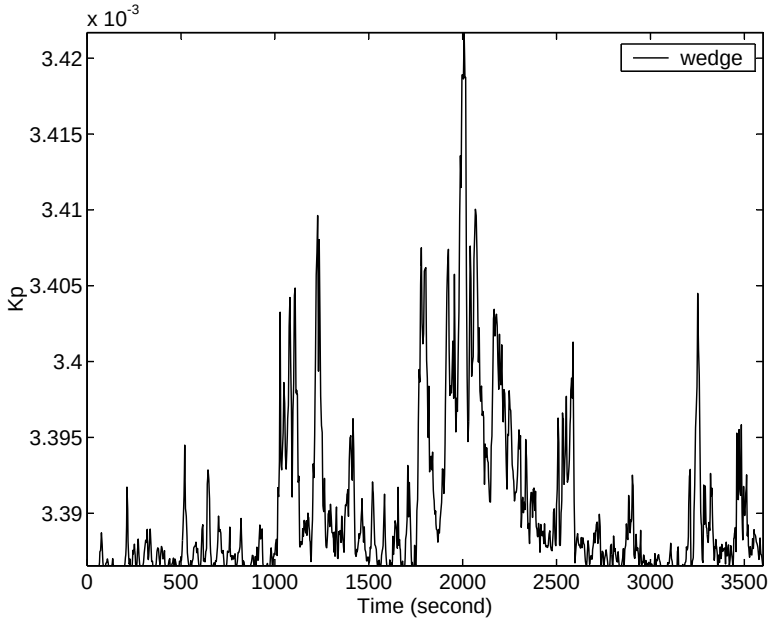

Figure 7.9: Proportional gain (K_P) of control area 1.

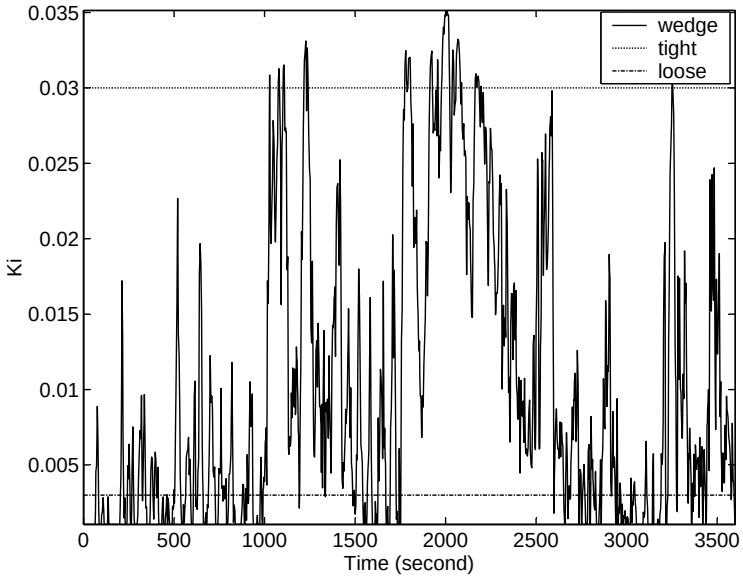

Figure 7.10: Integral gain (K_I) of control area 1.

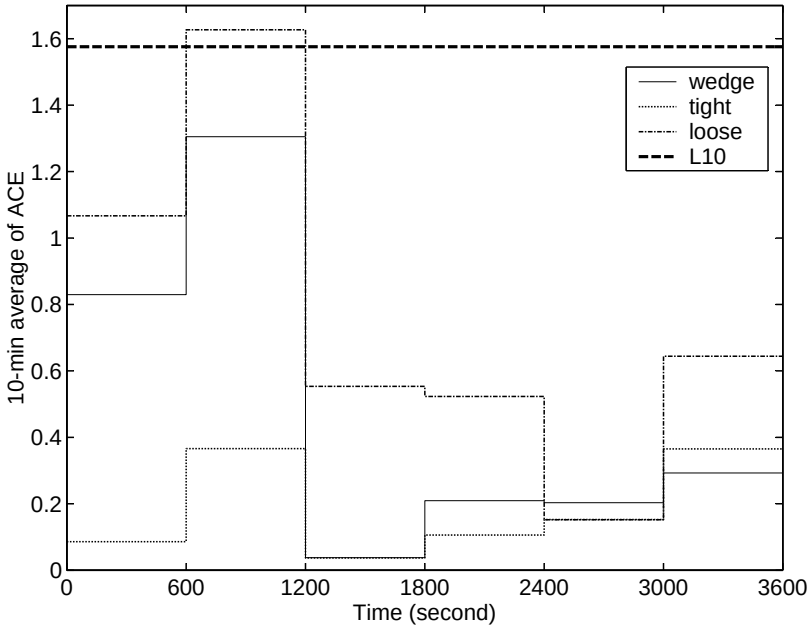

Figure 7.11: 10-minute average of ACE of control area 1.

To be seen closely, the changes in governor load setpoint (ΔP_C) over the first 400 seconds obtained from different LFCs are illustrated in Figure 7.12. The response of the proposed LFC looks similar to that of the loose LFC. Upon closer inspection, the response is higher in magnitude but fewer in number of reversals. Meanwhile, the response of the tight LFC is the highest in magnitude. This consequently results in the highest RMS of ΔP_C as shown in Figure 7.13. This parameter is generally used to indicate the amount of control effort. Nevertheless, it also reflects the amount of uneconomical generation (MW) deviated from an economic dispatch operating point, which will be discussed in detail in the next section. Incidentally, although the loose LFC yields the least RMS of ΔP_C, it is not preferred because of its poor capability in complying with NERC's control performance standards.

According to simulation results, the proposed load frequency control appears to be the best candidate, which complies well with NERC's control performance standards with low control effort. Nevertheless, the results will be more convincing, if the assessment includes more parameters other than the control effort. In section 7.4, new parameters including the area requirement and unit reversals will be introduced and used in the final assessment of load frequency control.

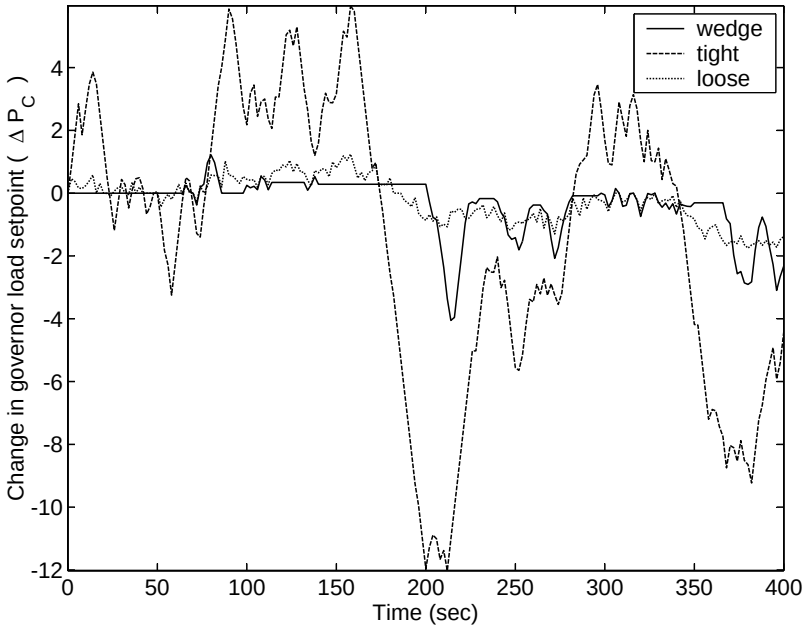

Figure 7.12: Change in governor load setpoint (ΔP_C) of control area 1.

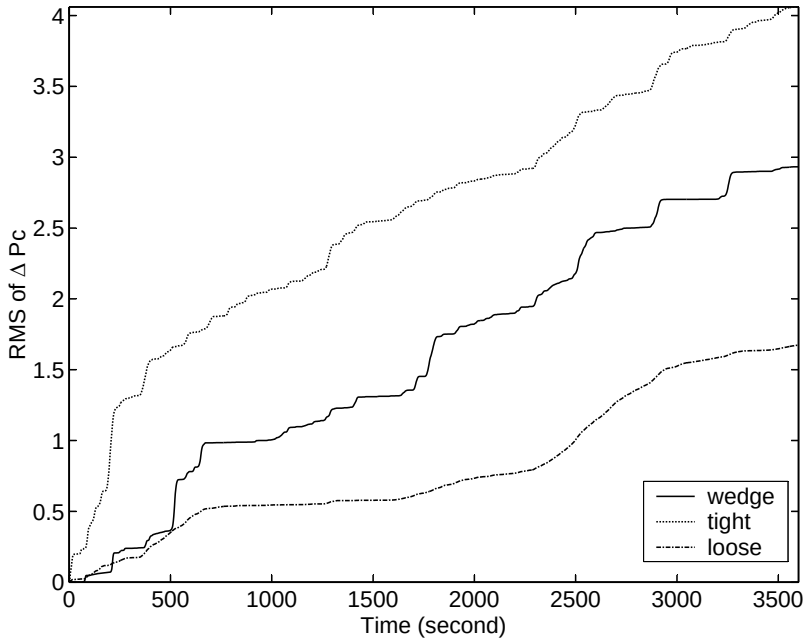

Figure 7.13: RMS of change in governor load setpoint (ΔP_C) of control area 1.

7.4 Economic assessment of load frequency control

This section presents a method of assessing load frequency control costs associated with control actions. Subsequently, the proposed LFC and tight conventional LFC, which are capable of complying with NERC's control performance standards, will be compared in terms of their operational and maintenance costs. However, quantifying these costs in real dollars will probably not be possible, due to the inaccessibility of the necessary information, which the electric utilities will not disclose.

Here, three parameters are introduced, which are 1) the area requirement (AR), 2) the RMS of uneconomic generation (MW) deviated from an economic dispatch (ED) solution, and 3) the number of unit reversals. They are used as indices to express LFC costs in another way. The meanings and determination of these parameters will be explained in the following sections.

7.4.1 Area requirement

In this dissertation, the area requirement (AR) is the megawatt capacity of the LFC or regulation service required for a control area to maintain good reliability. Normally, the system operator will first estimate the appropriate area requirement. Next, the operator will purchase that regulation capacity (MW) from generating units, and later sell it to customers on the demand side. As a result, a lesser area requirement would yield more savings for the demand-side customers. The amount of savings can be expressed in eq. (7.17).

$$AR\ saving \quad = \quad (MW\ less\ in\ AR) \cdot Regulation\ price \tag{7.17}$$

where

AR saving:	Dollars ($) saved in reduction of AR over a one-hour period
MW less in AR:	MW capacity reduced in area requirement for a specific hour
Regulation price:	Regulation price ($/MW) for a specific hour

The above equation results in an amount of dollars saved by the reduction of the area requirement over a one-hour period. This time frame is used because the area requirement and regulation price are usually changed each hour through a market mechanism.

Normally, the area requirement is estimated as 5-10 % of the peak load. This number for each area may vary according to the performance of the LFC and the characteristic of local loads. For instance, it can be very high for areas, which include the steel mill industry. However,

this percentage number may be reduced when the proposed load frequency control is in use. Figure 7.14 shows the actual regulation capacity in terms of MW used by the conventional and proposed LFCs to meet the demand as given in Figure 7.8.

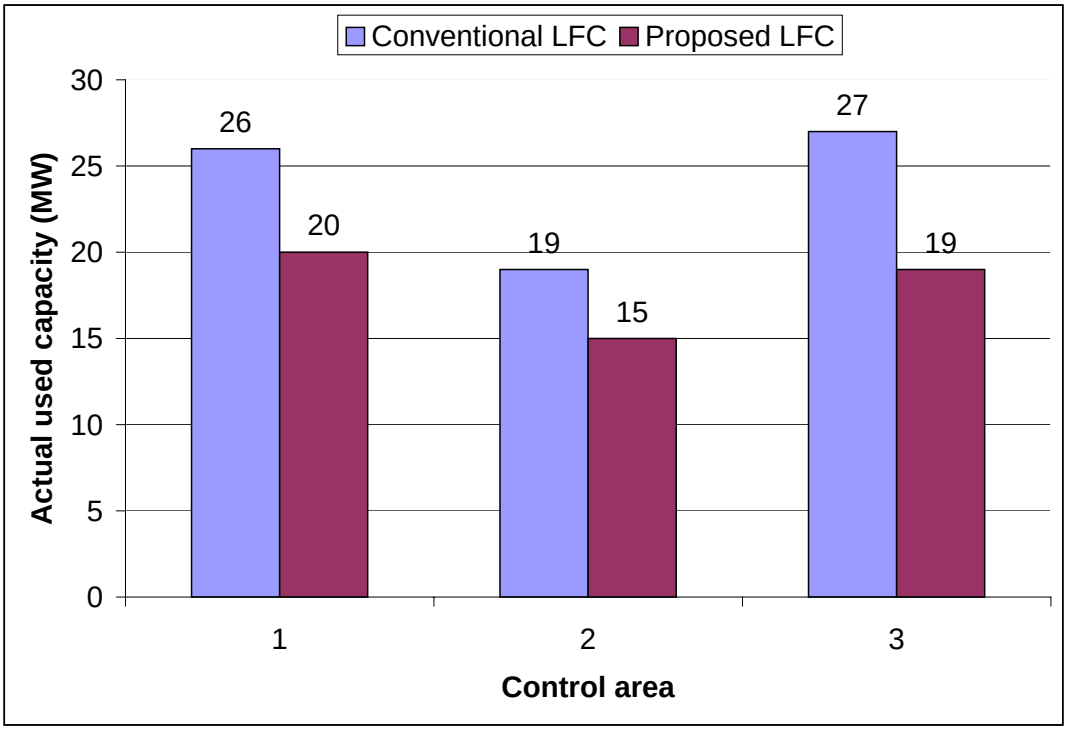

Figure 7.14: Actual regulation capacity (MW) used by load frequency control.

According to Figure 7.14, the actual megawatts for regulation used by the proposed LFC are approximately 25% less than that used by the conventional LFC. As a result, the area requirement will be eventually reduced after the proposed LFC is installed. The demand customers should significantly benefit from this outcome.

7.4.2 RMS of megawatts deviated from economic dispatch operating point

The function of regulation service is to move generation up and down around an economic dispatch (ED) operating point to satisfy fluctuations in the demand. Generally, the ED operating point is an optimal schedule of real power, obtained from the constrained optimization that minimizes operating costs of committed generating units. For a general economic dispatch problem,

the cost function is the cost of fuel (F) consumed in generation.

As shown in Figure 7.15, the economic dispatch solution (P_1^*, P_2^*, and P_3^*) for three units are obtained, where the incremental costs ($\frac{dF_i}{dP_i}$) of all units are equal, and the total scheduled power of all units equals the given demand [60], i.e. $\sum_{i=1}^{3} P_i^* = P_D$.

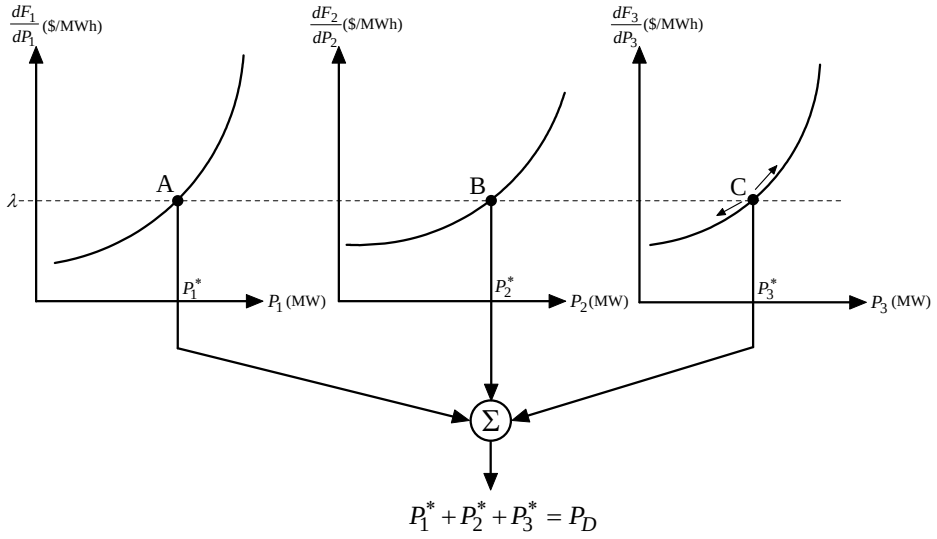

Figure 7.15: Graphical solution to economic dispatch.

According to the results, the optimal operating points of the three units are located at points A, B and C respectively. However, if the third unit also provides regulation service, the load frequency control will frequently move the operating point away from point C. As a result, this move yields an accumulation of uneconomic generation, which can be expressed by the root mean squares (RMS) of megawatts deviated from the ED operating point (P_3^* in this case). In Figure 7.16, this parameter is determined for all units in each control area.

In comparison to the conventional LFC, the proposed LFC yields by average 50% less in the RMS of megawatt deviations. This result confirms that uneconomical generation for regulation has been significantly reduced. In other words, those providing regulation pay less in fuel costs, which will ultimately help bring the regulation price down.

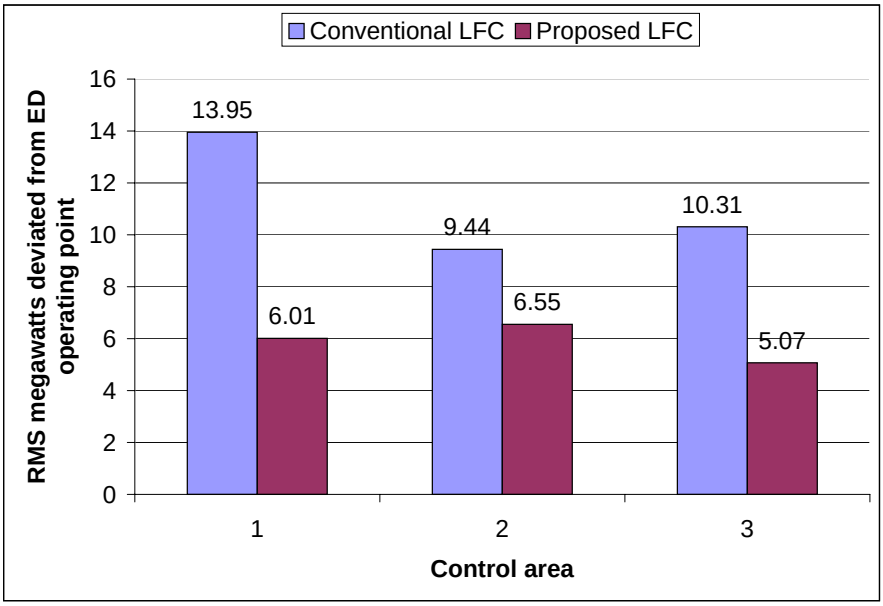

Figure 7.16: RMS of megawatts deviated from economic dispatch operating point.

7.4.3 Unit reversals

Unit reversals are of the most concern to regulation units. Raising and lowering signals sent from the automatic generation control (AGC) system continuously steer the unit up and down. This mechanism leads to accumulated wear and tear on unit equipment, and accelerates the time table of the maintenance schedule. As a result, the maintenance cost is included as a major part of the regulation cost.

Here, the number of reversals of the raising and lowering signals are counted over a one-hour period. As shown in Figures 7.17-7.19, the reversal counts are separated into six 10-minute intervals. According to the results, the proposed LFC, which yields considerably fewer reversals, outperforms the conventional one in terms of cost reduction. Presumably, if the maintenance cost associated with the LFC is proportional to the number of reversals, the proposed LFC could save the maintenance cost up to 50%.

This section has shown that the proposed LFC is attractive for restructured power systems, which are run according to economic incentives. Based on the above results, the operational and maintenance costs of the LFC are significantly reduced by the proposed strategy. Moreover, the

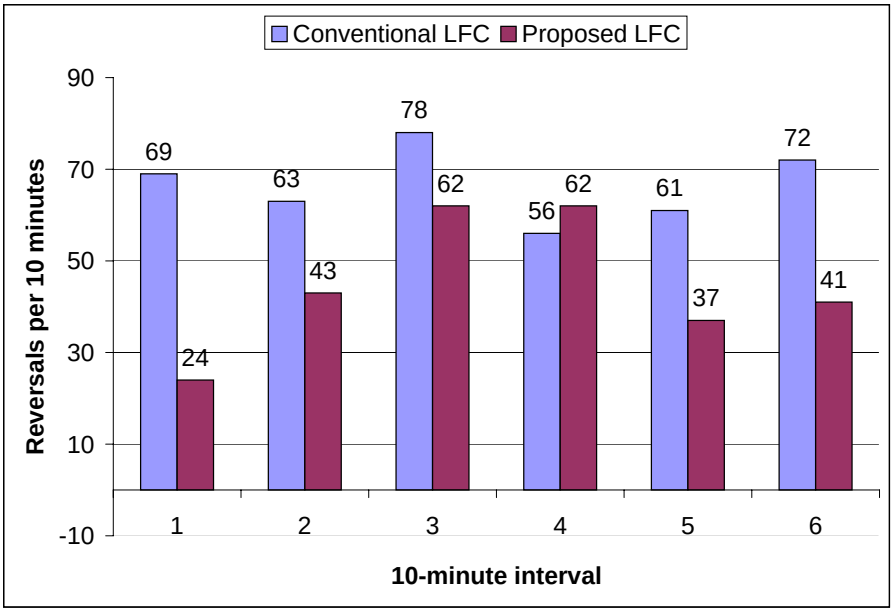

Figure 7.17: Area 1 - number of reversals per 10 minutes over a 1-hour period.

previous sections show that the new LFC provides efficient capability to comply with NERC's control performance standards. This strengthens the proposed load frequency control system, making it the optimal solution to real-world LFC problems.

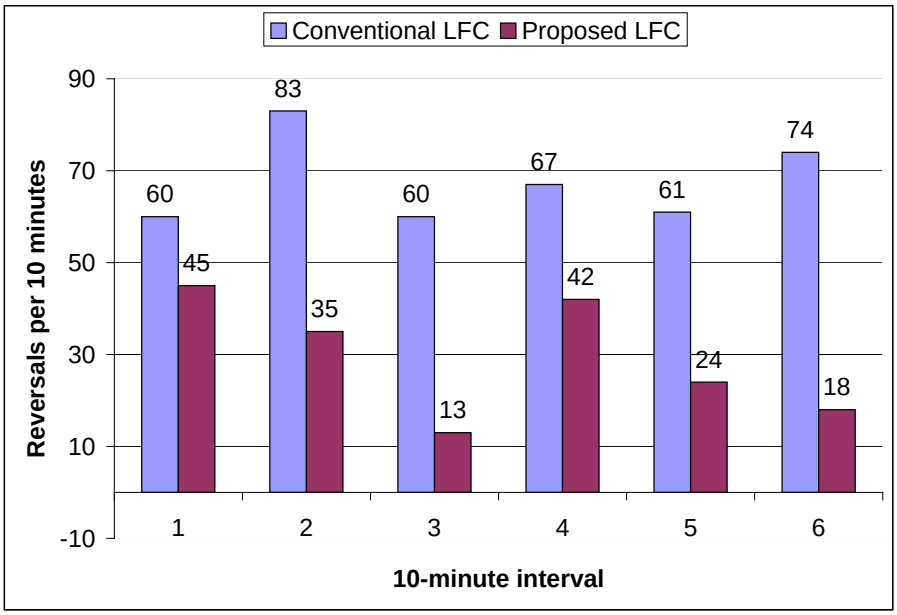

Figure 7.18: Area 2 - number of reversals per 10 minutes over a 1-hour period.

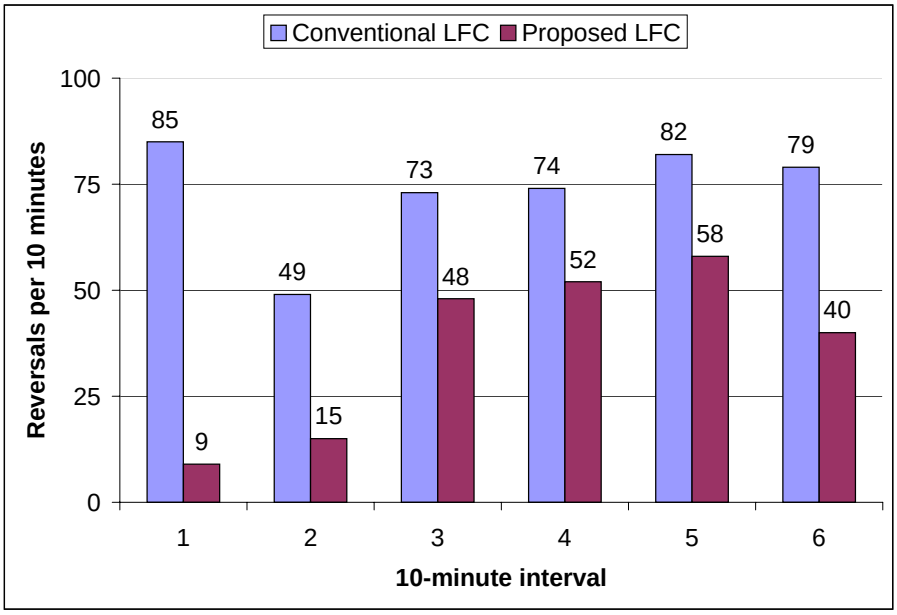

Figure 7.19: Area 3 - number of reversals per 10 minutes over a 1-hour period.

Chapter 8

Conclusions

In interconnected power systems, load frequency control is a very crucial mechanism in balancing power generated and demand. As described in the literature survey, extensive research has been conducted in this area. Load frequency control design is considered to be one of the most interesting issues because many different control designs have been developed. Nevertheless, most designs result in complicated high-order controllers. On the other hand, some methods lack theoretical support, and therefore cannot guarantee any dynamic performance (in a closed-loop system). Consequently, the development of a canonical load frequency control design that overcomes these disadvantages is a very desirable goal.

8.1 Summary of work

In Chapter 4, new decentralized control designs were developed for load frequency control applications. All methods consider the interface between areas as a disturbance. The first control design presented in section 4.1 models the disturbance as a dynamic equation driven by a white noise signal. Next, it is integrated with the dynamics of the subsystem. Then, a Kalman filter is developed to estimate all states of the augmented system which are needed for an LQR controller.

The second control design in section 4.2 is based on the H_∞ control theory. It was developed to improve the robustness of closed-loop power systems. A special feature is that the robust H_∞ control problem is formulated into linear matrix inequalities (LMIs) as a constrained optimization problem. It is solved by using the LMI control toolbox, which results in a dynamic controller. Under a variety of disturbances, the resulting controller has shown its robustness by regulating the system frequency and driving the area control error (ACE) back to zero effectively.

The above two methodologies have yielded observer based controllers whose dynamic order equals the size of system. As a result, the dynamic order of the closed-loop system can be very high if the power system being studied is large. In section 4.3, the third method was proposed in order to make the load frequency control design more practical in terms of implementation. The concept is based on collaboration between the linear matrix inequalities and genetic algorithms (GAs). More specifically, the controller type was pre-specified as proportional-integral (PI) control, which is simple and normally used in LFC applications. Next, GAs were employed to search for PI control parameters that satisfy the LMI based robust control constraints. Iteratively, once a pair of PI control parameters was chosen by the GAs, it was substituted into the LMIs, which were solved by the LMI control toolbox to achieve the minimum performance index. Eventually, the final solution consisted of the control parameters that yielded the robust PI load frequency controller with the minimum robust performance index. In a comparison between the performances of this method and the second control design, the simulation results of both were almost identical, which consequently justifies the robust performance of the proposed PI controller.

Subsequently, a global stability analysis was performed on the entire power system equipped with decentralized controllers. The perturbation theory of eigenvalues was used to determine the perturbation bounds of eigenvalues after a perturbation. However, these bounds proved to be unreasonably wide. A new parameter, departure angle, was introduced to reshape the bounds to be more accurate. The new bounds are much more reasonable, and indicate the appropriate stability margin.

Next, the excitation effects on load frequency control were investigated using the Power Analysis Toolbox (PAT). In LFC studies, the excitation system is normally neglected in the power system model used in control design because its dynamics are much faster than those of the turbine-governor system, which provides the main source of steering of the load frequency control. In the PAT simulation, the proposed LFC was tested with a full-blown power system, including the detailed model of a synchronous generator, excitation system, and transmission system. The simulation results show that there is no observable deterioration of the LFC performance caused by the voltage loop. This confirms the above assumption, and assures the feasibility of applying the proposed LFC to real-world systems.

The North American Electric Reliability Council (NERC) adopted control performance standards, CPS1 and CPS2, to evaluate the load frequency control performance on a monthly basis. All control areas are strictly required to comply with these standards. According to CPS data

reported to the NERC, a few control areas failed to comply with CPS2 for three consecutive months, and they were penalized afterwards. Hence, a control strategy to assure control areas of complying with the NERC control performance standards such as is proposed here is useful and cost saving to the industry.

The above LFC strategy using fuzzy logic technique was developed in Chapter 6 to help control areas comply with the standards. The levels of compliance with CPS1 and CPS2 were used as the inputs of the fuzzy logic system. While either level is low, which means close to violating the standard, the load frequency control will control the system more tightly. In contrast, the control parameter of the LFC will decrease to relax control actions, when the level of compliance is high. This action is to reduce the excess unit maneuvering that causes extra fuel costs for regulation service.

Since the deregulation of power systems, cost minimization has become the primary goal of all parties in the power market. Especially, regulation service providers can benefit considerably from savings in LFC costs. The cost minimization is the objective of work presented in Chapter 7. A new LFC system was developed primarily to reduce LFC associated costs. At the same time, this LFC system ensures that the control area complies with NERC's control performance standards. The wedge-shaped control method presented in section 7.1 is used as criteria to adjust the control tightness, and to direct control actions of adaptive robust load frequency control. The simulation results show that compliance with the NERC standards is achieved. Furthermore, three LFC cost indicators including 1) the area requirement, 2) the RMS of megawatts deviated from the economic dispatch operating point and 3) the number of reversals, are all significantly reduced as compared with those of a conventional LFC. In other words, a significant amount of LFC costs have been saved by using the load frequency control system proposed.

The contributions of this dissertation have been summarized above, which mainly consists of load frequency control designs and strategies. Through the simulation results, the proposed control designs and strategies have shown their advantages and effectiveness in terms of control performance, intelligence, practicality, and economy. By applying the findings of this dissertation, substantial benefits can be gained for load frequency control providers, control areas, and the society.

8.2 Future work

Load frequency control is a basic energy balancing problem. Generally, the characteristic of demand fluctuations is similar to a random signal that has high-frequency oscillations. Therefore, it is impossible to perfectly match the demand by controlling generated power whose response is much slower. The discrepancy between power generation and demand is called area control error (ACE) and used as the input of load frequency controllers. A large ACE normally causes adverse effects such as poor compliance with NERC's control performance standards. In addition, a large control effort is needed to bring the ACE back close to zero, which may require extra operational and maintenance costs. Consequently, a study on short-term load prediction would be helpful for this problem. In other words, if the probable trend of demand can be foreseen, the load frequency control will have better intelligence to enhance its performance and avoid uneconomical actions. Nevertheless, an enormous amount of load data is required to develop a model of short-term load prediction. Therefore, a tight collaboration with power industries is necessary to carry out this work.

Nowadays, using load as a resource has become an option for balancing energy. Electrical load can be a dependable resource in a case of power inadequacy. Loads can provide operating reserve or supplemental reserve services by turning themselves off when they are requested to do so by the system operator. Interestingly, preliminary research shows that some types of load can be controlled to function as load frequency control [61]. For instance, water-pumping load with variable-speed drive can be commanded by automatic generation control signals from the system operator. There are still a lot of opportunities for research in this new area. An advantage of using load as a resource is a benefit resulting from increased capacity of units, which becomes available for energy and other more profitable ancillary services. Moreover, market power at the generation side is mitigated because of additional choices of resources on the demand side.

Another suggestion for further research concerns the possibility of a modification or revision of the NERC control performance standards. Although they have proved better than the old control performance criteria, some experts still question their judgement, and predict that NERC may adopt new standards in the future. In this situation, the related work presented in this dissertation has provided a generalized concept, which could be modified and applied to a new problem without difficulty. Nevertheless, further research is necessary to optimize the performance of the new strategy.

Under other circumstances, regulation bids may soon include the quality of compliance with the NERC control performance standards, if control areas tend to barely comply with the standards in order to minimize their responsibility for interconnection burden. This possible consequence will definitely make load frequency control a very challenging optimization problem, including complex engineering and economic constraints.

Appendix A

Publications

Eleven publications are the results of this dissertation. Abstracts of these publications and citations are given in this appendix.

[1] **Decentralized Control of Nonlinear Electric Power Systems Thru Excitation and Governor Systems Using Local Measurements and Feedback Linearization**
Abstract: This paper applies feedback linearization to control a multimachine nonlinear electric power system thru the excitation and governor subsystems. The rotor angles are estimated in real-time from local measurement to achieve decoupling. The nonlinear decentralized controller effectively regulates the terminal voltage and also stabilizes the power system when a fault is applied. Two test systems are used to illustrate the proposed method: one-machine-infinite-bus and nine-bus three-machine power systems.
Reference: D. Rerkpreedapong, A. Feliachi, "Decentralized Control of Nonlinear Electric Power Systems Thru Excitation and Governor Systems Using Local Measurements and Feedback Linearization," *Proc. of Midwest Symposium on Circuits and Systems*, Lansing, MI, Aug. 8-10, 2000.

[2] **Decentralized Load Frequency Control in a Deregulated Environment**
Abstract: In this paper, a decentralized controller is proposed for the load frequency control problem in a deregulated environment. Decentralization is achieved by developing a model for the interface variables, which consist of frequencies of other subsystems. To account for the modeling uncertainties, a local Kalman filter is designed to estimate each subsystem's own and interface variables. The controller uses these estimates, optimizes a given performance index, and allocates generating units's outputs according to a deregula-

tion scenario. Two test systems are given to illustrate the proposed methodologies.

Reference: D. Rerkpreedapong, A. Feliachi,"Decentralized Load Frequency Control in a Deregulated Environment," *Proc. of the North American Power Symposium*, College Station, TX, Oct. 15-16, 2001.

[3] **Decentralized Load Frequency Control for Load Following Services**

Abstract: This paper proposes a decentralized controller for the load frequency control operated as a load following service. Decentralization is achieved by developing a model for the interface variables, which consist of frequencies of other subsystems. To account for the modeling uncertainties, a local Kalman filter is designed to estimate each subsystem's own and interface variables. The controller uses these estimates, optimizes a given performance index, and allocates generating units's outputs according to a deregulation scenario. Two test systems are given to illustrate the proposed methodologies.

Reference: D. Rerkpreedapong, A. Feliachi,"Decentralized Load Frequency Control for Load Following Services," *Proc. of the IEEE Power Engineering Society Winter Meeting*, New York, NY, Jan. 2002.

[4] **Fuzzy Rule Based Load Frequency Control in Compliance with NERC's Standards**

Abstract: In this paper, a set of fuzzy logic rules is designed to manipulate load frequency controllers of generating units providing regulation and load following services. The fuzzy based load frequency controllers take smart actions that (1) assure compliance with NERC's control performance standards, CPS1 and CPS2, and (2) also reduce wear and tear of generating units' equipments. A test system with multiple generation and distribution companies that takes into account regulation and load following services is used to illustrate the proposed methodologies.

Reference: D. Rerkpreedapong, A. Feliachi,"Fuzzy Rule Based Load Frequency Control in Compliance with NERCs Standards," *Proc. of the IEEE Power Engineering Society Summer Meeting*, Chicago, IL, July 2002.

[5] **Load Frequency Control Using Model Predictive Control**

Abstract: In this paper a Model Predictive Control (MPC) design is proposed for the LFC problem. The MPC controller is implemented in a completely decentralized fashion, using Area Control Error (ACE) signal as the controller input. To achieve decentralization, interfaces between interconnected power system control areas are treated as disturbances.

MPC controllers's performance is tested on a three-area power system with three different load disturbance scenarios. Simulation results are presented and compared with those obtained using a robust H_∞ controller.

Reference: A. Hasanović, N. Atić, D. Rerkpreedapong, A. Feliachi, "Load Frequency Control Using Model Predictive Control," *Proc. of the North American Power Symposium*, Phoenix, AZ, Oct. 14-15, 2002.

[6] **PI Gain Scheduler for Load Frequency Control Using Spline Techniques**

Abstract: This paper proposes a new gain scheduler for Proportional-Integral (PI) based load frequency control (LFC) using spline techniques. LFC operation has to comply with the North American Electric Reliability Council (NERC)'s control performance standards. This can be achieved by tuning the control gains of the load frequency controller. Furthermore, excess maneuvering of the generating units can be reduced if the gains are adjusted properly. Various PI gains are generated by a robust control design, where each one yields different control performance. Subsequently, those gains are interpolated and approximated using spline techniques, which finally result in robust gain paths. An appropriate pair of PI gains will be scheduled from the gain paths to achieve the LFC objective. Simulation results are shown to illustrate performance of the proposed methods.

Reference: D. Rerkpreedapong, A. Feliachi, "PI Gain Scheduler for Load Frequency Control Using Spline Techniques," *Proc. of the IEEE Southeastern Symposium on System Theory*, Morgantown, WV, March 2003.

[7] **Implementing an Auction Market for Regulation Service Using Software Agents**

Abstract: Software agent based systems have long been used in the design and implementation of complex systems. This paper discusses a framework for the regulation service auction market for investigating the behavior of software agents representing the various participants including the auction coordinator (ISO). The main emphasis is to consider the profit maximizing bidding strategies employed by the power suppliers to gain from the competitive market setup. The Java Multi-Agent Development Kit (Madkit) is used for the auction simulations and Java Native Interface (JNI) methods are employed to invoke Matlab computations. Finally, two examples are shown for procurement of Regulation Service involving five suppliers over a twenty-four hour auction period.

Reference: R. Srinivasan, D. Rerkpreedapong, S. Kankanahalli, A. Feliachi, "Implementing an Auction Market for Regulation Service Using Software Agents," *Proc. of the IEEE*

Southeastern Symposium on System Theory, Morgantown, WV, March 2003.

[8] Economy Oriented Model Predictive Load Frequency Control

Abstract: In this paper, Model Predictive Control (MPC) scheme is used to develop the proposed load frequency controller. In each sampling interval, an optimization procedure is performed to calculate optimal control actions. In addition, it has the ability to incorporate economic objectives as part of control requirements. Here, it applies the wedge control philosophy to minimize unit maneuvering and reversals, which affect load frequency control (LFC) costs. The proposed methodology is tested with a three-area power system. Simulation results show that the proposed LFC successfully complies with NERC's control performance standards, and also achieves the economic objective.

Reference: D. Rerkpreedapong, N. Atić, A. Feliachi, "Economy Oriented Model Predictive Load Frequency Control," *Proc. of Large Engineering Systems Conference on Power Engineering*, Montreal, Canada, May 2003.

[9] Robust Load Frequency Control Using Genetic Algorithms and Linear Matrix Inequalities

Abstract: In this paper, two robust decentralized control design methodologies for load frequency control (LFC) are proposed. The first one is based on H_∞ control design using linear matrix inequalities (LMI) technique in order to obtain robustness against uncertainties. The second controller has a simpler structure, which is more appealing from an implementation point of view, and it is tuned by a proposed novel robust control design algorithm to achieve the same robust performance as the first one. More specifically, Genetic Algorithms (GAs) optimization is used to tune the control parameters of the proportional-integral (PI) controller subject to the H_∞ constraints in terms of LMI. Hence, the second control design is called GALMI. Both proposed controllers are tested on a three-area power system with three scenarios of load disturbances to demonstrate their robust performances.

Reference: D. Rerkpreedapong, A. Hasanović, A. Feliachi, "Robust Load Frequency Control Using Genetic Algorithms and Linear Matrix Inequalities," *IEEE Transactions on Power Systems*, Vol. 18, No. 2, May 2003.

[10] Decentralized H_∞ Load Frequency Control Using LMI Toolbox

Abstract: In this paper, a decentralized controller for the load frequency control (LFC) problem in power systems is designed based on a robust H_∞ control technique formulated as

a Linear Matrix Inequalities (LMI) problem. To achieve decentralization, interfaces between interconnected power system's control areas are treated as disturbances. The LMI control toolbox is used to solve such a constrained optimization problem for LFC applications. The robust performance of the proposed controller is illustrated and compared with that of a conventional controller through simulation of a two-area power system with a variety of disturbances. Results show that H_∞ control technique via the LMI approach is an ideal tool for decentralized load frequency control design.

Reference: D. Rerkpreedapong, A. Feliachi,"Decentralized H_∞ Load Frequency Control Using LMI Toolbox," *Proc. of the IEEE International Symposium on Circuits and Systems*, Bangkok, Thailand, May 2003.

[11] NERC Compliant Decentralized Load Frequency Control Design Using Model Predictive Control

Abstract: This paper presents a decentralized Model Predictive Control (MPC) design for the Load Frequency Control (LFC) problem. The proposed algorithm has two objectives, (1) to assure compliance with control performance standards $CPS1$ and $CPS2$ set by NERC, and (2) to reduce wear and tear of generating units. A nonlinear simulation of a test system with multiple generation and distribution companies including regulation and load following services is performed to illustrate the proposed control scheme.

Reference: N. Atić, D. Rerkpreedapong, A. Hasanović, A. Feliachi, "NERC Compliant Decentralized Load Frequency Control Design Using Model Predictive Control," *Proc. of the IEEE Power Engineering Society General Meeting*, Toronto, Canada, July 2003.

Appendix B

Power system data used in Power Analysis Toolbox

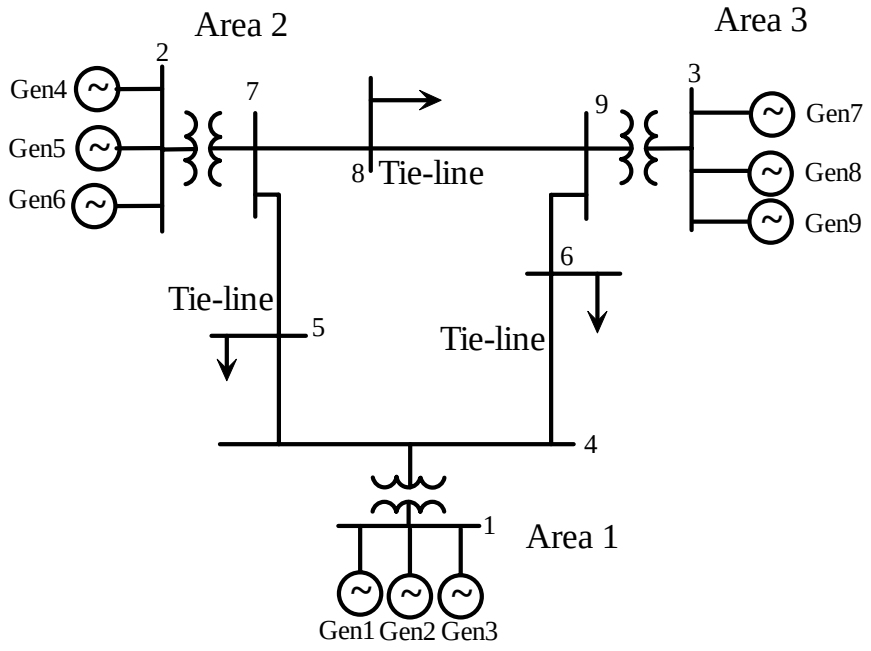

Figure B.1: A three-area power system.

```
% System base MVA setting (if none default of 100 MVA is taken)
basmva = 1000;

% Bus data format
%
%  bus  information    GENERATION    LOAD       SHUNT    Bus    Limits    Voltage   Limits
%   #   |V|    angle   Pg    Qg    P     Q     G     B  type  Qmax Qmin level kV  Vmax  Vmin
%       1  2      3    4     5     6     7     8     9   10    11    12    13     14    15
bus = [  1  1.04   0   0     0.0  0.0   0.0   0.00  0.00  1    20    -20   138    1.10  0.9;
         2  1.025  0   1.63  0.0  0.0   0.0   0.00  0.00  2    20    -20   138    1.10  0.9;
         3  1.025  0   0.85  0.0  0.0   0.0   0.00  0.00  2    20    -20   138    1.10  0.9;
         4  1.0    0   0.0   0.0  0.0   0.0   0.00  0.00  3    20    -20   138    1.10  0.9;
         5  1.0    0   0.0   0.0  1.25  0.5   0.0   0.00  3    20    -20   138    1.10  0.9;
         6  1.0    0   0.0   0.0  0.9   0.3   0.0   0.00  3    20    -20   138    1.10  0.9;
         7  1.0    0   0.0   0.0  0.0   0.0   0.0   0.00  3    20    -20   138    1.10  0.9;
         8  1.0    0   0.0   0.0  1.0   0.35  0.0   0.00  3    20    -20   138    1.10  0.9;
         9  1.0    0   0.0   0.0  0.0   0.0   0.0   0.00  3    20    -20   138    1.10  0.9];

% Line data
%
%         from  to    R    reactance  line charg-   tap   phase   tap  tap  tap
%         bus   bus  (pu)    (pu)      ing (pu)    ratio  shift   max  min  step
%         1      2    3        4          5          6      7      8    9    10
line = [  1      4   0.0     0.0567     0.0          0.0    0.0    0.0  0.0  0.00;
          2      7   0.0     0.0625     0.0          0.0    0.0    0.0  0.0  0.00;
          3      9   0.0     0.0586     0.0          0.0    0.0    0.0  0.0  0.00;
          4      5   0.01    0.085      0.176        0.0    0.0    0.0  0.0  0.00;
          4      6   0.017   0.092      0.158        0.0    0.0    0.0  0.0  0.00;
          5      7   0.032   0.161      0.306        0.0    0.0    0.0  0.0  0.00;
          6      9   0.039   0.170      0.358        0.0    0.0    0.0  0.0  0.00;
          7      8   0.0085  0.072      0.149        0.0    0.0    0.0  0.0  0.00;
          8      9   0.0119  0.1008     0.209        0.0    0.0    0.0  0.0  0.00];

% Machine data
%
%  1.  machine number,
%  2.  bus number,
%  3.  base mva,
%  4.  leakage reactance x_l(pu)
%  5.  resistance r_a(pu)
%  6.  d-axis sychronous reactance x_d(pu)
%  7.  d-axis transient reactance x'_d(pu)
%  8.  d-axis subtransient reactance x"_d(pu)
%  9.  d-axis open-circuit time constant T'_do(sec)
%  10. d-axis open-circuit subtransient time constant T"_do(sec)
%  11. q-axis sychronous reactance x_q(pu)
%  12. q-axis transient reactance x'_q(pu)
%  13. q-axis subtransient reactance x"_q(pu)
%  14. q-axis open-circuit time constant T'_qo(sec)
%  15. q-axis open circuit subtransient time constant T"_qo(sec)
%  16. inertia constant H(sec)
%  17. damping coefficient d_o(pu)
%  18. dampling coefficient d_1(pu)
%  19. bus number
%  20. saturation factor S(1.0)
%  21. saturation factor S(1.2)
%  22. and 23. fraction of P and Q

% column   1 2   3     4      5      6     7     8   9     10   11    12    13
mac_con = [1 1 1000  0.200  0.0025  1.8  0.30  0.25 8.00  0.03  1.7  0.55  0.25
           2 1  800  0.200  0.0025  1.8  0.30  0.25 8.00  0.03  1.7  0.55  0.25
           3 1 1000  0.200  0.0025  1.8  0.30  0.25 8.00  0.03  1.7  0.55  0.25
           4 2 1100  0.200  0.0025  1.8  0.30  0.25 8.00  0.03  1.7  0.55  0.25
           5 2  900  0.200  0.0025  1.8  0.30  0.25 8.00  0.03  1.7  0.55  0.25
           6 2 1200  0.200  0.0025  1.8  0.30  0.25 8.00  0.03  1.7  0.55  0.25
           7 3  850  0.200  0.0025  1.8  0.30  0.25 8.00  0.03  1.7  0.55  0.25
           8 3 1000  0.200  0.0025  1.8  0.30  0.25 8.00  0.03  1.7  0.55  0.25
           9 3 1020  0.200  0.0025  1.8  0.30  0.25 8.00  0.03  1.7  0.55  0.25
% column    14   15    16    17  18  19  20  21   22   23
           0.4  0.05    5    15   0   1   0   0  1/3  1/3;
           0.4  0.05   4.5   14   0   1   0   0  1/3  1/3;
           0.4  0.05    6    15   0   1   0   0  1/3  1/3;
           0.4  0.05   5.5   16   0   2   0   0  1/3  1/3;
           0.4  0.05    5    14   0   2   0   0  1/3  1/3;
           0.4  0.05   4.9   14   0   2   0   0  1/3  1/3;
           0.4  0.05   4.4   15   0   3   0   0  1/3  1/3;
           0.4  0.05    5    16   0   3   0   0  1/3  1/3;
           0.4  0.05   5.5   15   0   3   0   0  1/3  1/3];

newDpu = mac_con(:,17)./mac_con(:,3);
mac_con(:,17) = newDpu;
```

```
% Exciter data
exc_con = [...
% IEEE DC2 exciter
%            filter    regulator regulator   lag      lead     max   min  exc. const.
%       gen  time Tr   gain Ka   time Ta   time Tb  time Tc    Vr    Vr       Ke
% type  no.   (sec.)     (pu)     (sec.)    (sec.)   (sec.)   (pu)  (pu)
% col.1 col.2  col.3    col.4     col.5     col.6     col.7   col.8  col.9   col.10
    2    1     0.01     300.0     0.01        0        0      4.95   -4.9     1.0
    2    2     0.01     300.0     0.01        0        0      4.95   -4.9     1.0
    2    3     0.01     300.0     0.01        0        0      4.95   -4.9     1.0
    2    4     0.01     300.0     0.01        0        0      4.95   -4.9     1.0
    2    5     0.01     300.0     0.01        0        0      4.95   -4.9     1.0
    2    6     0.01     300.0     0.01        0        0      4.95   -4.9     1.0
    2    7     0.01     300.0     0.01        0        0      4.95   -4.9     1.0
    2    8     0.01     300.0     0.01        0        0      4.95   -4.9     1.0
    2    9     0.01     300.0     0.01        0        0      4.95   -4.9     1.0

%exc. time const.  E1    Se(E1)   E2     Se(E2) Stabilizer  Stabilizer
%      Te                                angle    gain Kf     time
%    (sec)                               (deg.)
%    col.11      col.12  col.13  col.14  col.15    col.16    col.17
      1.33        3.05   0.279    2.29    0.117      0.1      0.675  ;
      1.33        3.05   0.279    2.29    0.117      0.1      0.675  ;
      1.33        3.05   0.279    2.29    0.117      0.1      0.675  ;
      1.33        3.05   0.279    2.29    0.117      0.1      0.675  ;
      1.33        3.05   0.279    2.29    0.117      0.1      0.675  ;
      1.33        3.05   0.279    2.29    0.117      0.1      0.675  ;
      1.33        3.05   0.279    2.29    0.117      0.1      0.675  ;
      1.33        3.05   0.279    2.29    0.117      0.1      0.675  ;
      1.33        3.05   0.279    2.29    0.117      0.1      0.675  ];

% Turbine-governor data
%column       data                      unit
%  1    turbine model number (=3)
%  2    machine number
%  3    speed set point                wf    pu
%  4    steady state gain             1/R    pu
%  5    maximum power order           Tmax  pu on generator base
%  6    servo time constant            Ts  sec,    T1            sec
%  7    governor time constant         Tc  sec,    T2            sec
%  8    transient gain time constant   T3  sec,    T3 (governor) sec
%  9    HP section time constant       T4  sec,    T4 (turbine)  sec
% 10    reheater time constant         T5  sec,    T5            sec
% 11    Time constant for Universal TG              T6            sec
% 12    Time constant for Universal TG              T7            sec
% 13    Gain constant for turbine                   K1
% 14    Gain constant for turbine                   K2
% 15    Gain constant for turbine                   K3
% 16    Gain constant for turbine                   K4
% 17    power loop 0/1 = off/on
% 18    frequency loop 0/gain = off/on

% Universal TG (Type=3)
Rp = [5 4 5.5 5 4 5 4 5 5];
R  = Rp/100;
tg_con = [...
% 1  2  3     4     5    6    7    8     9    10    11    12    13   14   15   16   17   18
  3  1  1  1/R(1)  1.0  0.0  0.0  0.08  0.40  0.0   0.0   0.0   1.0  0.0  0.0  0.0   0    1;
  3  2  1  1/R(2)  1.0  0.0  0.0  0.06  0.36  0.0   0.0   0.0   1.0  0.0  0.0  0.0   0    1;
  3  3  1  1/R(3)  1.0  0.0  0.0  0.07  0.42  0.0   0.0   0.0   1.0  0.0  0.0  0.0   0    1;
  3  4  1  1/R(4)  1.0  0.0  0.0  0.06  0.44  0.0   0.0   0.0   1.0  0.0  0.0  0.0   0    1;
  3  5  1  1/R(5)  1.0  0.0  0.0  0.06  0.32  0.0   0.0   0.0   1.0  0.0  0.0  0.0   0    1;
  3  6  1  1/R(6)  1.0  0.0  0.0  0.08  0.40  0.0   0.0   0.0   1.0  0.0  0.0  0.0   0    1;
  3  7  1  1/R(7)  1.0  0.0  0.0  0.07  0.30  0.0   0.0   0.0   1.0  0.0  0.0  0.0   0    1;
  3  8  1  1/R(8)  1.0  0.0  0.0  0.07  0.40  0.0   0.0   0.0   1.0  0.0  0.0  0.0   0    1;
  3  9  1  1/R(9)  1.0  0.0  0.0  0.08  0.41  0.0   0.0   0.0   1.0  0.0  0.0  0.0   0    1];

% Load configuration
load_con = [...
%  1  bus number
%  2  fracation of constant P
%  3  fracation of constant Q
%  4  fracation of constant active   current
%  5  fracation of constant reactive current
%  1  2  3   4  5
   5  1  0   0  0 .2 .2 .2 .2 2;
   6  1  0   0  0 .2 .2 .2 .2 2;
   8  1  0   0  0 .2 .2 .2 .2 2];
```

References

[1] R. J. Kafka, "Ancillary Services and Reliability," *IEEE PES Winter Meeting*, Columbus, Ohio, January 2001.

[2] Federal Energy Regulatory Commission (FERC), Standard Market Design and Structure NOPR RM01-12-000 [Online]. Available: http://www.ferc.gov/Electric/RTO/Mrkt-Strct-comments/discussion_paper.htm

[3] E. Hirst, and B. Kirby, "Ancillary Service Details: Regulation, Load Following, and Generator Response," Oak Ridge National Laboratory, Oak Ridge, TN, Tech. Rep. ORNL/CON-433, Sep. 1996.

[4] North American Electric Reliability Council (NERC), "Performance Standard Training Document," in Operating Manual, pp. ps1-20, Nov. 1996.

[5] Electric Power Research Institute (EPRI), "Interconnected Power System Dynamic Tutorial," EPRI TR-107726 1915-16 Final Report, Palo Alto, CA, March 1997.

[6] A. M. Stankovic, G. Tadmor, and T. A. Sakharuk, "On Robust Control Analysis and Design for Load Frequency Regulation," *IEEE Transactions on Power Systems*, Vol. 13, no. 2, pp. 481-489, May 1998.

[7] Y. L. Abdel-Magid, and M. M. Dawoud, "Genetic Algorithms Applications in Load Frequency Control," *The First International Conference on Genetic Algorithms in Engineering Systems: Innovations and Applications*, pp. 207-213, 1995.

[8] W. C. Schultz, and V. C. Rideout, "Control System Performance Measures: Past Present and Future," *IEEE Transactions on Automatic Control*, AC-6, 22 pp. 22-35, 1961.

[9] V. Donde, M. A. Pai, and I. A. Hiskens, "Simulation and Optimization in an AGC System after Deregulation," *IEEE Transactions on Power Systems*, Vol. 16, no. 3, pp. 481-489, August 2001.

[10] J. Kumar, K. H. Ng, and G. Sheble, "AGC Simulator for Price-Based Operation Part I," *IEEE Transactions on Power Systems*, Vol. 12, No. 2, pp. 527-532, May 1997.

[11] J. Kumar, K. H. Ng, and G. Sheble, "AGC Simulator for Price-Based Operation Part II: Case Study Results," *IEEE Transactions on Power Systems*, Vol. 12, No. 2, pp. 533-538, May 1997.

[12] M. L. Kothari, N. Sinha, and M. Rafi, "Automatic Generation Control of an Interconnected Power System Under Deregulated Environment," *Power Quality' 98*, pp. 95-102, 1998.

[13] A. Feliachi, "On Load Frequency Control in a Deregulated Environment," *Proceedings of the 1996 IEEE International Conference on Control Applications*, pp. 437-441, 1996.

[14] M. H. Rahi, and A. Feliachi, "H_∞ Robust Decentralized Controller for Nonlinear Power Systems," *Proceedings of the 30th Southeastern Symposium on Sysym Theory*, pp. 268-270, March 1998.

[15] A. Feliachi, "Reduced H_∞ load frequency controller in a deregulated electric power system environment," *Proceedings of the 36th IEEE Conference on Decision and Control*, Vol. 4, pp. 3100-3101, 1997.

[16] T. C. Yang, H. Cimen, and Q. M. Zhu, "Decentralized Load Frequency Controller Design Based on Structured Singular Values," *IEE Proceedings-Gener. Transm. Distrib.*, Vol. 145, No. 1, pp. 7-14, January 1998.

[17] M. Aldeen, and J. F. Marsh, "Decentralized Proportional-Plus-Integral Design Method for Interconnected Power Systems," *IEE Proceedings-C*, Vol. 138, No. 4, pp. 263-274, July 1991.

[18] H. Trinh, and M. Aldeen, "Decentralized Load-Frequency Control of Interconnected Power Systems," *IEE International Conference on Advances in Power System Control, Operation and Management*, Vol. 2, pp. 815-820, 1991.

[19] M. Aldeen, "Interaction Modeling Approach to Distributed Control with Application to Power Systems," *International Journal Control*, Vol. 53, pp. 1035-1054, 1991.

[20] S. S. Stankovic, X. Chen, M. R. Matausek, and D. D. Siljak, "Stochastic Inclusion Principle Applied to Decentralized Automatic Generation Control," *International Journal Control*, Vol. 72, No. 3, pp. 276-288, 1999.

[21] K. Y. Lim, Y. Wang, and R. Zhou, "Robust Decentralized Load-Frequency Control of Multi-Area Power Systems," *IEE Proceedings-Gener. Transm. Distrib.*, Vol. 143, No. 5, pp. 377-386, September 1996.

[22] K. Y. Lim, Y. Wang, G. Gua, and R. Zhou, "A New Decentralized Robust Controller Design for Multi-Area Load-Frequency Control via in Complete State Feedback," *Optimal Control Applications & Methods*, Vol. 19, pp. 345-361, 1998.

[23] P. P. Khargonekar, I. R. Petersen, and K. Zhou, "Robust Stabilization of Uncertain Systems: Quadratic Stabilizability and H^∞ Control Theory," *IEEE Transactions on Automatic Control*, Vol. 35, pp. 356-361, 1990.

[24] Y. Hsu, and C. Cheng, "Load Frequency Control Using Fuzzy Logic," *International Conference on High Technology in the Power Industry*, pp. 32-38, 1991.

[25] C. S. Indulkar, and B. Raj, "Application of Fuzzy Controller to Automatic Generation Control," *Electric Machines and Power Systems*, Vol. 23, No. 2, pp. 209-220, March 1995.

[26] M. Djukanovic, "Two-Area Load Frequency Control with Neural Nets," *Proceedings of the North American Power Symposium*, pp. 161-169, 1993.

[27] J. Talaq, and F. Al-Basri, "Adaptive Fuzzy Gain Scheduling for Load Frequency Control," *IEEE Transactions on Power Systems*, Vol. 14, No. 1, pp. 145-150, February 1999.

[28] B. Kirby, and E. Hirst, "Customer-Specific Metrics for The Regulation and Load Following Ancillary Services," Oak Ridge National Laboratory, Oak Ridge, TN, Tech. Rep. ORNL/CON-474, January 2000.

[29] B. Kirby, and E. Hirst, "Unbundling Electricity: Ancillary Services," *IEEE Power Engineering Review*, pp. 5-6, June 1996.

[30] R. D. Christie, and A. Bose, "Load Frequency Control Issues in Power System Operations after Deregulation," *IEEE Transactions on Power Systems*, Vol. 11, No. 3, pp. 1191-1200, August 1996.

[31] A. P. S. Meliopoulos, G. J. Cokkinides, and A. G. Bakirtzis, "Load-Frequency Control Service in a Deregulated Environment," *Proceedings of the Annual Hawaii International Conference on System Sciences*, pp. 24-31, 1998.

[32] G. B. Sheble, *Computational Auction Mechanisms for Restructured Power Industry Operation*, Kluwer Academic Publishers, Norwell, MA, 1999, ISBN 079238475X.

[33] N. Jaleeli, and L. S. VanSlyck, "NERC's New Control Performance Standards," *IEEE Transactions on Power Systems*, Vol. 14, No. 3, pp. 1092-1099, August 1999.

[34] G. Gross, and J. W. Lee, "Analysis of Load Frequency Control Performance Assessment Criteria," *IEEE Transactions on Power Systems*, Vol. 16, No. 3, pp. 520-525, August 2001.

[35] North American Electric Reliability Council (NERC), Control Performance Surveys (CPS). Compliance Enforcement Program [Online]. Available: http://www.nerc.com/ filez/cpc.html

[36] N. Jaleeli, and L. S. VanSlyck, "Tie-Line Bias Priortized Energy Control," *IEEE Transactions on Power Systems*, Vol. 10, No. 1, pp. 51-59, February 1995.

[37] M. Yao, R. R. Shoults, and R. Kelm, "AGC Logic Based on NERC's New Control Performance Standard and Disturbance Control Standard," *IEEE Transactions on Power Systems*, Vol. 15, No. 2, pp. 852-857, May 2000.

[38] H. Saadat, *Power System Analysis*, McGraw-Hill Companies, Inc., Singapore, 1999, ISBN 0071167587.

[39] The Department of Energy, Energy Information Administration [Online]. Available: http://www.eia.doe.gov/cneaf/electricity/page/prim2/chapter7.html

[40] A. S. Debs, *Modern Power Systems Control and Operation*, Kluwer Academic Publishers, Norwell, MA, 1998, ISBN 0898382653.

[41] E. Hirst, and B. Kirby, "Creating Competitive Markets for Ancillary Services," Oak Ridge National Laboratory, Oak Ridge, TN, Tech. Rep. ORNL/CON-448, October 1997.

[42] D. Rerkpreedapong, and A. Feliachi, "Decentralized Load Frequency Control in a Deregulated Environment," *Proceedings of North American Power Symposium*, Texas, pp. 316-321, October 2001.

[43] D. Rerkpreedapong, and A. Feliachi, "Decentralized Load Frequency Control for Load Following Services," *The 2002 Power Engineering Society Winter Meeting*, New York, Vol. 2, pp. 1252-1257, January 2002.

[44] J. B. Burl, *Linear Optimal Control: $\mathcal{H}_2$ and $\mathcal{H}_\infty$ Methods*, Addison Wesley Longman, Inc., Menlo Park, CA, 1998, ISBN 0201808684.

[45] H. Kwakernaak, and R. Sivan, *Linear Optimal Control Systems*, John Wiley & Sons, Inc., USA, 1972, ISBN 0471511102.

[46] P. Gahinet, A. Nemirovski, A. J. Laub, and M. Chilali, *LMI Control Toolbox*, The MathWorks, Inc., 1995.

[47] D. Rerkpreedapong, and A. Feliachi, "Decentralized H_∞ Load Frequency Control Using LMI Control Toolbox," *To appear in the Proceedings of IEEE International Symposium on Circuits and Systems*, Bangkok, Thailand, May 2003.

[48] D. Rerkpreedapong, A. Hasanović, and A. Feliachi, "Robust Load Frequency Control Using Genetic Algorithms and Linear Matrix Inequalities," *To appear in the IEEE Transactions on Power Systems.*

[49] K. Schoder, A. Hasanović, A. Feliachi, and A. Hasanović, "PAT: A Power Analysis Toolbox for MATLAB/Simulink," *IEEE Transactions on Power Systems*, Vol. 18, No. 1, pp. 42-47, February 2003.

[50] Chow, J., *Power System Toolbox Version 2.0 Dynamic Tutorial and Functions*, Cherry Tree Scientific Software, Colborne, Ontario, Canada, 1997.

[51] S. D. Kaehler, Fuzzy Logic - An Introduction: Part 1 [Online]. Available: http://www.seattlerobotics.org/encoder/mar98/fuz/fl_part1.html

[52] D. Rerkpreedapong, and A. Feliachi, "Fuzzy Rule Based Load Frequency Control in Compliance with NERC's Standards," *The 2002 Power Engineering Society Summer Meeting*, Chicago, July 2002.

[53] MathWorks, *Fuzzy Logic Toolbox User's Guide*, The MathWorks, Inc., September 2000, p. 2-20.

[54] H. Demuth, and M. Beale, *Neural Network Toolbox For Use with MATLAB*, The MathWorks, Inc., March 2001.

[55] G. W. Stewart, and J. Sun, *Matrix Perturbation Theory*, Academic Press, Inc., CA, 1990, ISBN 0126702306.

[56] G. H. Golub, and C. F. Van Loan, *Matrix Computations*, The Johns Hopkins University Press, MD, 1989, ISBN 0801837391.

[57] J. W. Demmel, *Applied Numerical Linear Algebra*, SIAM, PA, 1997, ISBN 0898713897.

[58] D. Rerkpreedapong, and A. Feliachi, "PI Gain Scheduler for Load Frequency Control Using Spline Techniques," *Proceedings of IEEE Southeastern Symposium on System Theory*, Morgantown, WV, pp. 259-263, March 2003.

[59] C. De Boor, *A Practical Guide to Splines*, Springer-Verlag New York Inc., 2001.

[60] A. J. Wood, and B. F. Wollenberg, *Power Generation Operation & Control*, John Wiley & Sons, Canada, 1984, ISBN 0471091820.

[61] B. Kirby, and E. Hirst, "Load as a Resource in Providing Ancillary Services," *Proceedings of the American Power Conference*, Vol. 61, Chicago, IL, April 1999.